

## Nondestructive Testing to Identify Concrete Bridge Deck Deterioration

### DETAILS

---

85 pages | 8.5 x 11 | PAPERBACK

ISBN 978-0-309-12933-6 | DOI 10.17226/22771

BUY THIS BOOK

FIND RELATED TITLES

### AUTHORS

---

Gucunski, Nenad; Imani, Arezoo; Romero, Francisco; Nazarian, Soheil; Yuan, Deren; Wigggenhauser, Herbert; Shokouhi, Parisa; Taffe, Alexander; and Kutrubes, Doria

### Visit the National Academies Press at [NAP.edu](http://NAP.edu) and login or register to get:

---

- Access to free PDF downloads of thousands of scientific reports
- 10% off the price of print titles
- Email or social media notifications of new titles related to your interests
- Special offers and discounts



Distribution, posting, or copying of this PDF is strictly prohibited without written permission of the National Academies Press. (Request Permission) Unless otherwise indicated, all materials in this PDF are copyrighted by the National Academy of Sciences.

**The Second**  
**S T R A T E G I C   H I G H W A Y   R E S E A R C H   P R O G R A M**

 **SHRP 2 REPORT S2-R06A-RR-1**

# Nondestructive Testing to Identify Concrete Bridge Deck Deterioration

**NENAD GUCUNSKI, AREZOO IMANI, AND FRANCISCO ROMERO**  
Rutgers University—Center for Advanced Infrastructure and Transportation

**SOHEIL NAZARIAN AND DEREN YUAN**  
The University of Texas at El Paso—Center for Transportation Infrastructure Systems

**HERBERT WIGGENHAUSER, PARISA SHOKOUHI, AND ALEXANDER TAFFE**  
Federal Institute for Materials Research and Testing (BAM), Germany

**DORIA KUTRUBES**  
Radar Systems International, Inc.

---

**TRANSPORTATION RESEARCH BOARD**

WASHINGTON, D.C.  
2013  
[www.TRB.org](http://www.TRB.org)

## **Subscriber Categories**

Bridges and Other Structures

Construction

Highways

Maintenance and Preservation

Materials

## The Second Strategic Highway Research Program

America's highway system is critical to meeting the mobility and economic needs of local communities, regions, and the nation. Developments in research and technology—such as advanced materials, communications technology, new data collection technologies, and human factors science—offer a new opportunity to improve the safety and reliability of this important national resource. Breakthrough resolution of significant transportation problems, however, requires concentrated resources over a short time frame. Reflecting this need, the second Strategic Highway Research Program (SHRP 2) has an intense, large-scale focus, integrates multiple fields of research and technology, and is fundamentally different from the broad, mission-oriented, discipline-based research programs that have been the mainstay of the highway research industry for half a century.

The need for SHRP 2 was identified in *TRB Special Report 260: Strategic Highway Research: Saving Lives, Reducing Congestion, Improving Quality of Life*, published in 2001 and based on a study sponsored by Congress through the Transportation Equity Act for the 21st Century (TEA-21). SHRP 2, modeled after the first Strategic Highway Research Program, is a focused, time-constrained, management-driven program designed to complement existing highway research programs. SHRP 2 focuses on applied research in four areas: Safety, to prevent or reduce the severity of highway crashes by understanding driver behavior; Renewal, to address the aging infrastructure through rapid design and construction methods that cause minimal disruptions and produce lasting facilities; Reliability, to reduce congestion through incident reduction, management, response, and mitigation; and Capacity, to integrate mobility, economic, environmental, and community needs in the planning and designing of new transportation capacity.

SHRP 2 was authorized in August 2005 as part of the Safe, Accountable, Flexible, Efficient Transportation Equity Act: A Legacy for Users (SAFETEA-LU). The program is managed by the Transportation Research Board (TRB) on behalf of the National Research Council (NRC). SHRP 2 is conducted under a memorandum of understanding among the American Association of State Highway and Transportation Officials (AASHTO), the Federal Highway Administration (FHWA), and the National Academy of Sciences, parent organization of TRB and NRC. The program provides for competitive, merit-based selection of research contractors; independent research project oversight; and dissemination of research results.

SHRP 2 Report S2-R06A-RR-1

ISBN: 978-0-309-12933-6

Library of Congress Control Number: 2012955018

© 2013 National Academy of Sciences. All rights reserved.

### Copyright Information

Authors herein are responsible for the authenticity of their materials and for obtaining written permissions from publishers or persons who own the copyright to any previously published or copyrighted material used herein.

The second Strategic Highway Research Program grants permission to reproduce material in this publication for classroom and not-for-profit purposes. Permission is given with the understanding that none of the material will be used to imply TRB, AASHTO, or FHWA endorsement of a particular product, method, or practice. It is expected that those reproducing material in this document for educational and not-for-profit purposes will give appropriate acknowledgment of the source of any reprinted or reproduced material. For other uses of the material, request permission from SHRP 2.

*Note:* SHRP 2 report numbers convey the program, focus area, project number, and publication format. Report numbers ending in "w" are published as web documents only.

### Notice

The project that is the subject of this report was a part of the second Strategic Highway Research Program, conducted by the Transportation Research Board with the approval of the Governing Board of the National Research Council.

The members of the technical committee selected to monitor this project and review this report were chosen for their special competencies and with regard for appropriate balance. The report was reviewed by the technical committee and accepted for publication according to procedures established and overseen by the Transportation Research Board and approved by the Governing Board of the National Research Council.

The opinions and conclusions expressed or implied in this report are those of the researchers who performed the research and are not necessarily those of the Transportation Research Board, the National Research Council, or the program sponsors.

The Transportation Research Board of the National Academies, the National Research Council, and the sponsors of the second Strategic Highway Research Program do not endorse products or manufacturers. Trade or manufacturers' names appear herein solely because they are considered essential to the object of the report.



### SHRP 2 Reports

Available by subscription and through the TRB online bookstore:

[www.TRB.org/bookstore](http://www.TRB.org/bookstore)

Contact the TRB Business Office:  
202-334-3213

More information about SHRP 2:  
[www.TRB.org/SHRP2](http://www.TRB.org/SHRP2)

# **THE NATIONAL ACADEMIES**

## *Advisers to the Nation on Science, Engineering, and Medicine*

The **National Academy of Sciences** is a private, nonprofit, self-perpetuating society of distinguished scholars engaged in scientific and engineering research, dedicated to the furtherance of science and technology and to their use for the general welfare. On the authority of the charter granted to it by Congress in 1863, the Academy has a mandate that requires it to advise the federal government on scientific and technical matters. Dr. Ralph J. Cicerone is president of the National Academy of Sciences.

The **National Academy of Engineering** was established in 1964, under the charter of the National Academy of Sciences, as a parallel organization of outstanding engineers. It is autonomous in its administration and in the selection of its members, sharing with the National Academy of Sciences the responsibility for advising the federal government. The National Academy of Engineering also sponsors engineering programs aimed at meeting national needs, encourages education and research, and recognizes the superior achievements of engineers. Dr. Charles M. Vest is president of the National Academy of Engineering.

The **Institute of Medicine** was established in 1970 by the National Academy of Sciences to secure the services of eminent members of appropriate professions in the examination of policy matters pertaining to the health of the public. The Institute acts under the responsibility given to the National Academy of Sciences by its congressional charter to be an adviser to the federal government and, on its own initiative, to identify issues of medical care, research, and education. Dr. Harvey V. Fineberg is president of the Institute of Medicine.

The **National Research Council** was organized by the National Academy of Sciences in 1916 to associate the broad community of science and technology with the Academy's purposes of furthering knowledge and advising the federal government. Functioning in accordance with general policies determined by the Academy, the Council has become the principal operating agency of both the National Academy of Sciences and the National Academy of Engineering in providing services to the government, the public, and the scientific and engineering communities. The Council is administered jointly by both Academies and the Institute of Medicine. Dr. Ralph J. Cicerone and Dr. Charles M. Vest are chair and vice chair, respectively, of the National Research Council.

The **Transportation Research Board** is one of six major divisions of the National Research Council. The mission of the Transportation Research Board is to provide leadership in transportation innovation and progress through research and information exchange, conducted within a setting that is objective, interdisciplinary, and multimodal. The Board's varied activities annually engage about 7,000 engineers, scientists, and other transportation researchers and practitioners from the public and private sectors and academia, all of whom contribute their expertise in the public interest. The program is supported by state transportation departments, federal agencies including the component administrations of the U.S. Department of Transportation, and other organizations and individuals interested in the development of transportation. **[www.TRB.org](http://www.trb.org)**

**[www.national-academies.org](http://www.national-academies.org)**

## SHRP 2 STAFF

**Ann M. Brach**, *Director*  
**Stephen J. Andrie**, *Deputy Director*  
**Neil J. Pedersen**, *Deputy Director, Implementation and Communications*  
**James Bryant**, *Senior Program Officer, Renewal*  
**Kenneth Campbell**, *Chief Program Officer, Safety*  
**JoAnn Coleman**, *Senior Program Assistant, Capacity and Reliability*  
**Eduardo Cusicanqui**, *Financial Officer*  
**Walter Diewald**, *Senior Program Officer, Safety*  
**Jerry DiMaggio**, *Implementation Coordinator*  
**Shantia Douglas**, *Senior Financial Assistant*  
**Charles Fay**, *Senior Program Officer, Safety*  
**Carol Ford**, *Senior Program Assistant, Renewal and Safety*  
**Elizabeth Forney**, *Assistant Editor*  
**Jo Allen Gause**, *Senior Program Officer, Capacity*  
**Rosalind Gomes**, *Accounting/Financial Assistant*  
**Abdelmenane Hedhli**, *Visiting Professional*  
**James Hedlund**, *Special Consultant, Safety Coordination*

**Alyssa Hernandez**, *Reports Coordinator*  
**Ralph Hessian**, *Special Consultant, Capacity and Reliability*  
**Andy Horosko**, *Special Consultant, Safety Field Data Collection*  
**William Hyman**, *Senior Program Officer, Reliability*  
**Michael Marazzi**, *Senior Editorial Assistant*  
**Linda Mason**, *Communications Officer*  
**Reena Mathews**, *Senior Program Officer, Capacity and Reliability*  
**Matthew Miller**, *Program Officer, Capacity and Reliability*  
**Michael Miller**, *Senior Program Assistant, Capacity and Reliability*  
**David Plazak**, *Senior Program Officer, Capacity*  
**Monica Starnes**, *Senior Program Officer, Renewal*  
**Charles Taylor**, *Special Consultant, Renewal*  
**Onno Tool**, *Visiting Professional*  
**Dean Trackman**, *Managing Editor*  
**Connie Woldu**, *Administrative Coordinator*  
**Patrick Zelinski**, *Communications/Media Associate*

## ACKNOWLEDGMENTS

This work was sponsored by the Federal Highway Administration in cooperation with the American Association of State Highway and Transportation Officials. It was conducted in the second Strategic Highway Research Program (SHRP 2), which is administered by the Transportation Research Board of the National Academies. The project was managed by Monica Starnes, Senior Program Officer for SHRP 2 Renewal.

The research reported herein was performed by the Center for Advanced Infrastructure and Transportation (CAIT) at Rutgers University (RU); the Center for Transportation Infrastructure Systems (CTIS) at The University of Texas at El Paso (UTEP); the Federal Institute for Materials Research and Testing (BAM), Germany; and Radar Systems International, Inc. (RSI). Rutgers University was the coordinator and contractor for this project. Dr. Nenad Gucunski, professor and chair of Civil and Environmental Engineering and director of CAIT's Infrastructure Condition Monitoring Program at RU, was the principal investigator. The other authors of this report are Dr. Soheil Nazarian, professor of Civil Engineering and director of CTIS at UTEP; Dr. Deren Yuan, research associate at CTIS at UTEP; Dr. Herbert Wiggenhauser, head of Non-Destructive Testing (NDT) in Civil Engineering at BAM; Dr. Alexander Taffe, leader of Combination and Automation of NDT of Buildings at BAM; Dr. Parisa Shokouhi, Alexander von Humboldt Research Fellow, hosted by BAM; and Doria Kutrubes, president of RSI. Arezoo Imani and Touraj Tayebi, graduate research assistants at RU, helped conduct the validation testing, data analysis, and web manual content preparation. Hoda Azari, a graduate research assistant, and Dr. Manuel Celaya, a research engineer at UTEP, assisted in the validation study as well. Hooman Parvardeh, research assistant at RU, helped build the reference database and develop the framework for the web manual, while Erica Erlanger, a research staff member at RU, edited the manuscript. Their contributions are gratefully acknowledged.

The research team also gratefully acknowledges contributions of the participants from industry and academia in the validation testing. The participants include NDT Corporation; Germann Instruments; Olson Engineering; Dr. Ralf Arndt, National Research Council associate at FHWA Turner-Fairbank Highway Research Center; Ingegneria Dei Sistemi S.p.A. (IDS), Italy; 3D-RADAR, Norway; Dr. John Popovics, University of Illinois at Urbana-Champaign; Dr. Jinying Zhu, The University of Texas at Austin; Rutgers University—Center for Advanced Infrastructure and Transportation; and The University of Texas at El Paso—Center for Transportation Infrastructure Systems. The contributions of these participants were critical for the evaluation and grading of the performance of NDT technologies.

## FOREWORD

Monica A. Starnes, PhD, *SHRP 2 Senior Program Officer, Renewal*

The extensive number of concrete bridge decks in poor structural conditions is one of the biggest problems affecting U.S. bridges. Highway agencies have an increased need to evaluate bridge deck condition in order to optimize the effective timing, scope, and approaches for preventive maintenance, repair, and replacement.

The difficulty is that bridge deck deterioration often takes place below the surface where it cannot be evaluated by visual means. Nondestructive testing (NDT) techniques have the potential of providing the needed information about the under-the-surface deteriorated condition of the deck.

---

Over the past few decades, new techniques and equipment have been developed that can provide high-speed testing potentially capable of being used for bridge deck condition assessment. These technologies, however, have not been widely accepted in part because of less than positive experiences that may have occurred from unrealistic expectations or improper use.

This research project has been carried out with the goal of offering an independent evaluation of the capabilities and limitations of the most common NDT techniques to detect and characterize typical deterioration mechanisms in concrete bridge decks. As designed, the independent evaluation depended on a participation of manufacturers of NDT equipment, service providers, research institutions, and consultants. All the participants were evaluated on the basis of the same series of tests, the same environmental factors, and the same performance metrics. As such, their individual performances were tested in an environment analogous to a rodeo.

The independent evaluation, or rodeo, was conducted in both laboratory and field conditions. Through this rodeo, the research team evaluated the NDT technologies from the perspective of speed, accuracy, precision, and ease of use. The information gathered from the tested technologies has been organized in an electronic repository called the NDToolbox.

Additional tasks were recently added to this project in order to expand the coverage of the NDToolbox. Once completed, the NDToolbox will include the results from all the NDT research projects studied under SHRP 2; thus the NDToolbox could serve as a quick reference of validated methods for identifying deterioration on concrete bridge decks, as well as methods for conducting quality control of construction materials and pavements and for assessing the condition of pavements and tunnels.

## CONTENTS

1	Executive Summary
5	<b>CHAPTER 1</b> Background
7	<b>CHAPTER 2</b> Common Defects of Concrete Bridge Decks
7	Common Deterioration Types in Bridge Decks
11	Overlay Debonding
12	<b>CHAPTER 3</b> Candidate Methods for Deterioration in Concrete Bridge Decks
12	Impact Echo
14	Ultrasonic Pulse Echo
16	Ultrasonic Surface Waves
18	Impulse Response
19	Ground-Penetrating Radar
21	Half-Cell Potential
22	Galvanostatic Pulse Measurement
24	Electrical Resistivity
25	Infrared Thermography
25	Chain Dragging and Hammer Sounding
29	<b>CHAPTER 4</b> Criteria and Methodology for Evaluating NDT Methods for Assessment of Bridge Decks
29	Performance Measures and Deterioration Types Selection
29	Description and Definition of Main Deterioration Types
30	Elements Constituting Performance Measures
32	Conclusions
34	<b>CHAPTER 5</b> Approach to Validation Testing
34	Field Validation Testing
36	Laboratory Validation Testing
48	<b>CHAPTER 6</b> Results and Discussion
48	Field Validation Testing
53	Laboratory Validation Testing: Fabricated Bridge Deck
60	Laboratory Validation Testing: Retrieved Bridge Deck
68	<b>CHAPTER 7</b> Evaluation and Ranking of NDT for Condition Assessment of Bridge Decks
68	Assessment of NDT Technologies
76	Summary Grades
78	<b>CHAPTER 8</b> Implementation of the Results from the Study
82	<b>CHAPTER 9</b> Summary, Conclusions, and Recommendations
84	References



# Executive Summary

Providing the means for the rapid, nondestructive, and accurate condition assessment and performance monitoring of bridge decks will significantly reduce the necessary resources and expenditures for bridge renewal. Aside from reducing the duration of traffic interruption during field operation, the more dense measurements yield a more accurate characterization of the condition of the bridge deck, a better prediction of the deterioration progression, and a better assessment of the rehabilitation needs. Such comprehensive and accurate assessments could also reduce the frequency of detailed regular and follow-up inspections. In addition, data collected from the nondestructive testing (NDT) of bridge decks should complement other information in our search to better understand life-cycle costs, deterioration mechanisms, and the effectiveness of preservation techniques at various stages of the aging process. Most important, the information gained should prevent the premature and unexpected failure of bridge decks.

The dominant practice used by state departments of transportation (DOTs) in the evaluation of bridge decks has been visual inspection and simple nondestructive methods such as chain dragging and hammer sounding. Modern NDT for concrete and concrete bridge decks exploits various physical phenomena (e.g., acoustic, seismic, electric, electromagnetic, and thermal) to detect and characterize specific deterioration processes or defects. In general, the objective of all NDT techniques is to learn about the characteristics of a given medium from its response to an applied excitation.

The ultimate goal of this research was to identify and describe the effective use of NDT technologies that can detect and characterize deterioration in bridge decks. To achieve this goal, the following four specific objectives needed to be accomplished:

1. Identifying and characterizing NDT technologies for the rapid condition assessment of concrete bridge decks;
2. Validating the strengths and limitations of applicable NDT technologies from the perspectives of accuracy, precision, ease of use, speed, and cost;
3. Recommending test procedures and protocols for the most effective application of the promising technologies; and
4. Synthesizing the information regarding the recommended technologies needed in an electronic repository for practitioners.

This report summarizes all the tasks conducted during the project. The first part concentrates on the elements related to the identification and selection of technologies included in the NDT technology validation tasks. This part provides a synthesis of the common concrete bridge deck deterioration types and the NDT technologies used to evaluate them. The methodology developed for the grading and ranking of NDT technologies is also presented. The second part concentrates on the tasks related to the validation of the promising NDT technologies. These tasks

are the plan for validation testing, including the selection of the test beds; the conduction of the validation testing; and the analysis of the results of the validation testing. The analyses of the information provided by the participants in the validation testing, and the associated efforts and costs, are also included in the second part. Finally, the third part concentrates on the formulation of the generic features of the NDT technologies for bridges and the development of an electronic repository for practitioners, a web-based tool named NDTtoolbox. All the research tasks were described in more detail in the project progress reports.

One of the early deliverables of the project was a comprehensive literature synthesis report on the deterioration processes in concrete decks and the most important NDT technologies for their detection. The synthesis concentrated on four groups of NDT technologies that use acoustic/seismic, electromagnetic, electrochemical, and thermal principles of operation. More traditional and commonly used techniques, such as visual inspection, chain dragging, hammer sounding, and chloride concentration measurements, were also described. The principle of operation and types of structural and material defects that can be detected and characterized with each technology were synthesized. The application and performance parameters—accuracy, precision, ease of use, speed, and cost—were also summarized. Clear information about the advantages and limitations of each technology was provided whenever available in the literature. The conclusion of this search was that a single technology cannot detect or provide information about all the deterioration processes and defects of interest. Also, it was obvious that the technologies significantly differ in terms of the ease of use, cost, level of expertise needed in data collection, analysis and interpretation, speed of data collection, and accuracy of the provided information. All of this provided a clear need and justification for this research study.

A methodology for categorizing and ranking the most promising NDT technologies was the first essential part in the development of the recommendations. Such a methodology was structured in a way so that information relating to (1) the value of the technology with respect to the detection of a particular deterioration type and (2) the overall value to an agency in bridge deck deterioration detection can be qualified. Technologies that could detect and characterize four deterioration types—corrosion, delamination, vertical cracking, and concrete degradation—were of interest in the grading and later selection for validation testing. The NDT technologies were evaluated from the perspective of five performance measures: accuracy, precision (repeatability), ease of use, speed, and cost. The methodology was first implemented to identify the most promising NDT technologies, based on the literature search. The ranking developed served as the basis for the solicitation of participants in the validation testing.

The validation testing and the follow-up analysis of the results were the most important and, at the same time, the most challenging parts of the project. The first step in the validation testing was identifying and planning the validation test beds. The validation test beds were identified, and the corresponding validation test plans were developed to enable an objective assessment of the previously defined performance measures. The first validation testing included an evaluation under controlled laboratory conditions. The controlled laboratory validation included a concrete slab with built-in defects and simulated deteriorations. In addition, a section of a deck removed from a highway bridge was used in the laboratory validation. The main foci of the laboratory validation were on the assessment of the accuracy and repeatability of the NDT technologies because broad ground truth information was available from cores and conducted autopsies. Field testing was supposed to enable the testing under actual, production-level conditions; therefore, the field validation testing concentrated on the evaluation of speed, ease of use, precision, and cost. It was expected that it would be possible to evaluate the accuracy of NDT technologies to a lesser extent because of limited ground truth information.

The field validation testing was first conducted in late October and early November of 2010 on a bridge over I-66 in Haymarket, Virginia, in coordination with the FHWA's Long-Term Bridge Performance (LTBP) Program. The LTBP Program evaluated the same bridge in 2009, which provided a wealth of information from preliminary evaluations, using destructive and non-destructive means, and assisted in identifying the most suitable area for the validation testing.

The testing area was about 1,000 ft<sup>2</sup>. A 2-ft by 2-ft grid was marked on the deck, identifying seven survey lines in the longitudinal bridge direction, with 43 test points along each line. The participants were required to take measurements and report results at all test points. They were also required to repeat the measurement along one of the survey lines.

The laboratory validation was conducted at a site near the main campus of the University of Texas at El Paso in early to mid-December 2010. Two test sections were prepared for the validation testing. The first test section was a newly fabricated concrete slab with simulated defects, and the other test section was a section of bridge along I-10 in El Paso demolished earlier in that year. The fabricated slab was 20 ft long, 8 ft wide, and about 8.5 in. thick and was supported by three 1.5-ft-wide prestressed girders. Delaminated areas of different sizes and depths of embedment, vertical cracks of different depths, and a corroded section were artificially created. The distressed highway bridge section consisted of a 9-ft by 14-ft arch-type concrete section. For the fabricated bridge section, the grid test points were 1 ft apart, while they were 1.5 ft apart for the actual bridge section. Altogether, 10 teams participated in the validation testing, five of them from industry, four from academia, and one from an agency. The ten technologies represented in the validation testing were ground-penetrating radar, impact echo, ultrasonic surface waves, impulse response, half-cell potential, electrical resistivity, galvanostatic pulse, infrared thermography, ultrasonic pulse echo, and chain dragging and hammer sounding. Some of the technologies were represented by multiple participants, each using a different system.

The results from the validation testing were analyzed to evaluate the performance of the participating NDT technologies with respect to the five performance measures: accuracy, precision, ease of use, speed, and cost. Grades used in the evaluation of technologies varied between 1 and 5, where 5 was used for excellent and 1 for poor performance. The accuracy was in most cases obtained from the percent of test points where the technology provided an accurate assessment. The precision, or repeatability, of technologies was examined through the coefficient of variance of the submitted results from triplicate tests during both field and laboratory testing. The challenge in making an objective comparison among technologies and participants was that the repeatability results provided were for different levels of data analysis and interpretation and, in some cases, only graphical presentations of raw data. The speed of NDT technologies was evaluated with respect to the data collection and data analysis and interpretation. The data collection speed grades were assigned on the basis of the actual time measurements of the field surveys. The data analysis and interpretation speed were graded on the basis of information provided by the participants regarding time needed. Similarly, the ease of use of technologies was evaluated. The data collection ease-of-use grade was defined on the basis of the observed, or perceived, physical effort and level of expertise needed to accomplish the task. The data analysis and interpretation ease-of-use grading, however, relied on the provided information and perceived conclusions regarding the expertise needed to successfully accomplish the task. Finally, the cost was defined and graded on the basis of the information provided by the participants.

The following conclusions were drawn regarding the performance and overall value of the examined NDT technologies for concrete bridge deck deterioration detection:

1. For each of the main deterioration types, there are technologies that have demonstrated a fair-to-good potential for detection. However, there is not a single technology that has shown potential for evaluating all deterioration types.
2. Four technologies were identified as having a fair-to-good potential for delamination detection and characterization. Those are impact echo, chain dragging and hammer sounding, infrared thermography, and ground-penetrating radar.
3. Four technologies were identified as having a fair-to-good potential for corrosion detection or characterization of a corrosive environment. Those include half-cell potential, electrical resistivity, galvanostatic pulse measurement, and ground-penetrating radar.
4. Only one technology, surface wave testing, was validated as a fair technology in the vertical crack characterization.

**4**

5. Only one technology, ultrasonic surface waves, was validated as having a good potential in concrete deterioration detection and characterization.
6. The top technologies, based on their overall value in detecting and characterizing deterioration in concrete decks, include ground-penetrating radar, impact echo, and ultrasonic surface waves. However, the ultimate decision on which equipment to acquire and which technology to use will primarily depend on (1) the type of deterioration that is of the highest concern to the agency and (2) whether the evaluation is being done for network-level condition monitoring or for project-level maintenance or rehabilitation.
7. The overall value and ranking were to some extent influenced by the selected performance measures and by the applied weights and significance factors in the grading process.

Finally, an electronic repository of NDT technologies for bridge decks that targets practitioners was developed as the ultimate goal of SHRP 2 Renewal Project R06A. The electronic repository or NDToolbox is a web-based open-source database system that allows users to easily navigate through the content and find the information they seek. The NDToolbox primarily allows a user to explore different NDT technologies and examine their use in the deterioration detection. The NDT technology information includes a description of the technology, physical principle behind it, applications, performance, limitations, equipment, test procedures and protocols, and sample results. The NDToolbox also provides recommendations regarding the best technologies for a particular deterioration detection application.

## CHAPTER 1

# Background

Society is more dependent than ever on transportation for its economic vitality and quality of life. Highways are the foremost of all transportation modes. As our dependency on infrastructure is growing, the engineered components of transportation infrastructure are aging, deteriorating, and exhausting their capacity to meet the ever-expanding operational demands. Ensuring operational and structural safety and security of the transportation infrastructure represents a paramount task that requires a fundamental change in the way we plan, design, build, and operate our transportation infrastructure. This task can only be effectively addressed through broad political and public support and the integration of talents in diverse areas. These areas are financing, planning, asset management, design, construction, materials, inspection, and so forth.

With this broad challenge identified, the second Strategic Highway Research Program (SHRP 2) has gathered and deployed the intellectual, experiential, and financial resources necessary to answer the questions about highway safety, renewal, travel-time reliability, and capacity. Methods must be identified to rapidly rebuild the infrastructure system with long-lasting facilities. Renewal of our highway system has become especially challenging because much of the aging infrastructure is in heavily congested highway corridors. Therefore, minimizing traffic disruptions during highway renewal projects is a paramount goal. In addition, developing and implementing the means for the rapid and accurate inspection and performance monitoring of highways is of the essence, in order for the safety and durability experiences of the past to be avoided.

Bridges can and should be treated as critical nodes in the greater highway system. Developing and implementing the means for rapid rebuilding, quick and reliable inspection, and performance monitoring are even more critical than for most other components of the transportation network. This is especially true for bridge decks. They deteriorate faster than other bridge components and their inspection and rehabilita-

tion require traffic interruption. Providing the means for their rapid and accurate condition assessment and performance monitoring will lead to (1) more effective decision making, (2) better allocation of financial resources to renew and rehabilitate bridge decks, and (3) reduced frequency and duration of traffic interruption caused by slow and ineffective inspection and monitoring procedures.

Nondestructive testing (NDT) and nondestructive evaluation (NDE) provide engineers and bridge owners with the ability to rapidly and effectively inspect and monitor our aging infrastructure. Data collected from the NDT of bridge decks can complement other information in the search for a better understanding of their life-cycle costs and deterioration mechanisms. Also, NDT can evaluate the effectiveness of preservation techniques at various stages of the aging process, and, most important, it can prevent the premature and unexpected failure of bridge decks.

The ultimate goal of this project is to develop documents and resources that will motivate and enable transportation agencies to incorporate bridge deck NDT and NDE techniques into their inspection procedures and doctrine. Achieving this goal will ultimately contribute to the broader goals of the SHRP 2 Renewal Program, which is creating a reliable and optimum bridge asset management system by transportation agencies (Figure 1.1).

To accomplish the project goals, the overall work was divided into several main activities. The work was initiated with a thorough literature search of the main deterioration types in bridge decks and NDT technologies available or under development for their detection. The literature search resulted in the retrieval of more than 1,000 reference materials. The promising technologies were categorized, graded, and ranked from the perspectives of speed, accuracy, precision, ease of use, and other performance parameters of importance for bridge deck evaluation. The ranking of NDT technologies was the basis for their inclusion in the validation testing and evaluation of their generic features.

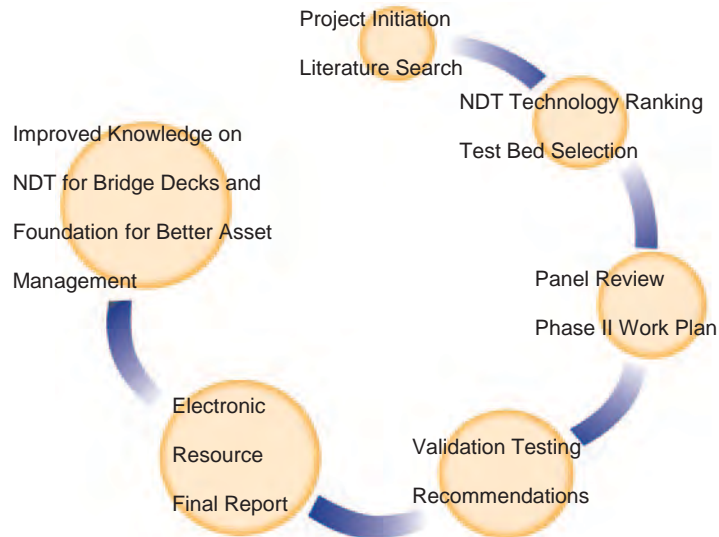


**Figure 1.1. Project contribution to longer-lasting and more economically managed bridges.**

To independently evaluate the performance of each of these technologies in detecting bridge deck deterioration, a validation program was designed and conducted in two phases: the laboratory and field validation testing. The laboratory validation testing provided a controlled environment in which the specimen deterioration and defect parameters were known in advance and could be controlled. The performance factors of highest importance during the laboratory validation were the technologies' accuracy and precision. The field validation enabled testing under actual, production-level conditions. Therefore, the parameters of highest importance in the field validation were the speed of data collection and analysis, ease of use, precision, and cost. A number of teams from industry and academia participated in the validation testing and demonstrated the application and performance of NDT technologies. Several technologies were implemented by multiple participants.

The analysis of the performance of NDT technologies was done on the basis of the results of the validation testing and records made by the project team. The technologies were compared with respect to the detection of a particular deterioration type. In the case in which a technology was represented by multiple participants, that technology was also evaluated to identify the best practices in data collection, and data analysis and interpretation. The results of these analyses were the bases for the identification of generic features of the NDT technologies and the development of recommendations for their practical

implementation. Finally, the information obtained about the technologies from the literature search and the performance from the validation testing was synthesized in an electronic repository on NDT technologies for bridge deck deterioration.

The organization of the report is as follows. The common deterioration types and consequential defects in concrete bridge decks are discussed in Chapter 2. The many forms of deterioration of highest importance have been summarized into four general deterioration and defect types: (1) reinforcement corrosion, (2) delamination, (3) vertical cracking, and (4) concrete degradation. Chapter 3 provides a discussion regarding the most promising NDT technologies for the evaluation of concrete decks. A summary of the criteria and methodology used to evaluate the NDT techniques is provided in Chapter 4. Selection of the test beds for validation testing and activities related to the field and laboratory validation testing are described in Chapter 5. Chapter 6 focuses on the analysis and presentation of the results from the laboratory and field validation testing. The results are primarily categorized based on the ability of a given technique to detect a certain deterioration type. The grading and ranking of the technologies from the perspectives of speed, accuracy, precision, ease of use, and cost are described in Chapter 7. Chapter 8 describes the electronic repository, the NDTtoolbox, developed for practitioners as one of the major products of SHRP 2 Renewal Project R06A. Finally, concluding remarks and recommendations for future work are presented in Chapter 9.

## CHAPTER 2

# Common Defects of Concrete Bridge Decks

Reinforced concrete structures such as bridge decks and pillars, highways, and other infrastructure facilities experience loss of integrity over time because of poor initial quality, damage from deicing salts, overloading, freeze–thaw cycle-induced stresses, fatigue, and, above all, corrosion of rebars (Figure 2.1). According to the Federal Highway Administration (FHWA), the cost of repairing and replacing deteriorating highway bridges in the United States is approximately \$100 billion (Lemieux et al. 2005; El-Safty 2008). The different kinds of deterioration observed in reinforced concrete structures are outlined in the following sections. The most frequent deterioration phenomena identified by Bien et al. (2007) are the following items:

- Corrosion;
- Carbonation;
- Alkali-silica reaction;
- Crystallization;
- Leaching;
- Oil and fat influence;
- Salt and acid actions;
- Creep;
- Fatigue;
- Influence of high temperature;
- Modification of founding conditions;
- Overloading;
- Shrinkage; and
- Water penetration.

### Common Deterioration Types in Bridge Decks

The deterioration of steel-reinforced concrete structures can be caused by the corrosion of steel or degradation of concrete. These deterioration processes are complex and often prompt one another. Among all the deterioration phenomena listed above, four deterioration mechanisms are of the

highest concern to bridge engineers and are the focus of this project. Those include the following:

- Rebar corrosion;
- Deck delamination;
- Vertical cracking; and
- Concrete degradation.

Each of the deterioration mechanisms is briefly discussed in the following sections.

### Rebar Corrosion

Reinforcing steel embedded in concrete is naturally protected from corrosion by the high alkalinity of the cement-based materials and an adequately thick concrete cover. High alkalinity can cause the formation of a passive and noncorroding protective oxide film on the steel surface. ACI 222R-01 (2001), which was reapproved in 2010, describes the process of metal corrosion in concrete. During this process, concrete allows electrolytic conduction and the flow of ions from anodes to cathodes. Once the oxide film is destroyed, an electric cell is formed along the steel or between steel bars, and the electrochemical process or corrosion begins. Some areas along the bar become anodes discharging current in the electric cell, and iron goes into the solution with oxygen. Other steel areas receive current resulting in the formation of hydroxide ions known as cathodes. A major contributor to this problem is chloride diffusion. Chlorides are derived primarily from the application of roadway deicing salts. Corrosion of steel reinforcement in a bridge deck can directly reduce the structural capacity of the deck. Furthermore, the corrosion process can cause internal stresses, cracking, delamination or surface fracture planes, and eventually spalling in concrete at, or just above, the level of the reinforcement (Figures 2.2 and 2.3).

The two most common steel corrosion processes are chloride-induced pitting corrosion and carbonation. Bridge



**Figure 2.1. Deck deterioration.**

engineers can often visually distinguish the two corrosion types. The locally confined, chloride-induced pitting corrosion leaves blackish rust marks, whereas red or brownish rust stains indicate carbonation-based corrosion. The rate of corrosion is dependent on numerous factors, including the composition of the metal, as well as humidity, temperature, water pH, and exposure to pollution and salt. Wet and dry cycles accelerate the corrosion process. Studies have shown that the corrosion rate is highest during the spring season and lowest during the winter. These rates can vary by a factor of about four or five during the year (Smith and Virmani 1996; Page et al. 1996).

### Deck Delamination

Delamination or horizontal cracking caused by corrosion of embedded reinforcing steel is a serious form of deterioration in concrete bridge decks. Reinforcing steel expands as it

corrodes. Such expansion may create a crack or subsurface fracture plane in the concrete at or just above the level of the reinforcement, as illustrated in Figure 2.4. Delamination may be localized or may extend over a substantial area, especially if the concrete cover is thin. It is possible that in a given area, delamination can occur along different planes between the concrete surface and the reinforcing steel. Delamination is not visible on the concrete surface; however, if repairs are not made in a timely fashion, the delamination progresses to open spalls. With continued corrosion, this process will eventually affect the structural integrity of the deck.

### Vertical Cracking

In addition to rebar corrosion, many other factors can cause cracking in bridge decks. These factors include plastic shrinkage, hydration heat, ambient temperatures, geometric constraint as the deck concrete cures, traffic load, and freeze–thaw

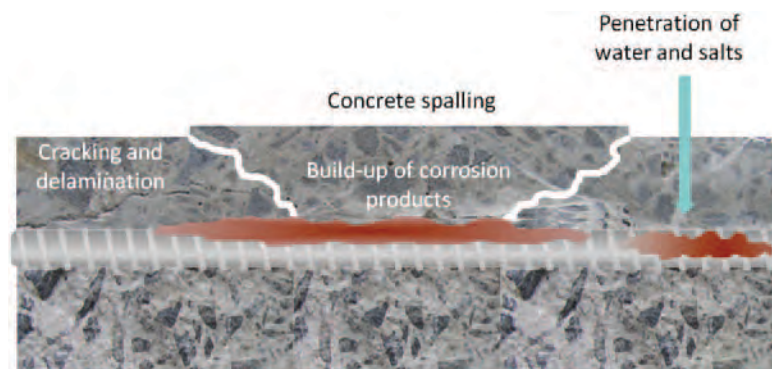


**Figure 2.2. Corrosion process.**





**Figure 2.3.** Corroded rebar in an excavated deck (top) and extracted core (bottom left), and delamination in a drill hole in a deck (bottom right).



**Figure 2.4.** Delamination observed in extracted cores.

cycles. The progression of rebar corrosion can further exaggerate these cracks. Vertically oriented cracks and load-related cracks will be the primary focus of the validation testing.

### Concrete Deterioration

A reduction in concrete strength or modulus is considered to be a form of concrete degradation. It may be the result of microcracking and macrocracking and other phenomena, such as alkali–silica reaction (ASR), delayed ettringite formation (DEF), plastic shrinkage, and freeze–thaw cycles. Each of the phenomena is briefly described in the following paragraphs.

*The alkali–silica reaction* is a reaction between reactive silica phases in aggregates and alkali hydroxides in the concrete pore solution. This reaction produces a silica gel that swells in the presence of water, causing internal and external cracking. The expansion of concrete resulting from ASR can cause two main problems: (1) the deformation of the structure, thereby impairing the serviceability, and (2) the development of a crack network through the structure (Figure 2.5).

*Delayed ettringite formation* is perceived as a form of internal sulfate attack. DEF is believed to be a result of improper heat curing of the concrete where the normal ettringite formation is suppressed. The highly concentrated sulfate in the pore



(a)



(b)

Source: ASR photograph courtesy of Dr. Moon Won, Texas Tech University. DEF damage photograph courtesy of Texas Department of Transportation Bridge Division.

**Figure 2.5. (a) ASR and (b) DEF damage.**

liquid may eventually react with calcium- and aluminum-containing phases of the cement paste to form the hydrated calcium sulfoaluminate mineral, ettringite. The formation of ettringite causes the concrete to expand, and empty cracks (gaps) may form around aggregates (see Figure 2.5)

*Plastic shrinkage (volume reduction)* can cause cracks in concrete. These cracks often occur on plane structures such as deck slabs, with no preferential crack orientation.

*Freeze–thaw* can increase the hydraulic pressure in concrete. The concrete will rupture once the pressure exceeds the tensile strength of the concrete. The exposure of concrete to repeated freeze–thaw cycles will ultimately cause extensive deterioration in the form of cracking, scaling, or crumbling.

## Overlay Debonding

Some old bridge decks are overlaid with asphalt concrete or portland cement concrete (PCC). In such bridge decks, the overlay can debond from the existing concrete decks. Once an overlay debonds, moisture and chlorides may enter the debonded region, further promoting deterioration. If repairs are not made, debonded overlay regions can eventually deteriorate into open spalls, which affect the ride quality of the deck and compromise the structural integrity of the deck. Furthermore, bonded and debonded overlays contribute to the complexity of the analysis of NDT methods and may impede their effectiveness.

## CHAPTER 3

# Candidate Methods for Deterioration in Concrete Bridge Decks

The literature review provided a number of NDT technologies that have the potential to detect and characterize deterioration in concrete bridge decks. The following 14 techniques were considered for grading and ranking on the basis of the literature search and possible inclusion in the validation testing program:

- Impact echo;
- Ultrasonic pulse echo;
- Ultrasonic surface waves;
- Impulse response;
- Ground-penetrating radar;
- Microwave moisture technique;
- Eddy current;
- Half-cell potential;
- Galvanostatic pulse measurement;
- Electrical resistivity;
- Infrared thermography;
- Visual inspection;
- Chain dragging and hammer sounding; and
- Chloride concentration measurement.

The following sections provide brief descriptions of the principle of operation and applications of each technology with respect to concrete deck deterioration detection. Advantages and limitations of the technologies according to the literature search are also described. The advantages and limitations of these technologies were not explicitly stated in most materials reviewed. In those cases, they are defined on the basis of the review of the reported results and reported or perceived technology performance. Because none of the participants in the validation tests used microwave moisture, eddy current, and chloride concentration measurement devices, these three techniques are not described or included in the final evaluation. Visual inspection is not described either, since it was not included in the validation testing.

## Impact Echo

### Description

The impact echo (IE) method is a seismic or stress wave–based method used in the detection of defects in concrete, primarily delaminations (Sansalone and Carino 1989). The objective of the IE survey is to detect and characterize wave reflectors or “resonators” in a concrete bridge deck, or other structural elements. This is achieved by striking the surface of the tested object and measuring the response at a nearby location. Simple or automated devices, such as those shown in Figure 3.1, can be used for this purpose.

### Physical Principle

The operation of the IE method is illustrated in Figure 3.2. The surface of the deck is struck by various means, such as wire-mounted steel balls, automated projectile sources, or solenoid-type impactors. The response is measured by a nearby contact or air-coupled sensor. The position of the reflectors is obtained from the frequency spectrum of the deck’s response to an impact. In a more rigorous sense, the response is related to the first symmetrical Lamb wave mode in the deck structure. The frequency of the reflection, called the “return frequency,” can be identified in the response spectrum of the recorded signal. The depth of the reflector can be obtained from the return frequency,  $f_T$  or  $f_p$ , and the measured or estimated compression-wave velocity of concrete,  $V_p$ , using the simple relationship shown in Figure 3.2. Because strong reflectors will be generated at all interfaces where there is a contrast in acoustic impedances of materials, such as the one between concrete and air, delaminated areas are typically recognized as shallow reflectors. In the case of a sound deck, the dominant reflector will be from the bottom of the deck, another concrete–air interface. Other reflectors may include voids, tendons, supporting structural elements, and so forth, and responses from various defects (initial delamination or cracking).



Figure 3.1. Stepper (left) and bridge deck scanner (right).

Different authors interpret the severity of the delamination in a given deck with the IE method in various ways. One of the ways used in this study is shown in Figure 3.2. A test point is described as intact if the dominant return frequency corresponds to the bottom of the deck. A delaminated point in the deck will theoretically demonstrate a shift in the return frequency toward higher values because the wave reflections occur at shallower depths. Depending on the extent and continuity of the delamination, the partitioning of the wave energy reflected from the bottom of the deck and the delamination may vary.

The initial or incipient delamination, described as occasional separation within the depth of the slab, can be identified through the presence of return frequencies associated with the reflections from both the bottom of the deck and the delamination. Progressed delamination is characterized by a single peak at a frequency corresponding to the depth of the delamination. Finally, in cases of wide or shallow delaminations, the dominant response of the deck to an impact is characterized by a low-frequency response of flexural-mode oscillations of the upper delaminated portion of the deck. This response is almost always

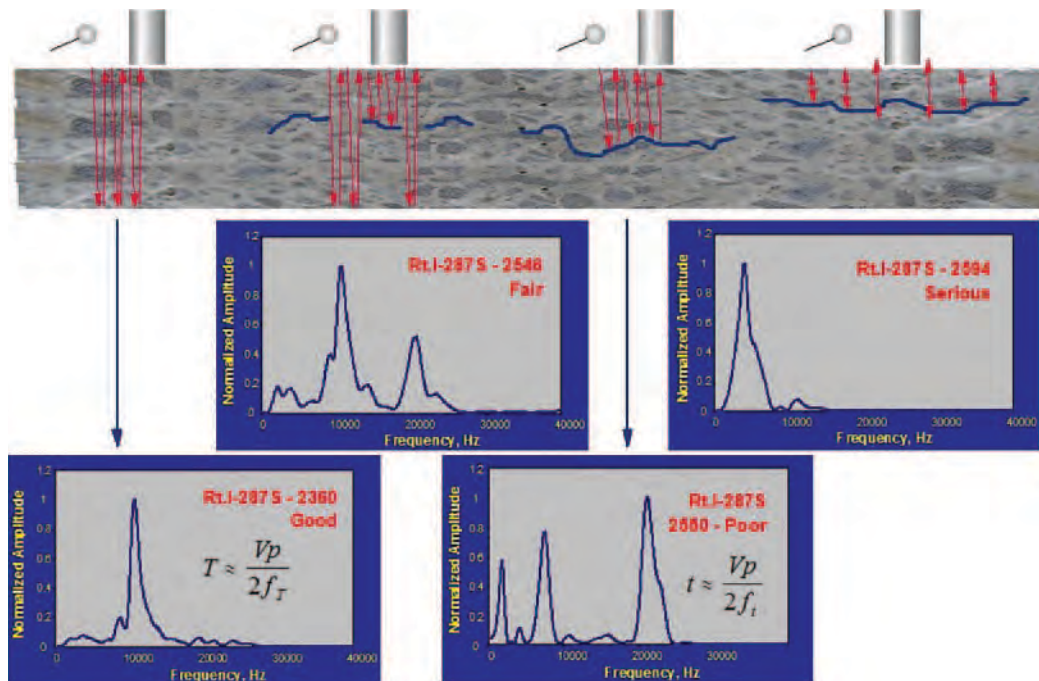


Figure 3.2. Grades for various degrees of deck delamination.

in the audible frequency range, unlike responses from the deck with incipient delamination that may exist only in the higher-frequency ranges (Gucunski et al. 2006; Cheng and Sansalone 1995; Lin and Sansalone 1996).

### Applications

The applications of IE can be divided into four general categories as follows:

- Condition assessment of reinforced concrete elements with respect to delamination;
- Characterization of surface-opening cracks (vertical cracks in bridge decks);
- Detection of ducts, voids in ducts, and rebars; and
- Material characterization.

The IE technique is primarily used to detect and characterize delaminations with respect to its horizontal and vertical position and its stage of development. The method has also been used with some success for the characterization of the depth and primary direction of surface-opening cracks and in the detection of rebars and ducts in cases in which the diameter-to-concrete cover ratio is above a certain threshold (roughly one-third). The detection of rebars and ducts requires a scanning approach and usually a higher level of expertise. It should be noted that, although the horizontal position of a rebar or duct can be defined, it is difficult to accurately define the concrete cover thickness. The IE method has also been used to evaluate concrete modulus and estimate concrete compressive strength. Other applications of the method include the characterization of grouting in tendon ducts and overlay debonding detection on decks with overlays.

### Limitations

The IE method can detect delaminations on decks with PCC overlays. However, on decks with asphalt concrete overlays,

detection is possible only when the asphalt concrete temperature is sufficiently low, so that the material is not highly viscous, or when the overlay is intimately bonded to the deck. It is necessary to conduct data collection on a very dense test grid to accurately define the boundaries of the delaminated areas. In the rare cases of impact echo testing on bridge decks near the deck edges, boundary effects should be taken into consideration. Such boundary conditions will produce reflections that will interfere with the sought signal. The boundary interference problem is more common during IE testing on other structural elements of limited dimensions (such as girders, piers, and pier caps) than on bridge decks.

## Ultrasonic Pulse Echo

### Description

Ultrasonic pulse echo (UPE) is a method that uses ultrasonic (acoustic) stress waves to detect objects, interfaces, and anomalies. The waves are generated by exciting a piezoelectric material with a short-burst, high-amplitude pulse that has high voltage and current. Civil engineering applications, for reinforced concrete structures in particular, were realized only in the recent past because of two reasons. First, traditional ultrasonic testing would lead to high scattering and attenuation of the transmitted pulses, mainly because of the very heterogeneous nature of concrete. Second, the transducers (ultrasonic probes) had to be coupled to the surface of the tested element using grease or wax. To overcome scattering problems, low-frequency transducers have been introduced, of a center frequency between 50 and 200 kHz that can be dry-coupled.

A dry-point contact, ultrasonic transducer unit consisting of 24 probes is shown in Figure 3.3 (left). Twelve probes in the

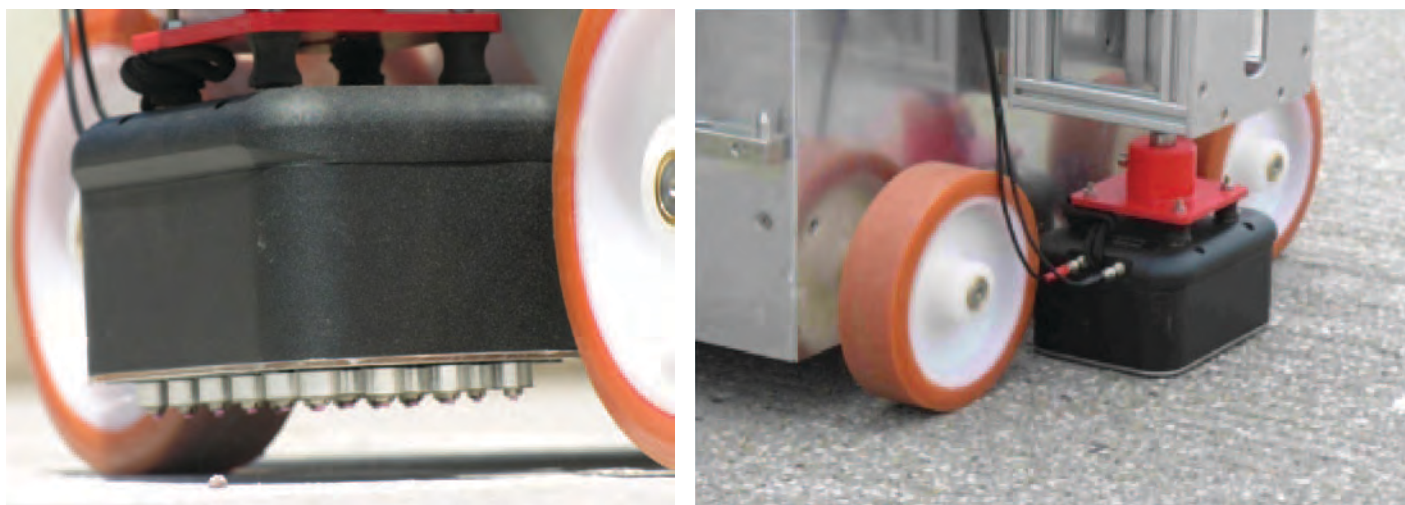


**Figure 3.3.** Shear-wave probe array A1220 (left), and automated A1220 measurements using stepper (right).

array act as pulsers, while the other 12 act as receivers. Depending on the transducer unit, these probes can emit both compressional and shear waves. The UPE test can also be performed by mounting the probe on an automatic device, like the one shown in Figure 3.3 (right).

### Physical Principle

A UPE test concentrates on measuring the transit time of ultrasonic waves traveling through a material and being reflected to the surface of the tested medium. Based on the transit time or velocity, this technique can also be used to indirectly detect the presence of internal flaws, such as cracking, voids, delamination or horizontal cracking, or other damages. An ultrasonic wave is generated by a piezoelectric element. As the wave interfaces with a defect, a small part of the emitted energy is reflected back to the surface. Defects, in this case, are identified as any anomaly of acoustical impedance different from the concrete element tested. The wave is then detected by a second piezoelectric element. In regions where there is significant deterioration

or microcracking, concrete will have a noticeably lower velocity compared with concrete in intact regions. A UPE B-scan (vertical cross section) of a deck along two survey lines is illustrated in Figure 3.4, using an ultrasonic system A1040 MIRA with almost real-time synthetic aperture focusing technique, or SAFT (Kozlov et al. 2006; Bishko et al. 2008; Gebhardt et al. 2006).

### Applications

Ultrasonic pulse echo surveys have been used for thickness measurements on objects with only one-sided access. The UPE is capable of assessing defects in concrete elements, debonding of reinforcement bars, shallow cracking, and delamination. The UPE was also successfully used in the detection of material interfaces, based on phase evaluations of the response. Examples include the interfaces between concrete and steel (e.g., reinforcement) or concrete and air (e.g., grouting defects) (Taffe and Wiggenhauser 2006; Afshari et al. 1996; Krause et al. 2008; Hevin et al. 1998).

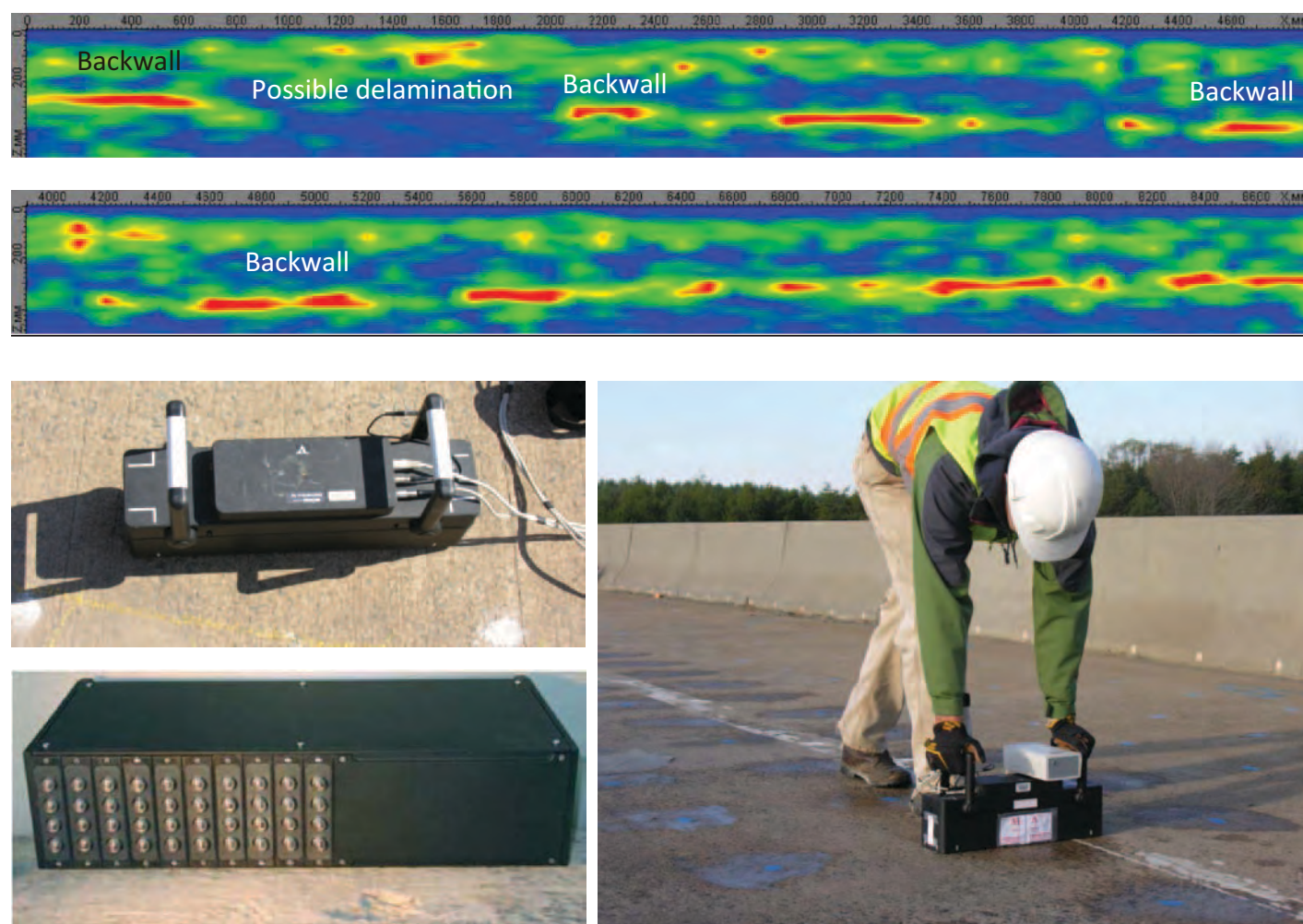


**Figure 3.4.** Bridge deck survey using MIRA ultrasonic system. B-scans (top) and equipment and data collection (bottom).

## Limitations

Ultrasonic pulse echo surveys require very close spacing between test points to develop images of the tested medium, making it time-consuming. The data quality depends strongly on the coupling of the sensor unit, which may be difficult on rough surfaces. Very shallow flaws may remain undetected because the surface waves mask the needed compressional or shear-wave signals. Also, as UPE works with lower frequencies, some of the defects might remain undetected.

## Ultrasonic Surface Waves

### Description

The ultrasonic surface waves (USW) technique is an offshoot of the spectral analysis of surface waves (SASW) method used to evaluate material properties (elastic moduli) in the near-surface zone. The SASW uses the phenomenon of surface wave dispersion (i.e., velocity of propagation as a function of frequency and wavelength, in layered systems to obtain the

information about layer thickness and elastic moduli). The USW test is identical to the SASW test, except that the frequency range of interest is limited to a narrow high-frequency range in which the surface wave penetration depth does not exceed the thickness of the tested object. In cases of relatively homogeneous materials, the velocity of the surface wave (phase velocity) does not vary significantly with frequency. The surface wave velocity can be precisely related to the material modulus, or concrete modulus in the case of bridge decks, using either the measured or assumed mass density, or Poisson ratio of the material. A USW test consists of recording the response of the deck, at two receiver locations, to an impact on the surface of the deck, as illustrated later in Figure 3.7. One of the devices that can be used for that purpose is shown in Figure 3.5.

### Physical Principle

Surface waves are elastic waves that travel along the free surface of a medium. They carry a predominant part of the energy on the surface, in comparison to body (compressive and shear)



**Figure 3.5.** USW testing using a portable seismic property analyzer (PSPA).



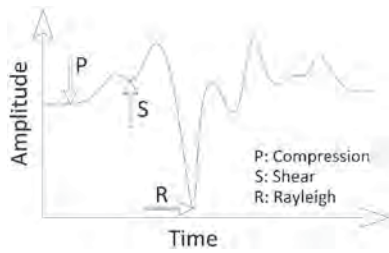


**Figure 3.6. Typical time record used in surface wave method.**

waves. This is illustrated in Figure 3.6, where the arrival of the surface (Rayleigh) wave follows the arrival of the two body-wave components because it is the slowest one (Nazarian et al. 1993; Stokoe et al. 1994; Yuan et al. 1999).

The surface waves propagate radially from the impact source, forming a cylindrical front with a velocity dependent on the elastic properties of the medium. The waves propagating in a heterogeneous medium are dispersive; that is, waves of different

wavelengths or frequencies travel with different velocities. Thus, information about the subsurface can be obtained through the measurement of the phase velocity versus frequency relationship, termed dispersion curve, and backcalculation of the dispersion curve to obtain the profile of the tested system. Unlike many seismic methods that base evaluation on the detection and measurement of first wave arrivals, the USW velocity evaluation is based on the spectral analysis of the recorded signal.

The body of a surface wave extends to the depth of approximately one wavelength. Therefore, if the measurement is limited to wavelengths not exceeding the thickness of the deck, the velocity of the surface waves will depend only on the concrete modulus. As sketched in Figure 3.7 for a two-layer half-space, at wavelengths less than or equal to the thickness of the layer, the velocity of the surface wave is more or less independent of wavelength. For the same reason, in the case of a sound and homogeneous deck, the velocity of the surface waves will show little variability. An average velocity is used to correlate it to the concrete modulus. Significant variation in the phase velocity will be

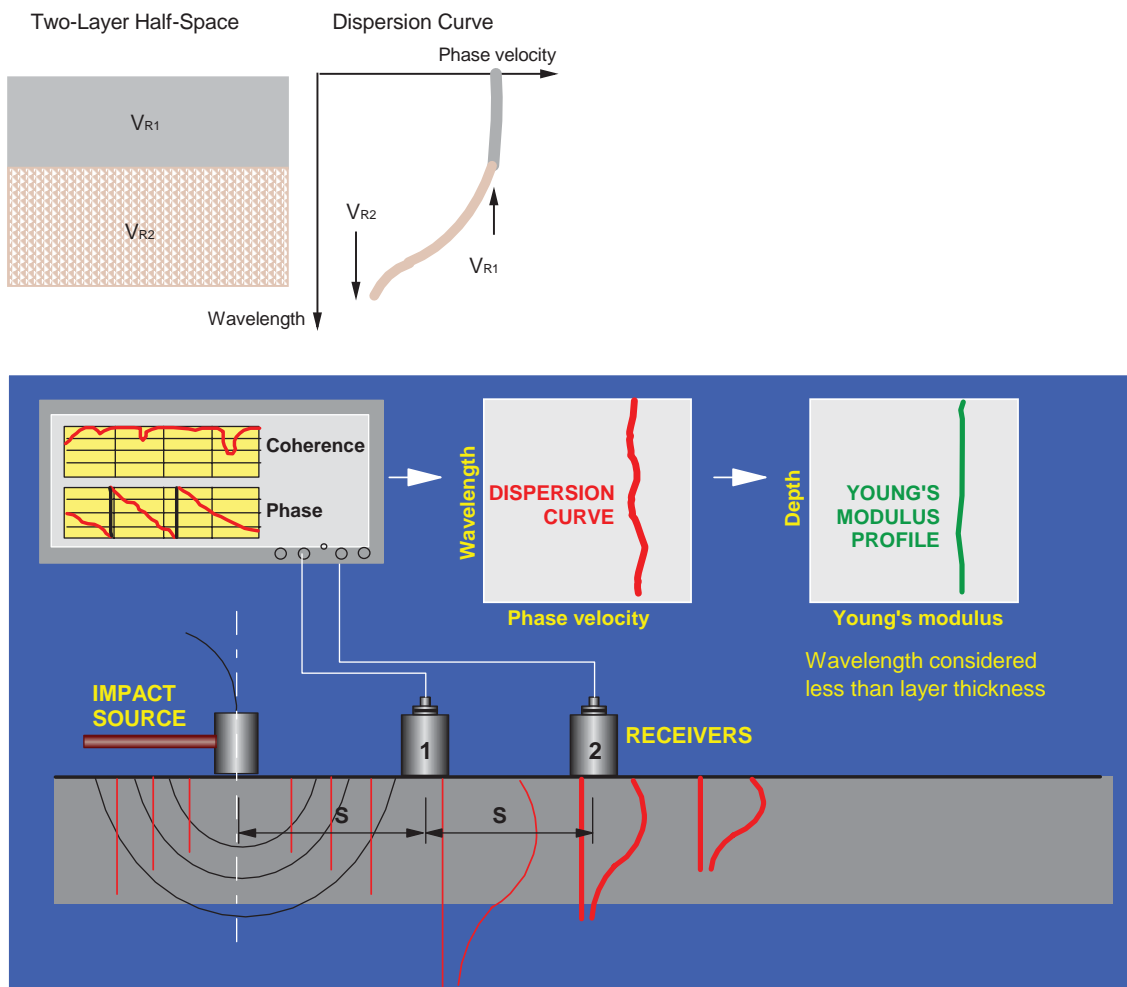


**Figure 3.7. Schematic of surface wave velocity versus wavelength (top) and evaluation of a layer modulus by SASW (USW) method (bottom).**

an indication of the presence of a delamination or other anomaly. A schematic of the USW (SASW) test is shown in Figure 3.7.

Elastic waves are generated by means of impacts (e.g., steel balls, automated projectile sources, solenoid-type impactors) detected by a pair or an array of receivers and recorded by a transient recorder.

## Applications

The USW is used in condition assessment for the purpose of evaluating probable material damage from various causes: ASR, DEF, freeze–thaw, and other deterioration processes. It is also used in material quality control and quality assurance of concrete and hot-mix asphalt, primarily to evaluate material modulus and strength, the second one using correlations with modulus. One of the USW’s applications is the measurement of the depth of vertical (surface) cracks in bridge decks or other elements. Finally, some results point to the USW’s ability to indirectly detect delaminations in bridge decks.

## Limitations

On deteriorated sections of a concrete deck, such as debonded or delaminated sections, the USW method cannot provide reliable modulus values. It can play only a supplemental role in deterioration detection, and experience is required for understanding and interpreting test results. The USW (SASW) modulus evaluation becomes significantly more complicated for layered systems, such as decks with asphalt concrete overlays, where the moduli of two or more layers differ significantly.

## Impulse Response

### Description

The impulse response method, also known as the transient dynamic or mechanical impedance method, is a nondestructive testing method that has been mostly used in quality control and condition assessment of pavements and deep foundations (Figure 3.8). The method was first developed in France in the late 1970s as an extension of a vibration test, used in the quality control of drilled shafts. Since then, the impulse response method has been used to determine the subgrade modulus and presence of voids or loss of support below rigid pavements, concrete tunnel linings and slabs, and in reinforced concrete bridges. The method was recently introduced as a screening tool for bridge decks, slabs, and tunnel linings for the detection of potentially damaged areas. The objective of the test is to measure the dynamic response of the element tested, often described in terms of the mobility or flexibility spectrum, in order to detect areas where the



**Figure 3.8. Impulse response testing.**

spectrum takes shapes and amplitudes significantly different from those at sound locations (Nazarian et al. 1993, 1994; Gucunski and Jackson, 2001; Jackson and Gucunski, 2002; Davis et al. 2001).

### Physical Principle

The impulse response method is a dynamic response method that evaluates the dynamic characteristics of a structural element to a given impulse. The typical frequency range of interest in impulse response testing is 0 to 1 kHz. The basic operation of an impulse response test is to apply an impact with an instrumented hammer on the surface of the tested element and to measure the dynamic response at a nearby location using a geophone or accelerometer.

The basic principle of impulse response is illustrated in Figure 3.9. The signal from the impact hammer sensor, the forcing function, and the response at the nearby displacement transducer, geophone (velocity transducer), or accelerometer are transformed into the frequency domain to obtain the corresponding spectra. The ratio of the displacement and impact spectra represents a flexibility spectrum, in the case of the measured displacement. The inverse ratio is termed *mechanical impedance* (dynamic stiffness spectrum). In some analyses, the flexibility spectrum is matched by a flexibility spectrum (response spectrum) for an assumed single-degree-of-freedom (SDOF) system. Once the two spectra are matched, the modal properties of the SDOF system provide information about the stiffness and damping properties of the system. The underlying assumption of this process is that a structure’s response can be approximated by the response of an SDOF system. If the measured response is velocity, the ratio of the velocity and impact spectra is termed *mobility spectrum*.

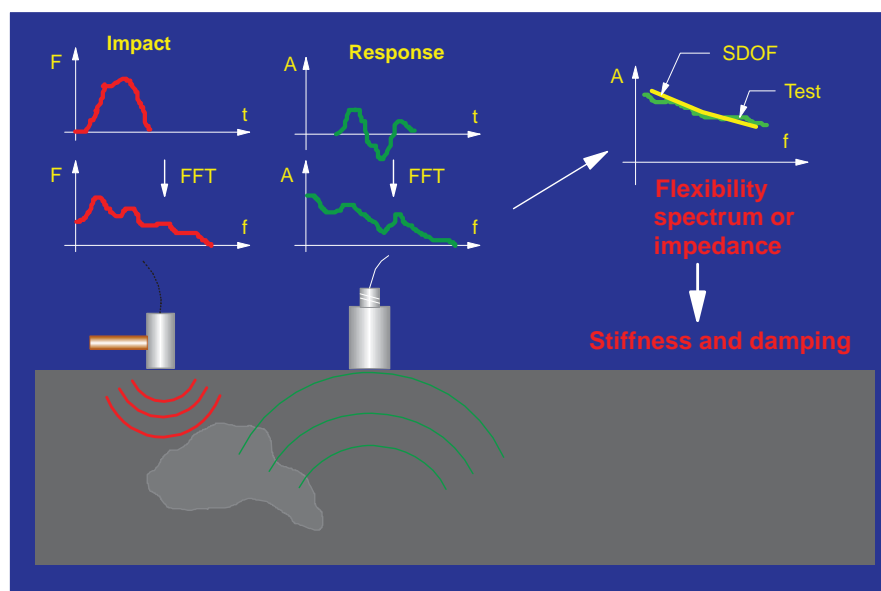


**Figure 3.9. Principle of impulse response testing.**

Even though the concept behind impulse response and impact echo is similar, there are significant differences in bridge deck testing. Impact echo is based on the excitation of particular wave propagation modes above the probable anomalies within the deck or between the top and bottom of the deck, which is typically in a frequency range of about 3 to 40 kHz. On the other hand, impulse response relies more on the structural response in the vicinity of the impact and, therefore, the frequency range of interest is much lower—that is, 0 to 1 kHz for plate structures.

### Applications

The impulse response method has been used in a number of pavement and bridge applications. These include the following:

- Detection of low-density concrete (honeycombing) and cracking in concrete elements;
- Detection of voids under joints of rigid pavements or under slabs;
- Concrete delamination in slabs, decks, walls, and other reinforced concrete structures, such as dams, chimneystacks, and silos;
- Load transfer at joints of concrete pavements; and
- Debonding of asphalt and concrete overlays on concrete deck and pavements.

### Limitations

The impulse response tests can be used to detect gross defects in structures while smaller defects might go undetected. In addition, reliable data interpretation is highly dependent on

the selection of test points. Finally, automated equipment is not available even though the automated analysis tools are available.

## Ground-Penetrating Radar

### Description

Ground-penetrating radar (GPR) is a rapid NDT method that uses electromagnetic waves to locate objects buried inside the structure and to produce contour maps of subsurface features (steel reinforcements, wire meshes, or other interfaces inside the structures). GPR can be used for a range of applications—namely, condition assessment of bridge decks and tunnel linings, pavement profiling, mine detection, archaeological investigations, geophysical investigations, borehole inspection, building inspection, and so forth. Antennas of different frequencies are used to facilitate different levels of needed detail and depth of penetration. In addition to ground-coupled antennas, like the one in Figure 3.10, air-coupled systems are used for faster bridge deck screening (Romero and Roberts 2002; Maser and Rawson 1992; Barnes and Trottier 2000).

### Physical Principle

Ground-penetrating radar provides an electromagnetic (EM) wave-reflection survey. A GPR antenna transmits high-frequency EM waves into the deck or the structure. A portion of the energy is reflected back to the surface from any reflector, such as rebar (or any other anomaly), and received by the antenna. The remainder of the GPR energy continues to penetrate beneath this interface, and additional energy is



**Figure 3.10. GPR testing.**

continually reflected back to the receiver from other interfaces until it is diminished.

GPR measures specific signal responses caused by variations in the electrical properties of the materials making up the deck. The signal responses are different for various interfaces because of two changing electrical properties: electrical conductivity (inverse of resistivity) and relative dielectric permittivity (dielectric constant). Relative permittivity values (dielectric constant,  $\epsilon_r$ ) for typical construction materials, including concrete, are shown in Table 3.1. These properties respectively govern (a) the ability of GPR energy to penetrate that particular medium and (b) the speed at which GPR waves propagate through the medium. In addition, the dielectric contrast between two adjacent materials will cause some of the penetrating GPR waveform to reflect back to the surface where it can be measured and recorded.

The condition assessment of bridge decks is based on the evaluation of the attenuation of EM waves at the top rebar level. The key point is that EM waves cannot penetrate into metals, like rebars. Therefore, rebars are excellent reflectors of

**Table 3.1. Dielectric Constants of Different Materials**

Medium	Dielectric Constant	Medium	Dielectric Constant
Air	1	Sand	4–6
Water (fresh)	81	Gravel	4–7
Ice	4	Clay	25–40
Asphalt	4–8	Silt	16–30
Concrete	8–10	Silty sand	7–10
Crushed base	6–8	Insulation board	2–2.5

EM waves. However, most construction materials are fair-to-good host materials for GPR. Concrete that is moist and high in free chloride ions (or other conductive materials) can significantly affect a GPR signal's penetration, or attenuation, in a measurable way. This is even more pronounced in cases where the deck is cracked or delaminated, and the cracks are filled with moisture, chlorides, and other conductive materials. An example is the GPR scan of a reinforced deck shown in Figure 3.11. The hyperbolae represent reflections from the top rebars. While most of the rebars on the right side can be described as providing a strong reflection, the far left rebar is somewhat fuzzy, which is an indication of strong attenuation at that location. To provide condition assessment, in most cases amplitude measurements from all the rebar locations are corrected for the rebar depth and plotted to create attenuation maps of a bridge deck. Zones of high attenuation are related to zones of likely deterioration, and vice versa.

## Applications

GPR has been used in a range of applications, such as condition assessment of bridge decks and tunnel linings, pavement profiling (pavement layer thickness evaluation) on both project and network levels, detection of voids and anomalies under pavements, mine detection, and archaeological investigations. Typical GPR applications for bridge decks include evaluation of the deck thickness, measurement of the concrete cover and rebar configuration, characterization of delamination potential, characterization of concrete deterioration, description of concrete as a corrosive environment, and estimation of concrete properties.

## Limitations

Although GPR has many advantages, there are also certain limitations. One of them is the inability to directly image and detect the presence of delamination in bridge decks, unless they are epoxy-impregnated or filled with water. Also, GPR data can be negatively influenced by extremely cold conditions. Moisture in the deck that is completely frozen will influence the acquired signal because it will no longer be detected. The application of deicing salts during winter months can also negatively influence GPR by affecting the dielectric constant.

Although GPR is capable of providing information about the layer structure, location, and layout of reinforcing steel, it cannot provide any information about the mechanical properties of the concrete (e.g., strength, modulus). Also, GPR cannot provide definitive information about the presence of corrosion, corrosion rates, or rebar section loss, even though it is sensitive to the presence of a corrosive environment and can be used to map the degree or severity of probable deterioration. GPR results generally require being correlated or validated by

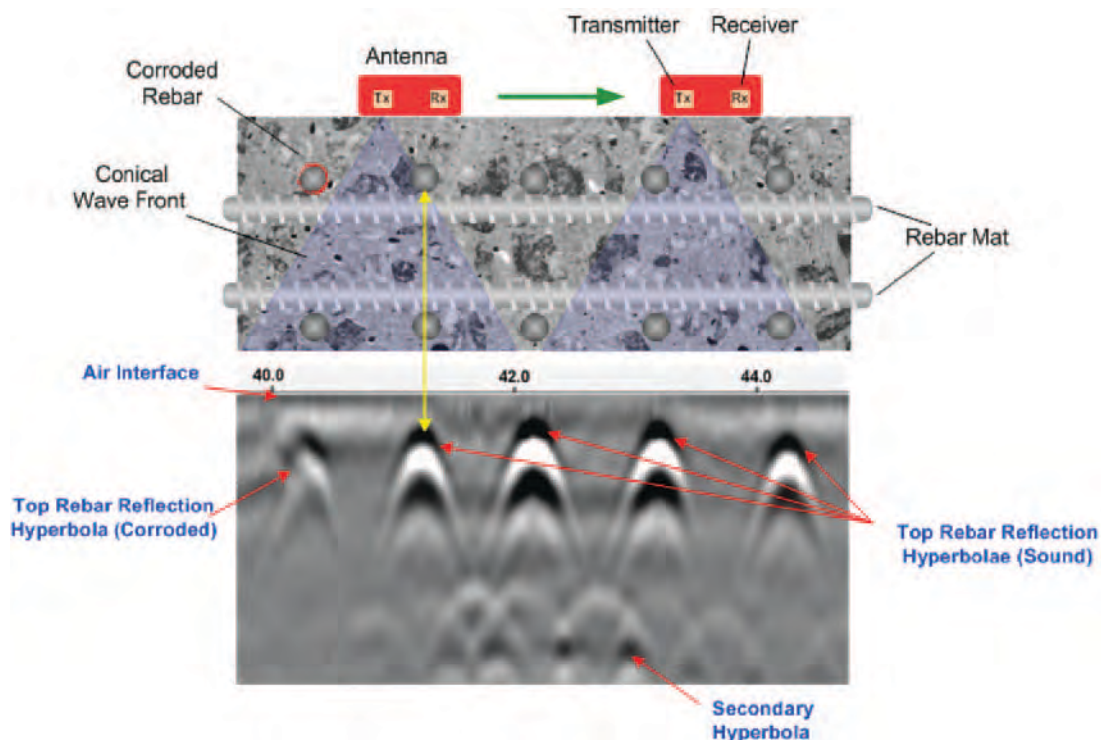


**Figure 3.11. GPR principle.**

some other NDE methods or limited destructive sampling (cores, chloride sampling and testing, or other ground truth).

GPR surveys may be less cost-effective than other methods when applied to either smaller or individual structures. Finally, Federal Communications Commission regulations controlling transmit power output and pulse repetition rate are limiting the ability to design and build newer systems, which would have a greater capability to cover larger areas in much less time using array platforms.

## Half-Cell Potential

### Description

The half-cell potential (HCP) measurement is a well-established and widely used electrochemical technique to evaluate active corrosion in reinforced steel and prestressed concrete structures. The method can be used at any time during the life of a concrete structure and in any kind of climate, provided the temperature is higher than 2°C (Elsener 2003). Half-cell measurements should be taken on a free concrete surface, because the presence of isolating layers (asphalt, coating, and paint) may make measurements erroneous or impossible. Using empirical comparisons, the measurement results can be linked to the probability of active corrosion. Half-cell testing and equipment are depicted in Figure 3.12. Generally, the potential difference between the reinforcement and a standard portable half-cell, typically a Cu/CuSO<sub>4</sub>

standard reference electrode, is measured when placed on the surface of a reinforced concrete element. When the reference electrode is shifted along a line or grid on the surface of a member, the spatial distribution of corrosion potential can be mapped (Baumann 2008; Gu and Beaudoin 1998).

### Physical Principle

When a metal is submerged into an electrolyte, positive metal ions will resolve (oxidation). Oxidation leads to a surplus of electrons in the metal lattice and a net negative charge at its surface. The positive metal ions will accumulate at the metal–liquid interface, which in consequence becomes positively charged, and a double layer is formed. Anions, from the electrolytic solution (in concrete  $\text{Cl}^-$  and  $\text{SO}_4^{2-}$ ), are attracted to the positively charged side of this double layer and accumulate there, forming the so-called half-cell. A potential difference between the metal and the net charge of the anions in the electrolyte builds up, which depends on the solubility of the metal and the anions present in the solution.

If two different metals are submerged into an electrolyte (two half-cells) and are electrically connected by a wire, a galvanic element is created. The two different metals will cause different electrical potentials in their half-cells, which in turn will cause a current flow through the wire. The less noble of the two metals is dissolved (anode) and the more noble remains stable (cathode). In the surface layer of the less noble metal, a surplus of electrons is formed. The potential difference



Figure 3.12. HCP testing.

between the two metals can be measured as a voltage with a high-impedance voltmeter (Figure 3.13).

### Applications

The main application of the method is to identify the corrosion activity of steel reinforcement in steel-reinforced concrete structures.

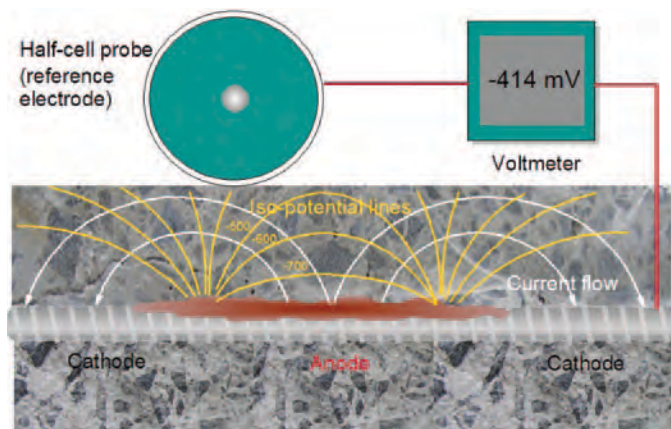


Figure 3.13. HCP principle.



### Limitations

Even though many bridge engineers have used the HCP method for years almost as a standard tool, the influence of concrete cover depth has not yet been thoroughly researched. As a consequence, correcting data for depth is not straightforward, just as it is not for moisture or salt content, which influence concrete resistivity.

### Galvanostatic Pulse Measurement

#### Description

Galvanostatic pulse measurement (GPM) is an electrochemical NDT method used for rapid assessment of rebar corrosion, based on the polarization of rebars using a small current pulse (Figure 3.14). Estimating the corrosion rate of reinforcing bars using the HCP measurement is often unreliable when concrete is wet, dense, or polymer modified, and thus the access to oxygen is limited. The GPM overcomes those problems in the interpretation of corrosion risk because of a different physical principle of operation. It provides more realistic measurements of the corrosion rate of steel rebars, which is often



**Figure 3.14. GPM testing.**

underestimated because of concrete electrical resistance (Elsener et al. 1996; Böhni and Elsener 1991; Klinghoffer et al. 2000; Baessler et al. 2003; Newton and Sykes 1988).

### Physical Principle

When a metal, such as steel reinforcement, is immersed in an electrolytically conducting liquid of adequate oxidizing power,

it undergoes corrosion by two complementary mechanisms. First, metal ions pass into the liquid, leaving a surplus of electrons on the base metal that forms an anodic site. Second, the excess electrons flow to a cathodic site where they are consumed by oxidizing agents in the liquid. These processes induce a corrosion current between the anodic and cathodic sites.

The corrosion current can be indirectly measured by galvanostatically (with constant current) imposing a short-time anodic current pulse between a counter electrode at the concrete surface and the steel reinforcement. The applied current polarizes the reinforcement anodically (with respect to the free corrosion potential), resulting in a measurable electrochemical potential drop (Figure 3.15). Actively corroding reinforcement possesses an active current between its anodic and cathodic sites and thus has a low resistance to current flow. Because of the applied current, this results in a low electrochemical potential change relative to its steady-state free corrosion potential. Noncorroding reinforcement possesses no current and thus has a high resistance to current flow. Because of the applied current, this results in a high electrochemical potential change relative to its free corrosion potential.

### Applications

The GPM is used primarily to identify the corrosion rate of steel reinforcement in reinforced concrete structures.

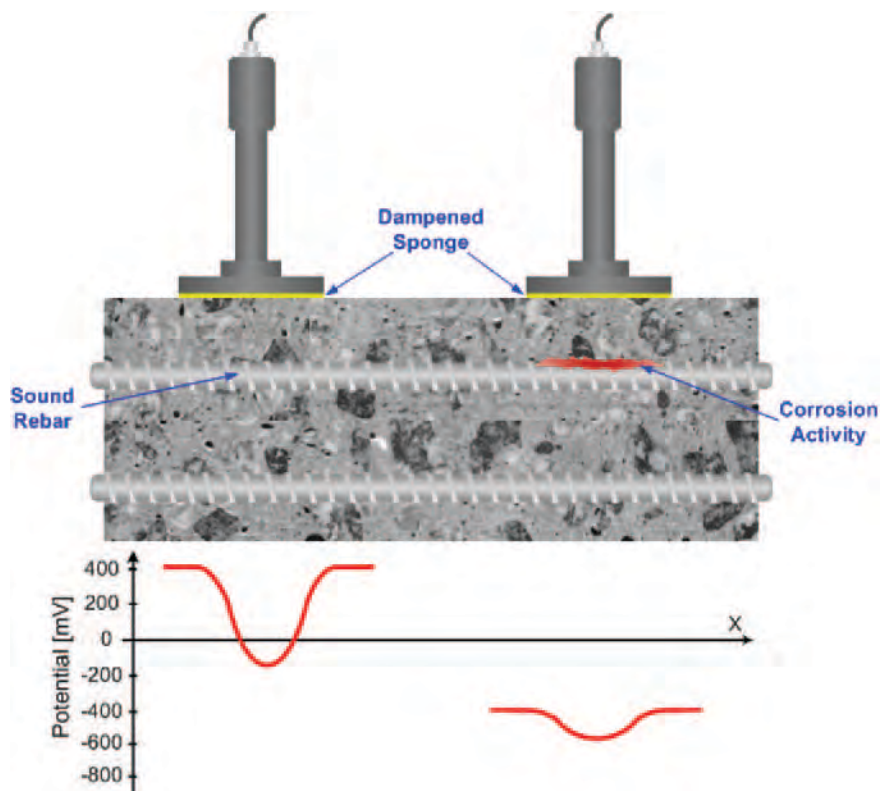


**Figure 3.15. GPM principle.**

## Limitations

High electrical resistivity in concrete cover leads to unstable measurements and, therefore, prewetting of the measurement area is essential. To avoid potential shifts due to wetting effects, the first reading should be recorded after a few minutes. Because there is a difference between the passive and active reinforcement area affected by the electrical signal, direct measurements of apparent polarization resistance do not provide appropriate results for corrosion status in these two cases.

## Electrical Resistivity

### Description

The electrical resistivity (ER) method is often used for moisture detection, which can be linked to the presence of cracks. The presence and amount of water and chlorides in concrete are important parameters in assessing its corrosion state or describing its corrosive environment. Damaged and cracked areas, resulting from increased porosity, are preferential paths for fluid and ion flow. The higher the ER of the concrete is, the lower the current passing between anodic and cathodic areas of the reinforcement will be. The relationship between ER and the normally observed corrosion rate of reinforced concrete is given in Table 3.2 (after Gowers and Millard 1999).

### Physical Principle

In practice, the voltage and current are measured at the surface of the object under investigation. The most common electrode layout in civil engineering applications is the Wenner setup (Figure 3.16). The Wenner setup uses four probes that are equally spaced. A current is applied between the outer electrodes, and the potential of the generated electrical field is measured between the two inner ones. The resistivity is then calculated according to the following:

$$\rho = \frac{2\pi a V}{I}$$

where

- $\rho$  = resistivity (in  $\Omega \cdot \text{m}$ );
- $a$  = electrode separation (in m);
- $V$  = voltage (in V); and
- $I$  = current (in A).

The inverse of the ER is the electrical conductivity,  $\sigma$  [S/m].

Building materials such as concrete, cement, or wood are ion conductors. This means that electrical conduction happens through the interconnected pore space. The resistivity of fully saturated concrete is on the order of 100 to 1,000  $\Omega \cdot \text{m}$ , depending on the conductivity of the saturating fluid. When

**Table 3.2. Correlation Between Resistivity Values and Corrosion Rates**

Resistivity ( $\text{k}\Omega \times \text{cm}$ )	Corrosion Rate
<5	Very high
5–10	High
10–20	Moderate–low
>20	Low

oven dried, the ER of concrete is as high as  $10^6 \Omega \cdot \text{m}$  and acts as an insulator. Because concrete is a composite material, its ER will always depend on its porosity, pore-size distribution, and factors such as the cement chemistry, water to cement ratio, types of admixtures, and so forth. To a large extent, resistivity values will also be a function of the ion type and content of the saturation fluid (Kruschwitz 2007; Hunkeler 1996; Bürchler et al. 1996). Phenomena such as carbonation, chloride attack (deicing salts), and secondary damage-like cracks also significantly influence the electrical properties of the concrete. Drying of the concrete surface, carbonation, and the presence of steel reinforcement in the vicinity of the electrodes significantly affect field resistivity measurements. Probably the most important parameter influencing the concrete resistivity is the fluid salinity. The fluid conductivity within a sample will depend on the saturating fluid and on the solubility of the concrete.

### Applications

Electrical resistivity is primarily used to characterize concrete's susceptibility to corrosion by characterizing its corrosive



**Figure 3.16. Electrical resistivity testing using a Wenner probe.**



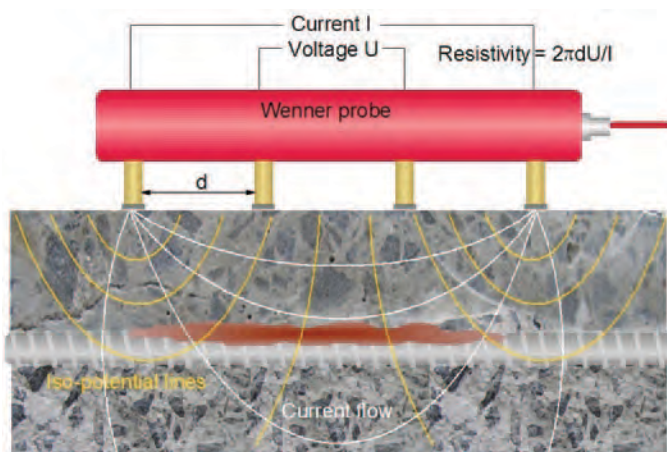


**Figure 3.17. Electrical resistivity principle.**

environment (Figure 3.17). It can also help to identify regions of the deck or other structural elements susceptible to chloride penetration. In addition, electrical resistivity surveys can be used to detect corrosion cells in tandem with another corrosion technique, such as half-cell potential, to map corrosion activity (Millard 1991; Gowers and Millard 1999).

### Limitations

Even though the data processing is not complicated and easily reduces to plotting the raw data, the interpretation is more challenging. The reason is that the ER depends on a number of material properties (e.g., moisture, salt content, porosity), and the delineation of their specific contributions to the bulk result is difficult. Even though it is technically possible, automated measurement systems for roads are not available on the market. Moreover, the electrodes need galvanic coupling to the concrete and, therefore, the surface of a test object has to be prewetted.

## Infrared Thermography

### Description

Infrared (IR) thermography has been used since the 1980s to detect concrete defects, such as cracks, delaminations, and concrete disintegration in roadways or bridge structures (Figure 3.18 to Figure 3.20). To detect subsurface defects, IR thermography keeps track of electromagnetic wave surface radiations related to temperature variations in the infrared wavelength. Anomalies, such as voids and material changes, can be detected on the basis of variable material properties, such as density, thermal conductivity, and specific heat capacity. The resulting heating and cooling behavior is compared with the surrounding material. Infrared cameras measure the infrared radiation (wavelength ranging from 0.7 to 14  $\mu\text{m}$ )

that is emitted by a body, and this radiation is then converted into an electrical signal. These signals are further processed to create maps of surface temperature. A qualitative data analysis can be done from the thermograms (temperature coded images) (Maierhofer et al. 2002; Maierhofer et al. 2004; Maierhofer et al. 2006; Maser and Bernhardt 2000).

### Physical Principle

Infrared radiation is part of the electromagnetic spectrum, with the wavelength ranging from 0.7 to 14  $\mu\text{m}$ . Infrared cameras measure the thermal radiation emitted by a body, based on the thermal properties of various materials, and capture the regions with temperature differences. The three main properties that influence the heat flow and distribution within a material include the thermal conductivity ( $\lambda$ ), specific heat capacity ( $C_p$ ), and the density ( $\rho$ ).

When the solar radiation or a heater, in the case of active thermography, heats up the deck, all the objects in the deck emit some energy back (Figure 3.20). The delaminated and voided areas are typically filled with water or air, which have a different thermal conductivity and thermal capacity than the surrounding concrete. These delaminated areas heat up faster and cool down more quickly compared with concrete. They can develop surface temperatures from 1°C to 3°C higher than the surrounding areas when ambient conditions are favorable.

### Applications

Infrared thermography is mostly used to detect voids and delaminations in concrete. However, it is also used to detect delaminations and debonding in pavements, voids in shallow tendon ducts (small concrete cover), cracks in concrete, and asphalt concrete segregation for quality control.

### Limitations

The method does not provide information about the depth of the flaw. Deep flaws are also difficult to detect. Finally, the method is affected by surface anomalies and boundary conditions. For example, when sunlight is used as a heating source, clouds and wind can affect the deck heating by drawing away heat through convective cooling.

## Chain Dragging and Hammer Sounding

### Description

Chain dragging and hammer sounding are the most common inspection methods used by state DOTs and other bridge



**Figure 3.18. Infrared thermography testing.**



Source: Photographs courtesy of Dr. Ken Maser.

**Figure 3.19. Infrared thermography.**

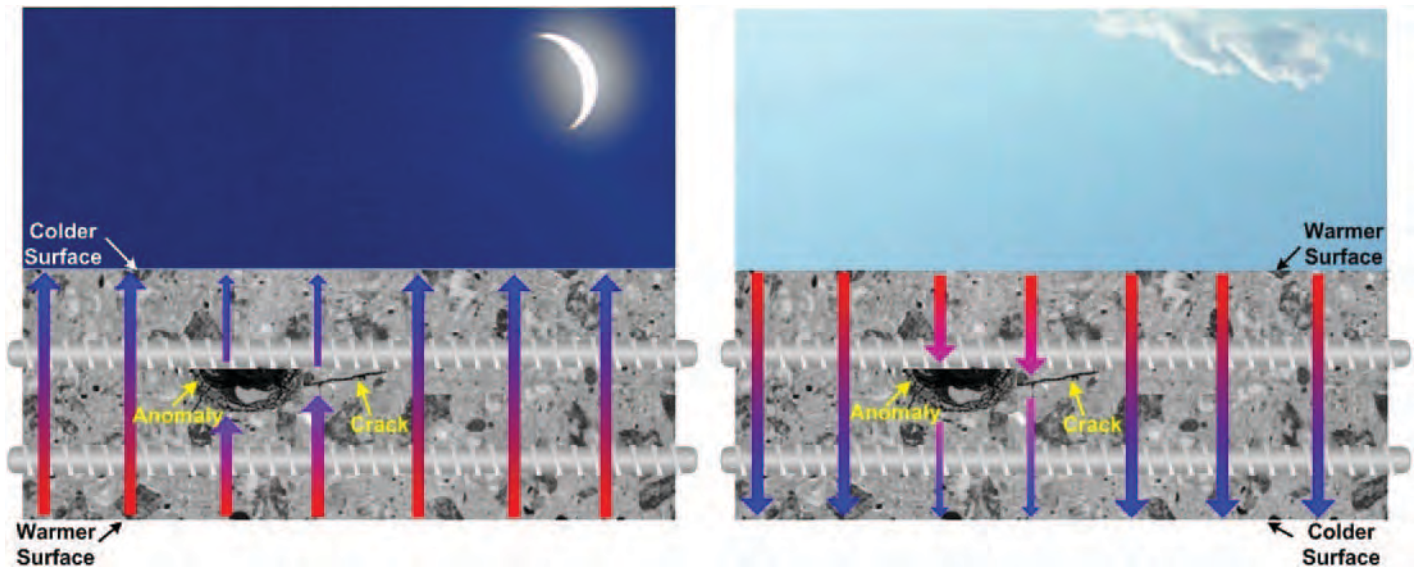


**Figure 3.20. Principle of passive infrared thermography.**

owners for the detection of delaminations in concrete bridge decks. The objective of dragging a chain along the deck or hitting it with a hammer is to detect regions where the sound changes from a clear ringing sound (sound deck) to a somewhat muted and hollow sound (delaminated deck). Chain dragging is a relatively fast method for determining the approximate location of a delamination. The speed of chain dragging varies with the level of deterioration in the deck. Hammer sounding is much slower and is used to accurately define the boundaries of a delamination. It is also a more appropriate method for the evaluation of smaller areas. The application of the two methods is shown in Figure 3.21.

Another technology that is close in principle to hammer sounding is called the rotary percussion system, which is also accepted as a standard procedure by ASTM D4580-86 (reapproved 1992) for measuring delaminations in concrete bridge decks. The rotary percussion system consists of multiple, gear-shaped wheels on the end of a pole. In some rotary percussion systems, a microphone and headphones are connected to the pole to amplify the sound and block out the ambient noise. The evaluation involves rolling the toothed wheel over a surface and listening for a change in the sound. Chain dragging and rotary percussion methods are relatively fast delamination detection devices that are also very simple to use.



**Figure 3.21. Chain dragging (left) and hammer sounding (right).**

### **Physical Principle**

Chain dragging and hammer sounding are categorized as an elastic wave test. The operator drags chains on the deck, listening to the sound the chains make. A clear ringing sound represents a sound deck, while a muted or hollow sound represents a delaminated deck. The hollow sound is a result of flexural oscillations in the delaminated section of the deck, creating a drumlike effect. Flexural oscillation of a deck resulting from an impact (the source of the impact can either be from chain dragging or hammer sounding) is typically found to be in a 1- to 3-kHz range. This is within the audible range of a human ear. The presence of any delamination changes the frequency of oscillation and, therefore, the audible response of the deck.

### **Applications**

Chain dragging and hammer sounding are mainly used to detect the late stages of delaminations in concrete structures. Although chain dragging is limited to horizontal surfaces, hammer sounding can be used for a wider range of structures.

### **Limitations**

Chain dragging and hammer sounding are dependent on the operator's skill and hearing, which makes both methods subjective. Initial or incipient delamination often produces oscillations outside the audible range and thus cannot be detected by the human ear. As a result, they are not detected by chain dragging and hammer sounding. Both methods are generally ineffective for delamination detection on decks with overlays.

## CHAPTER 4

# Criteria and Methodology for Evaluating NDT Methods for Assessment of Bridge Decks

In Chapter 3, all promising NDT techniques for bridge deck evaluation were summarized and described in terms of their principles of operation and their applications in the detection and characterization of certain defects. Limitations of the technologies were also described. This chapter describes the categorization, grading, and ranking of these promising technologies, according to a number of selected performance measures. Various steps in this process are illustrated in Figure 4.1.

Five performance measures, including accuracy, precision (repeatability), ease of use, speed, and cost were defined for each of the identified techniques and graded for the ultimate ranking of the technology. The ranking was based on a particular deterioration type and the overall value in evaluating and monitoring concrete bridge decks. Each performance measure was assigned a *weight factor*, on the basis of its importance in assessing deterioration in bridge decks.

The *overall grade* for a technology in detecting a particular deterioration or defect was calculated as the weighted sum of the grades for all performance measures. For techniques that can detect multiple types of deterioration and defects, the grade was determined for each of the deterioration or defect types. The *overall value* of the technology for concrete bridge deck evaluation was calculated as the weighted average from the grades for different deterioration types. The weight factors for different deterioration types are identified in the process as *significance factors*.

### Performance Measures and Deterioration Types Selection

The evaluation of NDT technologies was carried out for the following four deterioration types:

1. Delamination;
2. Corrosion;
3. Cracking; and
4. Concrete deterioration.

The rationale behind limiting the deterioration types into only four categories is the following. Although there are different causes for deterioration, in most cases the causes cannot be determined by NDT technologies; only their consequences can be determined. For example, corrosion and shrinkage-induced cracking will result in material degradation, which can be detected through reduced velocity, modulus, and so forth. In addition, from the list of all possible deterioration types and mechanisms, the four deterioration categories considered are of the highest concern to transportation agencies.

The following are the five performance measures selected for categorizing and ranking the technologies:

1. Accuracy;
2. Precision (repeatability);
3. Ease of data collection, analysis, and interpretation;
4. Speed of data collection and analysis; and
5. Cost of data collection and analysis.

The rationale used for concentrating on only five performance measures is the following. Although the description of a particular performance provides a more detailed description of that performance in terms of a large number of measures, for most technologies there is either no information regarding a specific performance measure or the measure is not applicable to that particular technology. In addition, analyses in terms of a smaller number of performance measures are believed to be of higher interest and practical value to transportation agencies and industry.

### Description and Definition of Main Deterioration Types

The descriptions of the deterioration categories below are based on the ability of the NDT technologies to detect them and thus do not include the causes of the deterioration.

- *Delamination*. Detection is targeted toward predominantly horizontally oriented cracks, whether those cracks are

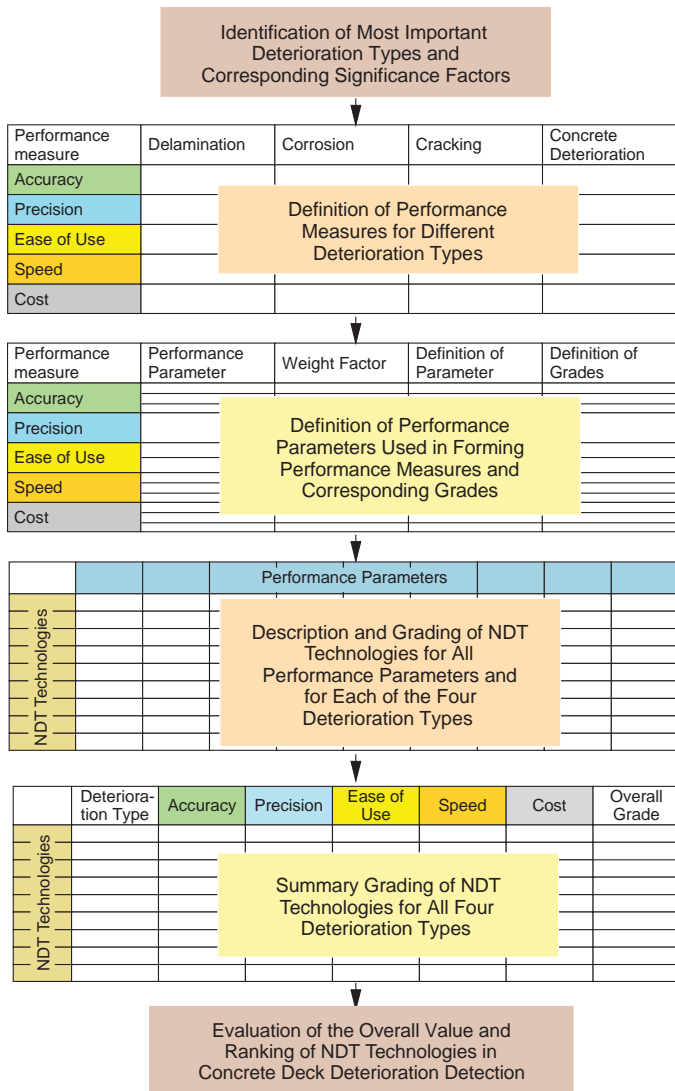


**Figure 4.1. Flowchart of the categorization and ranking process of NDT technologies.**

a result of rebar corrosion, overloading, or other types of deterioration.

- *Corrosion.* Detection is directed toward two main objectives: detection and evaluation of the intensity of active corrosion, and the severity of existing corrosion.
- *Cracking.* Detection concentrates on the detection and evaluation of dominantly vertically oriented cracks.
- *Concrete deterioration.* Detection involves measuring the change or variability of material properties, regardless of the cause (e.g., corrosion, ASR, carbonation, DEF).

Because various deterioration types have different impacts on the serviceability of the bridge deck, significance factors, presented in Table 4.1, were assigned to each deterioration type. The factors used in the technology ranking represent a consensus of the SHRP 2 Renewal Project R06A team. These

**Table 4.1. Significance Factors for Deterioration Types**

Deterioration Type	Significance Factor	
	SHRP 2 Team	DOT Bridge Engineers
Delamination	0.42	0.39
Corrosion	0.35	0.38
Cracking	0.10	0.12
Concrete degradation	0.13	0.11

factors are compared in the same table to the average weights provided by five DOT bridge engineers. The two groups similarly identify delamination and corrosion of primary significance and vertical cracking and concrete degradation evaluation of secondary significance.

### Elements Constituting Performance Measures

To rank the five major performance parameters in an accurate, repeatable, and practical manner, they were further subdivided into up to three subcategories, resulting in a total of 12 factors. These 12 factors, which are mapped into the major five performance measures in Table 4.2, can be summarized as follows:

1. Detectability extent;
2. Detectability threshold;
3. Evaluation of severity of deterioration;
4. Repeatability of measurement;
5. Speed of data collection;
6. Speed of data analysis and interpretation;
7. Expertise needed for data collection;
8. Expertise needed for data processing and data interpretation;
9. Extent and potential for automation and improvement;
10. Cost of data collection;
11. Cost of data analysis and interpretation; and
12. Cost of equipment, supplies, and equipment maintenance.

For each factor, a grade of 1, 3, or 5 was assigned, with 1 being the least favorable and 5 being the most favorable for a given technology. The definitions of these grades for each factor are summarized in Table 4.3.

On the basis of the above descriptions, the performance of each selected technology was graded for each of the four deterioration types. The final grades obtained for all the selected technologies and for all deterioration types are summarized in Table 4.4.

**Table 4.2. Definitions of Performance Measures for Different Deterioration Types**

Performance Measure	Delamination	Corrosion	Cracking	Concrete Deterioration
<b>Accuracy</b>	<ul style="list-style-type: none"> <li>• Estimation of boundaries (extent) of the delamination in the horizontal direction</li> <li>• Determination of the depth of the delamination</li> <li>• Detectability threshold and assessing the degree (severity) of delamination</li> </ul>	<ul style="list-style-type: none"> <li>• Detection of active corrosion</li> <li>• Determination of the depth and boundaries of corroding rebars</li> <li>• Detectability threshold</li> <li>• Determination of the degree (severity) of existing corrosion</li> </ul>	<ul style="list-style-type: none"> <li>• Determination of the crack depth and width</li> </ul>	<ul style="list-style-type: none"> <li>• Determination of the lateral boundaries and thickness of the deteriorated concrete</li> <li>• Detectability threshold</li> <li>• Determination of degree (severity) of deterioration</li> </ul>
<b>Precision</b>	<ul style="list-style-type: none"> <li>• Repeatability of the measurement in estimating boundaries, depth, detectability threshold, and severity of delamination</li> </ul>	<ul style="list-style-type: none"> <li>• Repeatability of the measurement in detection and evaluation of severity of active corrosion, existing corrosion degree, and depth of corroded rebars</li> </ul>	<ul style="list-style-type: none"> <li>• Repeatability of the measurement in evaluation of crack depth and width</li> </ul>	<ul style="list-style-type: none"> <li>• Repeatability of the measurement in detection, determination of deteriorated zone boundaries, and evaluation of severity of deterioration</li> </ul>
<b>Ease of use</b>	<ul style="list-style-type: none"> <li>• Ease and expertise level needed for data collection</li> <li>• Ease and expertise level needed for data analysis</li> <li>• Expertise level needed in interpretation (relating results of analyses to relevant engineering parameters)</li> </ul>			
<b>Speed</b>	<ul style="list-style-type: none"> <li>• Speed of data collection</li> <li>• Extent and potential for automation/improvement of data collection</li> <li>• Speed of data analysis</li> <li>• Extent and potential for automation/improvement in data analysis</li> </ul>			
<b>Cost</b>	<ul style="list-style-type: none"> <li>• Cost of the data collection (including traffic control and other)</li> <li>• Cost of the data analysis and interpretation</li> <li>• Cost of the equipment (initial), supplies, and maintenance</li> </ul>			

**Table 4.3. Definitions of Performance Parameters and Corresponding Grades**

Major Categories	Parameter	Weight Factor	Definition of Parameter	Definition of Grades		
				Very Favorable = 5	Favorable = 3	Not Favorable = 1
<b>Accuracy</b>	<b>Detectability extent—A1</b>	<b>0.3</b>	Minimum extent of deterioration that should occur before it can be detected	Localized deterioration can be detected	Extensive deterioration can be detected	Indirectly evaluated with low certainty
	<b>Detectability threshold—A2</b>	<b>0.3</b>	Stage of deterioration at which it can be detected	Onset of deterioration	Advanced deterioration	Indirectly detected with low certainty
	<b>Severity of deterioration—A3</b>	<b>0.4</b>	Ability of the method to quantify different degrees of deterioration	Fully/continuously quantifies	Quantifies one or more degrees	Cannot distinguish different degrees
<b>Precision</b>	<b>Precision/repeatability—R1</b>	<b>1.0</b>	Repeatability of data collection (even under changed environmental conditions), data analysis, interpretation, and so forth	High repeatability in all aspects	High repeatability only under certain conditions	Low repeatability for any reason

(continued on next page)

**Table 4.3. Definitions of Performance Parameters and Corresponding Grades (continued)**

Major Categories	Parameter	Weight Factor	Definition of Parameter	Definition of Grades		
				Very Favorable = 5	Favorable = 3	Not Favorable = 1
Speed	Speed of data collection—S1	0.6	Production rate in terms of area coverage (test point number) per hour for “good” quality data	More than 500 ft <sup>2</sup> /h or 120 test points	More than 100 ft <sup>2</sup> /h or 25 test points	Less than 100 ft <sup>2</sup> /h or 25 test points
	Speed of data analysis—S2	0.4	Production rate in terms of area coverage (test point number) for preprocessing and postprocessing analyses	More than 200 ft <sup>2</sup> /h or 50 test points	More than 50 ft <sup>2</sup> /h or 12 test points	Less than 50 ft <sup>2</sup> /h or 12 test points
Ease of use	Expertise data collection—E1	0.2	Expertise needed in setting up instrumentation, consideration of environmental and other effects, and survey conduct for high-quality data collection	Basic training and little experience needed	Medium expertise and experience needed	High expertise and extensive experience needed
	Expertise data analysis—E2	0.5	Expertise needed in pre- and postdata processing and delineation and classification of the deteriorated areas	Basic training and little experience needed	Medium expertise and experience needed	High expertise and extensive experience needed
	Extent and potential for automation—E3	0.3	Further potential for automation in data collection, analysis, and interpretation in the future	High potential for both data collection and data analysis	High potential for either data collection or data analysis	Little or no potential for automation of either data collection or data analysis
Cost	Cost of data collection—C1	0.5	Overall cost is based on direct data collection cost and need for traffic control	Low cost (<\$1/ft <sup>2</sup> ) and no need for traffic control	Low cost (<\$1/ft <sup>2</sup> ) and required traffic control	High cost (>\$1/ft <sup>2</sup> ) and required traffic control
	Cost of data analysis—C2	0.3	Overall cost is based on the expertise level and time needed to analyze and interpret	Low cost per unit area (<\$2/ft <sup>2</sup> )	Medium cost per unit area (\$2–4/ft <sup>2</sup> )	High cost per unit area (>\$4/ft <sup>2</sup> )
	Cost of equipment—C3	0.2	Overall cost from equipment purchase and maintenance, and supplies per year of operation	Less than \$5,000/year	Less than \$10,000/year	More than \$10,000/year

## Conclusions

The most important conclusions derived regarding the performance and overall ranking of the selected NDT technologies are provided below. It should be emphasized that these conclusions are only based on the literature search, which served as a guideline in the identification of NDT technologies for the validation testing.

- Even though several technologies have shown potential for detecting and evaluating each of the main deterioration

types, there is not a single technology that can potentially evaluate all deterioration types.

- Six technologies were identified as having a good potential for delamination detection and characterization. Those are impact echo, chain dragging and hammer sounding, ultrasonic pulse echo, impulse response, infrared thermography, and ground-penetrating radar.
- Three technologies were identified as having a good potential for corrosion detection and characterization. Those are half-cell potential, electrical resistivity, and galvanostatic pulse measurement.



**Table 4.4. Overall Value and Ranking of NDT Technologies**

Deterioration Type	Delamination	Corrosion	Cracking	Concrete Deterioration	Overall Value	Ranking
	WF-1 = 0.42	WF-2 = 0.35	WF-3 = 0.10	WF-4 = 0.13		
Impact echo	4.7	1.0	2.5	3.1	3.0	1
Ultrasonic pulse echo	3.6	1.0	2.6	3.4	2.6	1
Half-cell potential	1.0	4.9	0.0	1.0	2.3	2
Impulse response	3.6	1.0	0.0	2.6	2.2	2
Ultrasonic surface waves	2.5	1.0	3.0	3.4	2.2	2
Ground-penetrating radar	3.0	1.0	1.0	3.1	2.1	2
Chain dragging/hammer sounding	3.7	1.0	0.0	1.0	2.1	2
Electrical resistivity	1.0	3.9	0.0	1.0	1.9	3
Infrared thermography	3.2	1.0	0.0	1.0	1.8	3
Galvanostatic pulse measurement	1.0	3.0	0.0	1.0	1.6	3
Visual inspection	1.0	1.0	3.7	1.0	1.3	3
Microwave moisture technique	0.0	1.0	1.0	1.0	0.6	4
Chloride concentration	0.0	1.0	0.0	1.0	0.5	4
Eddy current	0.0	1.0	1.0	0.0	0.5	4

Note: Shaded areas indicate higher performance of the technology in detection and characterization of a particular deterioration type.

- Four technologies were identified as having a good potential for vertical cracking characterization. Those are visual inspection, ultrasonic surface waves, ultrasonic pulse echo, and impact echo.
- Five technologies were identified as having a potential in concrete deterioration detection and characterization. Those are ultrasonic surface waves and pulse echo, impact echo, ground-penetrating radar, and impulse response.
- The ranking of the technologies was to some extent influenced by the selected performance measures, weight factors, and significance factors. The closeness of some of the results necessitates validating the rankings through a series of field and laboratory testing.

## CHAPTER 5

# Approach to Validation Testing

High-speed NDT technologies such as ground-penetrating radar, infrared thermography, and impact echo scanning have been increasingly used in recent years for bridge deck condition assessment. Still, these technologies have not been widely adapted or accepted for two main reasons: (1) highway agencies are not fully aware of the capabilities and limitations of these methods or how they should best be used, and (2) some agencies have had less-than-positive experiences with NDT techniques, perhaps because of unrealistic expectations and improper use of these technologies. Therefore, a plan to evaluate the most promising technologies, both in the field under actual, production-level conditions and in the laboratory under controlled conditions, was developed for the second phase of the project. The performance factors of highest importance during the laboratory validation were accuracy and precision. The parameters of the highest importance in the field validation were speed of evaluation, including data collection and analysis; ease of use; precision; and cost. The following sections describe the validation testing, a task designed to evaluate the performance of candidate NDT technologies.

### Field Validation Testing

Field validation was conducted on the Route 15 bridge over I-66 in Haymarket, Virginia. Bridge selection and organization of testing were done in collaboration with the FHWA's Long-Term Bridge Performance (LTBP) Program, Virginia Department of Transportation, and Virginia Transportation Research Council. This bridge was selected because it had gone through a rigorous evaluation using both destructive and nondestructive means, visual inspection, and full-scale loading as a part of the LTBP activities. The instrumentation and monitoring of this particular bridge within the LTBP Program commenced in September 2009, which provided a wealth of information about the bridge condition. The Haymarket Bridge is a two-span concrete deck on a steel girder

structure and was constructed in 1979. The bridge has a 15° skew. The reinforced concrete deck is about 8 in. thick, with clearly visible deterioration on its surface (Figure 5.1).

In August 2010, the SHRP 2 research team released electronic announcements regarding the validation testing of 10 nondestructive testing technologies. This was done via targeted e-mails to industry vendors, manufacturers, and research centers, along with postings to the TRB, the American Society for Nondestructive Testing, and SHRP 2 websites. On receipt of invitee responses, the SHRP 2 team provided each respondent with a detailed description of the planned validation testing to be conducted. The descriptions included testing objectives, activity scope, participant and research team responsibilities, and result reporting methods. The final team comprised eight non-SHRP 2 project participants and two groups from the institutions of the SHRP 2 project team, but not the members of the project team. Thus 10 groups in total were involved in the validation testing. The participating teams in alphabetical order are as follows:

1. FHWA, Turner–Fairbank Highway Research Center (Dr. Ralf Arndt);
2. Germann Instruments;
3. IDS, Italy;
4. NDT Corporation;
5. Olson Engineering;
6. Rutgers University, CAIT;
7. 3D-RADAR, Norway;
8. University of Illinois (Dr. John Popovics);
9. The University of Texas at Austin (Dr. Jinying Zhu); and
10. The University of Texas at El Paso, CTIS.

Henceforth, each participant will be referred to by assigned numbers from the research teams.

The technologies participating in the validation testing included ground-penetrating radar, impact echo, surface wave testing, impulse response, half-cell potential, electrical



**Figure 5.1. Side view of Route 15 bridge over I-66 in Haymarket, Virginia.**

resistivity, galvanostatic pulse measurement, infrared thermography, ultrasonic pulse echo, and chain dragging and hammer sounding. Some of the technologies were represented by multiple participants, each using a different system.

Testing was conducted on a 1,008 ft<sup>2</sup> (84-ft × 12-ft) area, extending over parts of the shoulder and travel lane (Fig-

ure 5.2). A 2-ft by 2-ft rectangular grid was marked on the deck using washable paint. A blue, washable spray paint was used to mark the grid, rather than the commonly used white paint, to facilitate better imaging for infrared thermography. The origin of the test grid was located 24 ft from the north expansion joint and 3 ft from the west parapet wall. The grid had 301 test points. The grid schematic is depicted in Figure 5.3, and a part of the grid is shown in Figure 5.4. The participants were required to collect data on the grid points. However, they were also permitted to collect additional data, within the allocated time period, after obtaining the required test location data. Eight locations were marked on the deck for vertical crack evaluation for those participants who were engaged in their characterization. To evaluate technology repeatability, all participants were required to repeat measurements three times along the middle line (Line D).

Detailed testing plan instructions were provided to all participants both before the testing and at the bridge site. These instructions clearly delineated evaluation objectives, testing methods, results to be reported, elements of comparative

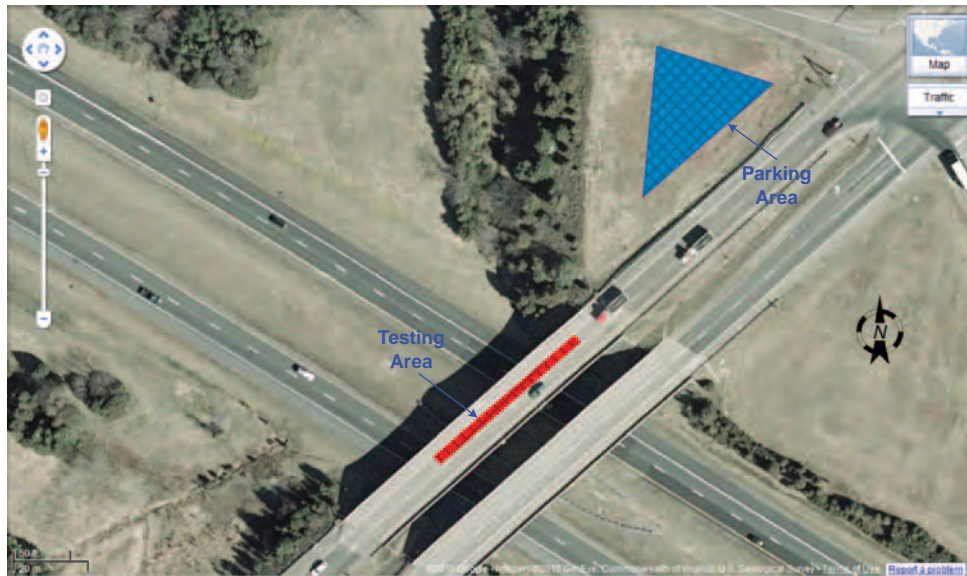


**Figure 5.2. Route 15 bridge over I-66 in Haymarket, Virginia.**

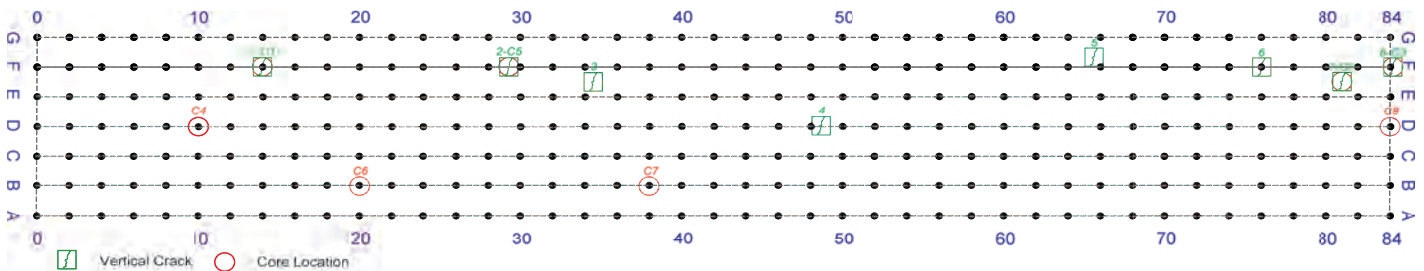


**Figure 5.3. Grid schematic with marked locations of vertical cracks (green squares) and extracted cores (red circles).**



**Figure 5.4. Test grid.**



**Figure 5.5. Impact echo: (left) Germann Instruments; (right) NDT Corporation.**



**Figure 5.6. Impulse response (left): Germann Instruments. Ground-penetrating radar (right): 3D-RADAR.**

evaluation, and technology ranking information. Figures 5.5 to 5.11 illustrate data collection by different participants.

After testing had been completed, eight cores were removed from the deck by a local contractor. These cores were used to provide ground truth. Four of the cores were taken at the vertical crack locations evaluated by the participating teams (Figure 5.12).

Images of eight cores removed from the deck are shown in Figure 5.13. All four defects of interest—delamination, corrosion, vertical crack, and concrete deterioration—can be observed in the cores.

## Laboratory Validation Testing

The laboratory validation testing commenced in December 2010 at El Paso, Texas. Two test decks were prepared for the validation testing. The first test deck was a newly fabricated



**Figure 5.7. Ground-penetrating radar: IDS.**

concrete deck with simulated defects, and the other test deck was removed from a bridge on I-10 in El Paso. The two test decks were embedded in the ground at a site near the main campus of the University of Texas at El Paso.

### Fabricated Bridge Deck

The fabricated bridge deck was 20 ft long, 8 ft wide, and about 8.5 in. thick and supported by three 1.5-ft-wide prestressed girders retrieved from a Texas Department of Transportation (Texas DOT) project (Figure 5.14). Class S concrete mix, as per Texas DOT Specification 421.4, was adapted for deck construction. This mix requires a minimum 28-day compressive strength of 4,000 psi and has been widely used in bridge deck



construction in Texas DOT projects. To simulate an actual concrete bridge deck, the slab was finished with a rough top surface. Water curing was applied to the slab for 7 days after concrete placement. The 28-day compressive strength and modulus of the mix were more than 5,000 psi and 4,000 ksi, respectively.

The deck was built with two mats of uncoated steel reinforcement. Each of the reinforcement mats consisted of No. 5 steel bars spaced at 8 in. in the transverse direction and spaced at 10 in. in the longitudinal direction. The top and bottom concrete covers of the deck were 2.5 to 3 in. and 2 in. thick, respectively. Nine artificially delaminated areas, two pieces of corroded reinforcement mats, and four vertical cracks were built in the deck. In addition, a natural crack was observed in the deck about 2 weeks after construction.



**Figure 5.8. Air-coupled ultrasonic surface wave: University of Texas at Austin.**



**Figure 5.9. Half-cell potential (left) and electrical resistivity (right): Rutgers University.**



**Figure 5.10. Impact echo and surface waves (left) and galvanostatic pulse measurement (right): Olson Engineering.**



**Figure 5.11. Infrared thermography (left): FHWA. Ground-penetrating radar (right): NDT Corporation.**

Figure 5.15 depicts an overview of the approximate distribution of the as-built defects in this deck. The information about each defect is summarized in Table 5.1. In Figure 5.15 and Table 5.1, DL denotes delaminations and CK denotes vertical cracks.

Ideally, corrosion should be built on the original steel bars used for the enforcement for HCP and ER testing. However,



**Figure 5.12. Vertical crack and core locations.**

because of the fund restriction and time limitation, it is practically impossible to build accelerated corrosion of 2 to 3 ft long on each 20-ft or 8-ft-long regular steel bar. Instead, thirty two 30-in.-long steel bars were pretreated in a manual way similar to the practice of ASTM B-117 [Standard Practice for Operating Salt Spray (Fog) Apparatus]. One-half of these bars were treated for 2 months and another one-half for 3 months. They were then used to build two sets of corrosion mats. The two sets of corrosion mats were merged parallel to one another and electrically connected to the normal reinforcement bars at one end of the fabricated deck (Figure 5.16).

To inspect the behavior of the materials used to simulate delaminations and to check the status of rebar corrosion, four cores (C1, C2, C3, and C4) were extracted from the deck at the locations shown in Figure 5.17 after all validation tests had been completed.

Images of the four cores from the fabricated deck are shown in Figure 5.18. Cores C1, C2, and C3 reflect three different levels of delamination. Core C4 shows the status of the corroded bar 8 months after placement; that is, red corrosion ( $\text{Fe}_2\text{O}_3$ ; also see Figure 5.16) turned to black

*(text continues on page 43)*



(a)



(b)



(c)



(d)



(e)



(f)

**Figure 5.13. Cores 1 (a), 2 (b), 3 (c), 4 (d), 5 (e and f).**

*(continued on next page)*





(g)



(h)



(i)



(j)

**Figure 5.13. (continued) Cores 6 (g and h), 7 (i), and 8 (j).**

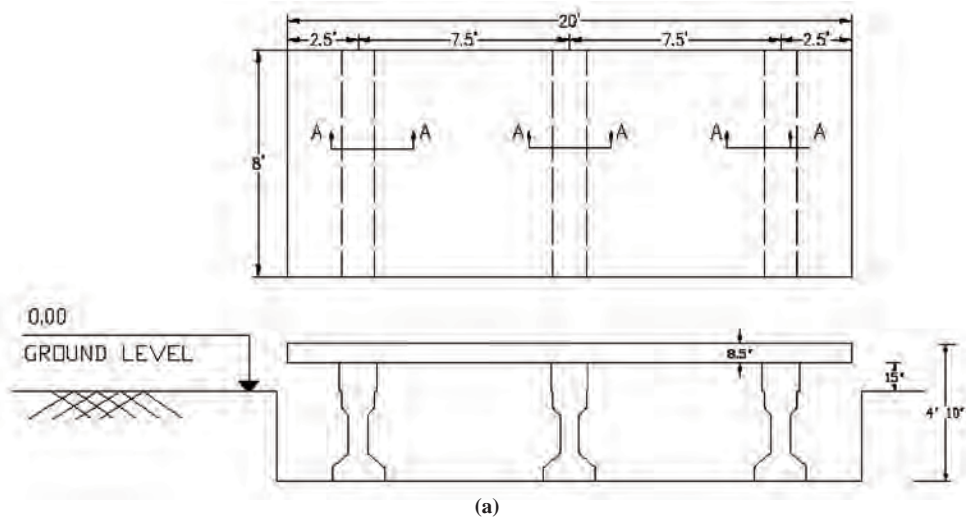


Figure 5.14. Fabricated slab: (a) schematic and (b) curing.

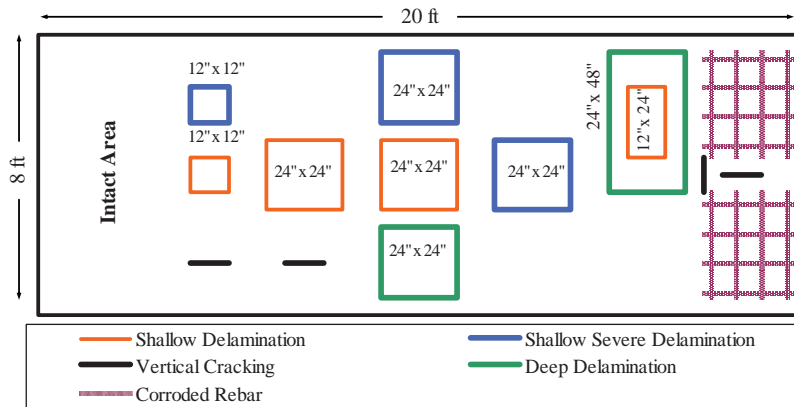
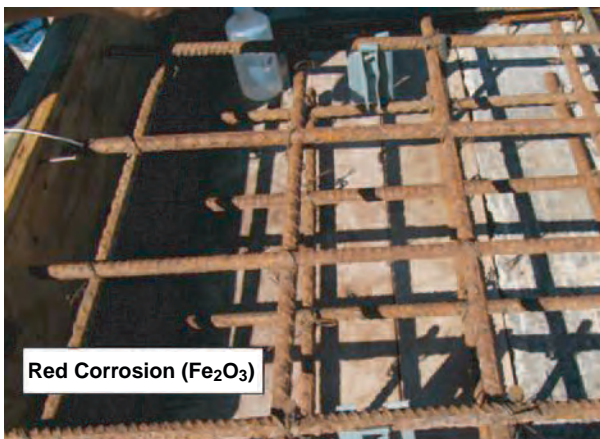


Figure 5.15. Overview of defect distributions in fabricated slab.

**Table 5.1. Detailed Information of Defects in Fabricated Concrete Deck**

Defect Type	Code	Size (in.)	Depth (in.)	Description
Delamination	DL1	12 × 12	2.5–3.0	Soft and high-strength, thin (about 1 mm) foam
	DL2, DL3	24 × 24	2.5–3.0	
	DL4	12 × 12	2.5–3.0	Soft and high-strength, thick (about 2 mm) foam
	DL5, DL6	24 × 24	2.5–3.0	
	DL7	24 × 24	6–6.5	Soft and high-strength, thin (about 1 mm) foam
	DL8	24 × 48	6–6.5	
	DL9	12 × 24	2.5–3.0	Very thin (about 0.3 mm), soft polyester fabric
Vertical crack	CK1, CK2	12 (length)	2.5	Soft thin cardboard
	CK3	12 (length)	3.0	Soft thick cardboard with void
	CK4	12 (length)	6.0	
	CK5	13 (length)	2.5–3.0	Natural, fine crack <sup>a</sup>
Rebar corrosion	30 in. × 30 in. (each mat)		2.5 and 6.5 (midpoints)	1- to 2-mm deep corrosion

<sup>a</sup> It extended to the edge of the deck, and its depth is measurable.



**Figure 5.16. Setup of the corroded steel bar mat in the fabricated deck.**

(continued from page 39)

corrosion (Fe<sub>3</sub>O<sub>4</sub>). The mechanism for this change is unclear in this situation.

**Recovered Bridge Deck**

A 9-ft by 14-ft section was removed from a distressed highway bridge along Interstate 10 near El Paso, Texas. The bridge deck consisted of arch-type concrete overlaid by a 4-in.-thick, hot-mix asphalt surface (Figure 5.19). The arch-type concrete showed continuous cracks at the bottom of each arch.

After all validation tests had been completed, seven cores were taken from the deck (Figure 5.20). These cores indicate that the deck is seriously delaminated and cracked, which seemed to be stress-induced by traffic loading, because almost no corrosion was observed from the cores.

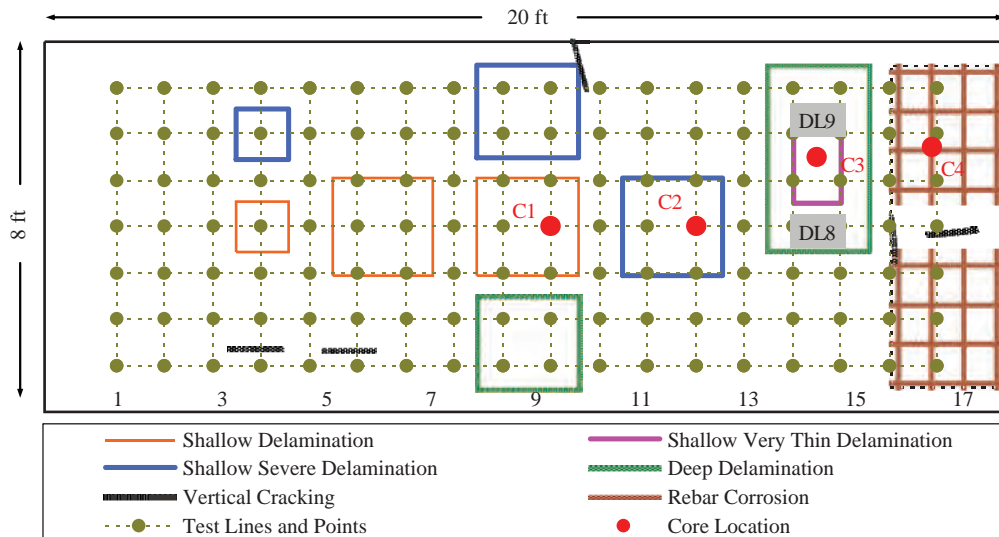


**Figure 5.17. Locations of coring on fabricated deck.**

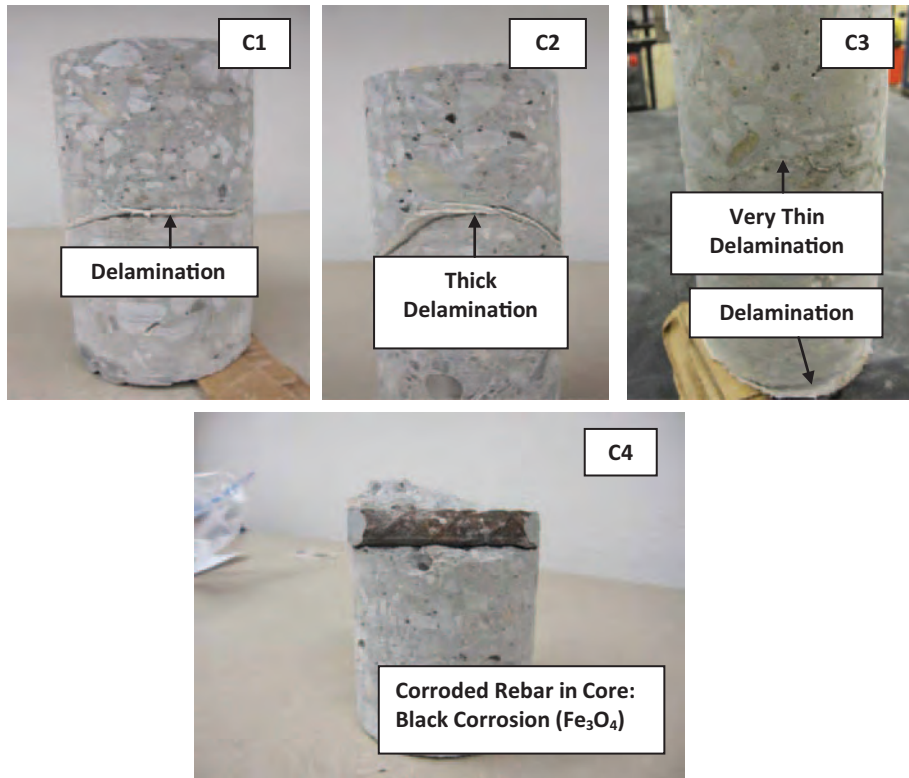
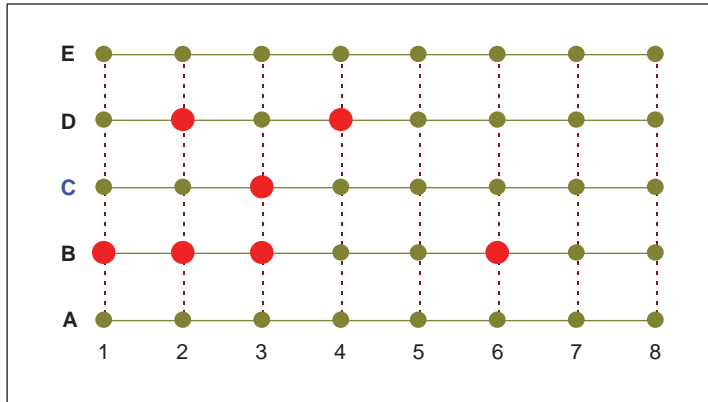


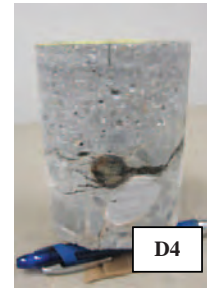
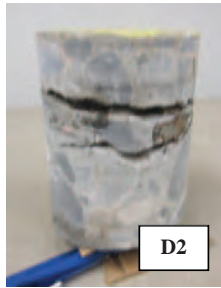
Figure 5.18. Cores from fabricated bridge deck.



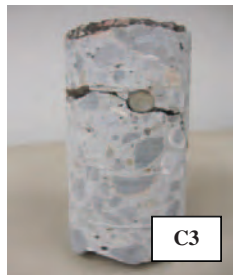
Figure 5.19. Bridge with arch deck.



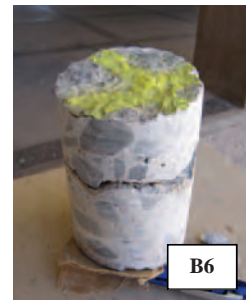
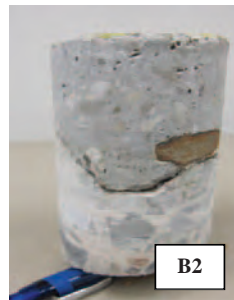
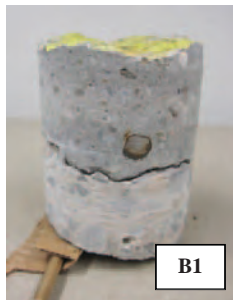
*Location of coring on the recovered bridge deck.*



*On line D (on arch).*



*On line C (between arches).*



*On line B (on arch).*

**Figure 5.20. Cores from recovered bridge deck.**

## Preparation for Validation Testing

To facilitate testing, compacted soil shoulders and ramps were built surrounding the fabricated slab, so that the surface was vehicle accessible, as shown in Figure 5.21. Similarly, the recovered bridge deck was placed into the soil ground. The hot-mix asphalt surface was removed from the deck before testing to eliminate any potential effect on the measurements. For the fabricated bridge deck, the grid test points were 1 ft apart, although the test points were 1.5 ft apart for the recovered bridge deck.

All the field validation testing participants took part in the laboratory testing as well. The participants were asked to submit the results no later than 2 weeks after conducting their tests. Figures 5.22 to 5.25 illustrate data collection by different participants.



**Figure 5.21.** Fabricated bridge deck (top) and recovered bridge deck (bottom) in place for testing.



**Figure 5.22.** Air-coupled impact echo (left): University of Illinois. Impact echo (right): NDT Corporation.



**Figure 5.23. Impact echo (left): Olson Engineering. Impact echo (right): Rutgers University.**



**Figure 5.24. Air-coupled impact echo (left): University of Texas at Austin. Ground-penetrating radar (right): Rutgers University.**



**Figure 5.25. Infrared thermography (left): FHWA. Ultrasonic surface waves (right): Rutgers University.**

## CHAPTER 6

# Results and Discussion

Each participant submitted a report within 2 weeks of testing, as per the instruction provided to them before testing. The results from both laboratory and field validation testing are presented and discussed in this chapter, as submitted by the participants.

### Field Validation Testing

As shown in Figures 5.12 and 5.13 in Chapter 5, the Virginia bridge section was distressed at least by delaminations and vertical cracking. Results from validation tests on that bridge section by different NDT methods and devices are as follows.

#### Impact Echo

Five participants conducted IE tests on the Haymarket Bridge section. Results from these tests are compared in Figure 6.1. All the participants identified five sections of the deck with predominant delaminations. Despite using various impact sources and different parameters (frequency, amplitude, thickness) for data analysis, the resulting contour maps and interpretations are generally in good agreement in defining the main areas of delamination. Comparing these maps with the observations made from the cores (Figure 5.13 in Chapter 5) confirms the capability of the impact echo method in detecting major delaminated areas. On each map, locations of the delaminated cores are marked with stars, and locations of the cores where no delamination was observed are marked with circles.

#### Ultrasonic Surface Waves, Impulse Response, Infrared Thermography, and Chain Dragging and Hammer Sounding

The ultrasonic surface waves (USW) data are presented in Figure 6.2a. The primary objective of the USW test is to provide the condition assessment and quality of concrete through measuring concrete modulus. However, the presented modulus

plot indicates that zones of very low moduli provide a good match with delaminated zones identified by other methods.

Other technologies that primarily targeted delaminations were impulse response, infrared thermography, and chain dragging and drag/hammer sounding. Chain dragging and drag/hammer sounding indicate delaminations at the correct locations on the deck (Figure 6.2b through 6.2d). The impulse response technology was not very successful in detecting the delaminated areas. Infrared thermography was not as successful in identifying the delaminated areas. One of the reasons for this was that there were many people on the deck running various tests simultaneously. The shadows cast from these people could have affected the results. Therefore, it was difficult to draw a reasonable conclusion from the infrared thermography data.

#### Ground-Penetrating Radar

Five participants conducted GPR tests on this bridge section. Results from these tests are compared in Figure 6.3. All GPR maps are based on signal attenuation of the top rebar level. The delaminated areas are indirectly detected based on the areas with high-energy attenuation. Despite some discrepancies between maps regarding boundaries and the intensity of the deterioration, they are generally in good agreement. The five sections of the deck with predominant delaminations were also identified as deteriorated areas by all participants using GPR (Figure 6.3). These areas to some extent match those identified by the impact echo method (Figure 6.1).

The depth of the concrete cover that was estimated by a participant using GPR is shown in Figure 6.4.

#### Electrical Resistivity and Half-Cell Potential

Electrical resistivity describes the corrosive environment, which in some cases is correlated to the corrosion rate, while the half-cell potential measurement yields the probability

*(text continues on page 52)*



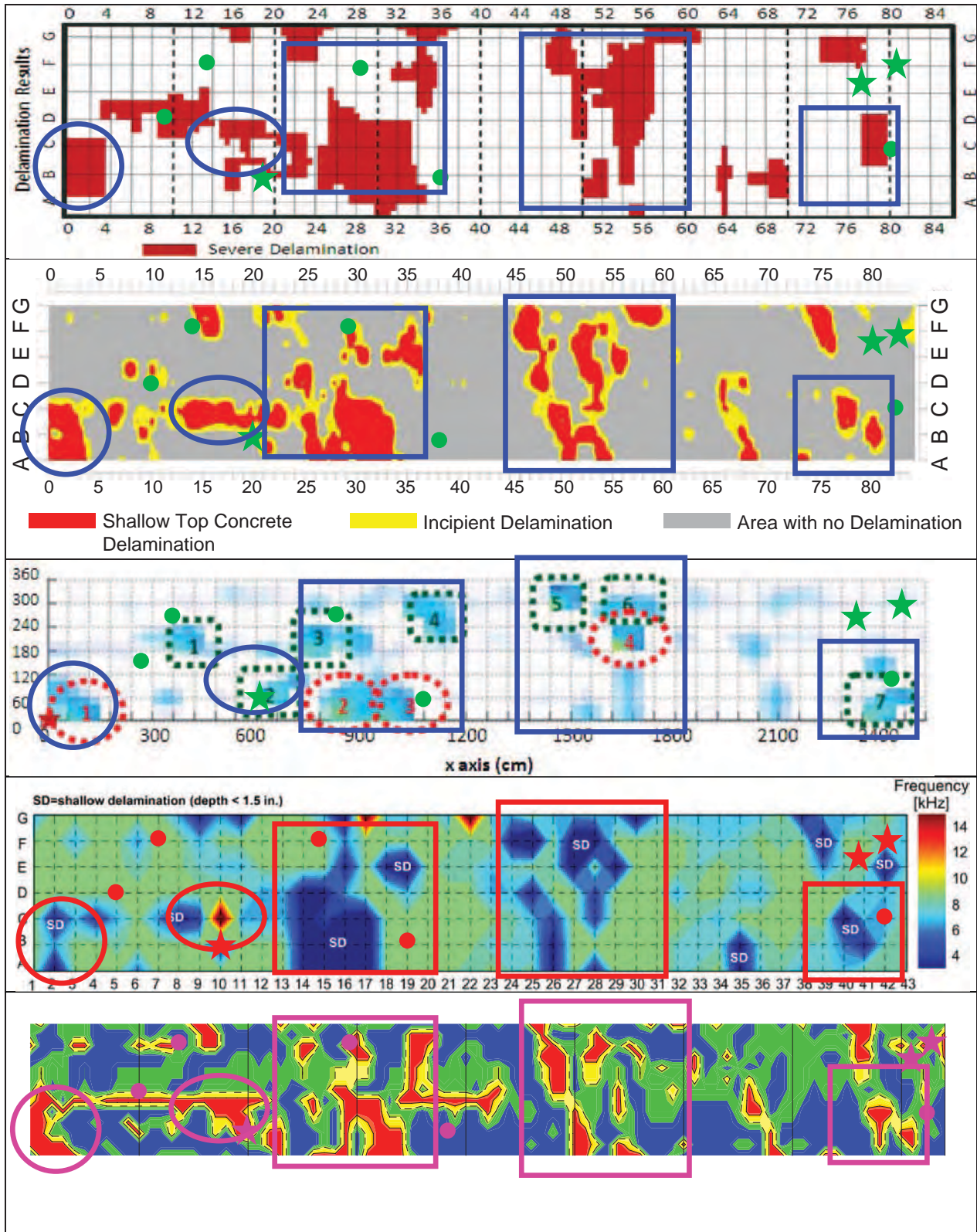
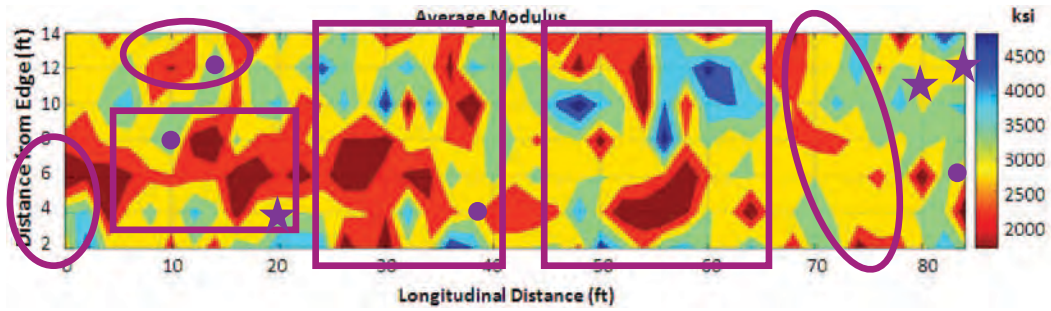
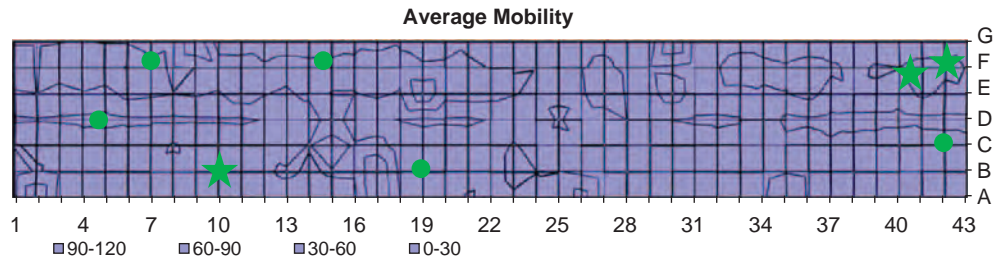


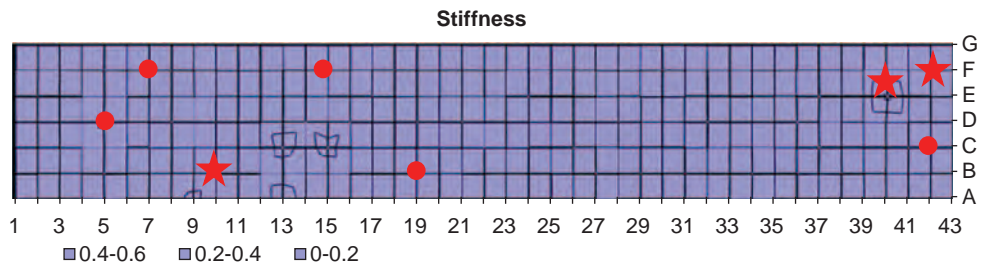
Figure 6.1. Comparison of results from IE tests on actual bridge section by different participants.



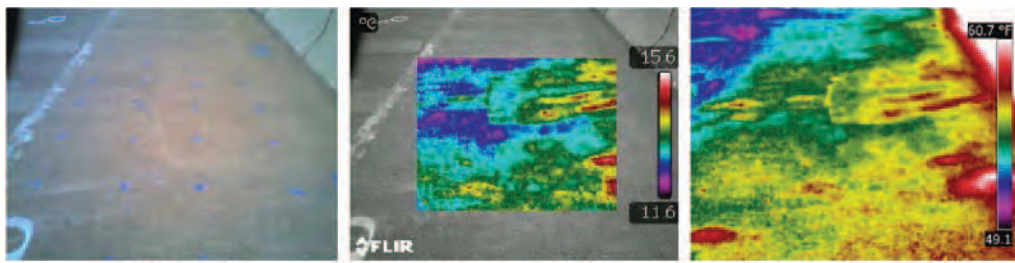
(a)



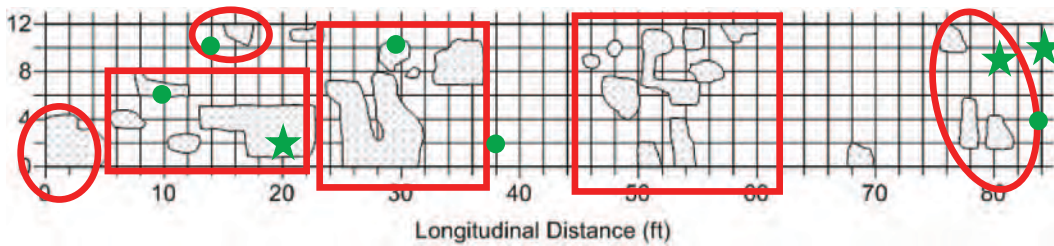
(b)



(c)



(d)



(e)

**Figure 6.2.** USW (a), impulse response (b, c), infrared thermography (d), chain dragging and hammer sounding (e).

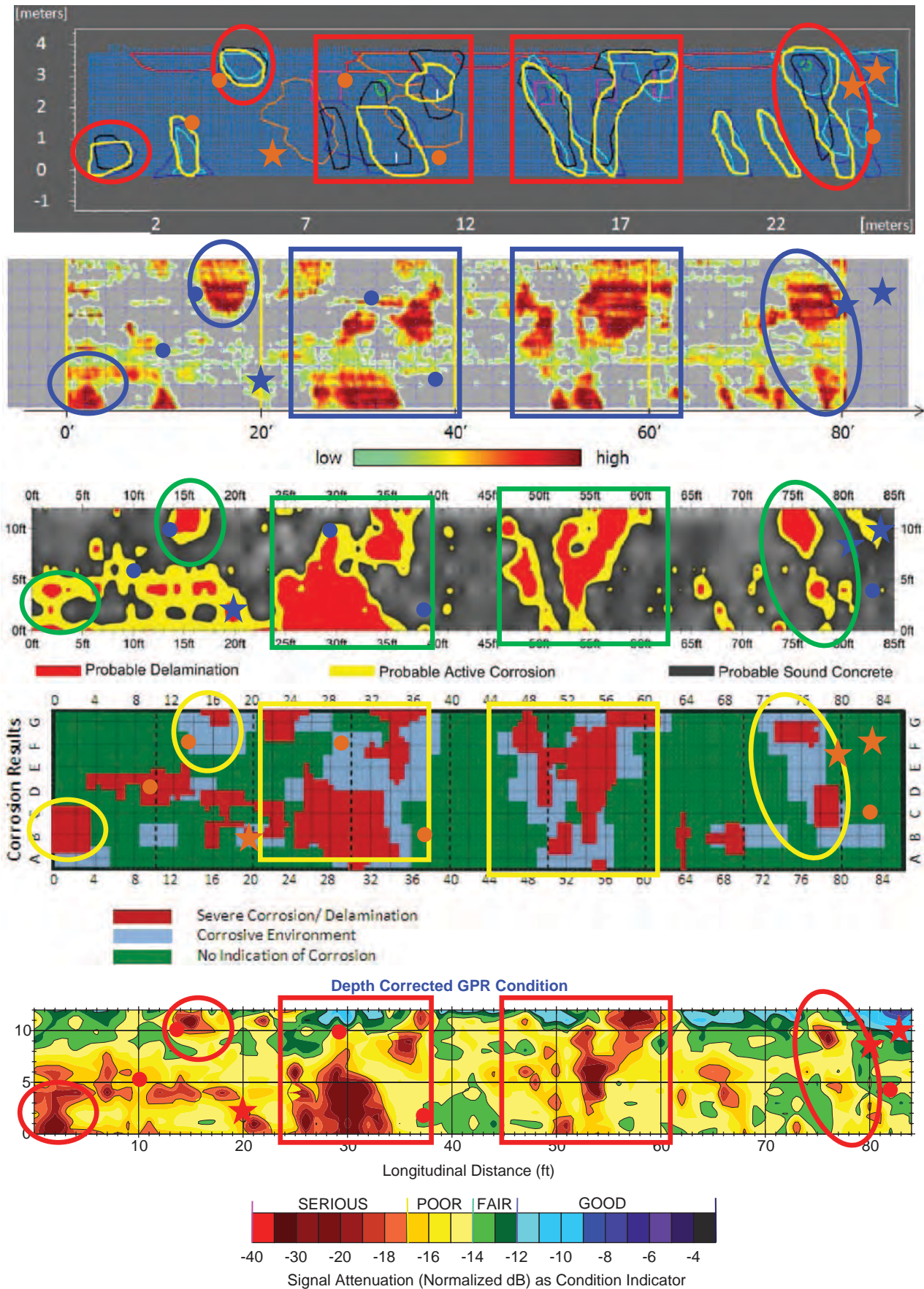
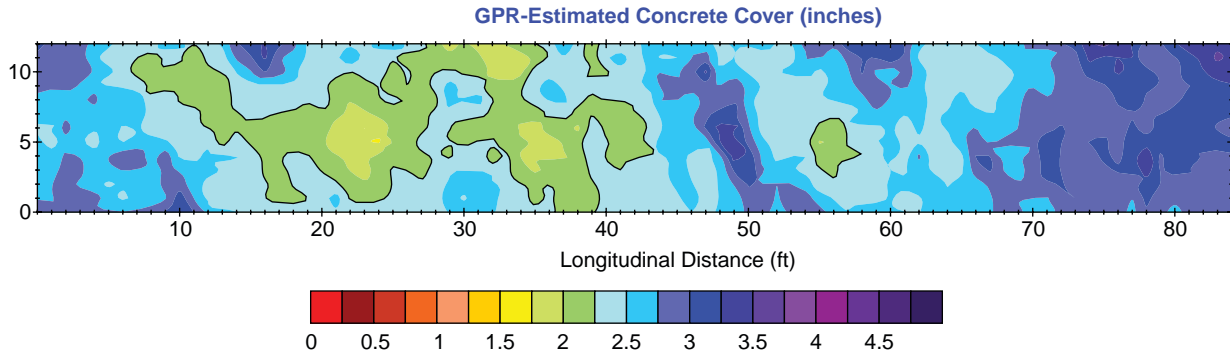


Figure 6.3. Comparison of results from GPR tests on actual bridge section by different participants.



**Figure 6.4. Concrete cover estimation based on GPR results.**

(continued from page 48)

of active corrosion. Although these measurements represent different parameters, maps obtained from the two techniques correlate well (Figure 6.5). It must be noted that this is not always the case, and one technique cannot replace the other.

Tables 6.1 and 6.2 show how well various participants' results were in agreement with the core conditions in terms of delamination detection. It should be again emphasized that

this evaluation is not technology centered; rather, it is based on the participants. In these two tables, the red cells correspond to a falsely detected delamination and the green cells correspond to a correctly detected delamination. A cell is yellow if the prediction was somewhat similar to the core condition. NA means that the participant did not provide data for that particular core. All technologies report a number of false readings; however, most major defects are detected.

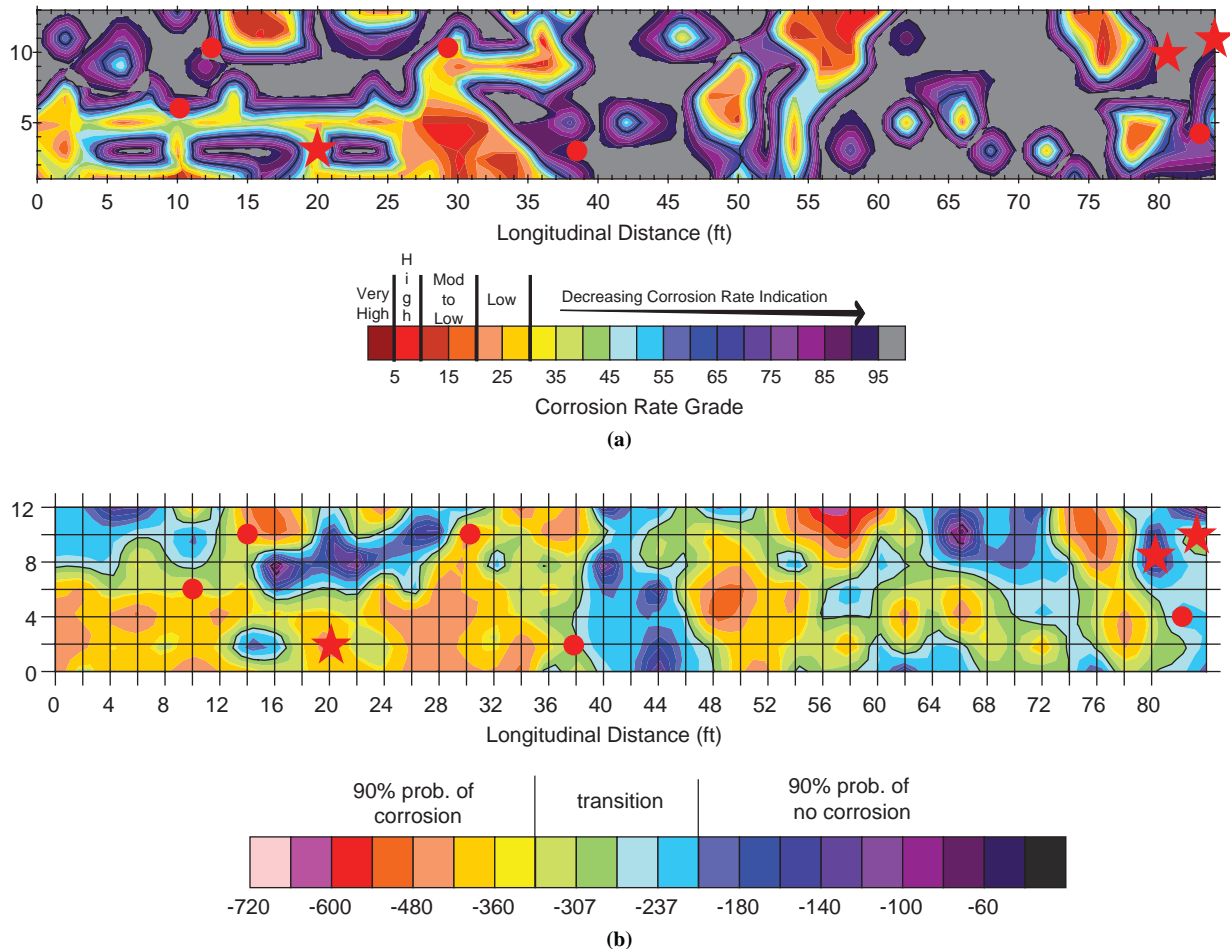


**Figure 6.5. Electrical resistivity (a) and HCP (b).**

**Table 6.1. Detectability of Delamination by IE and Chain Dragging and Hammer Sounding Methods**

Participant	Technology	C1	C2	C3	C4	C5	C6	C7	C8
9	IE	Green	Green	Green	Green	Green	Green	Green	Green
9	Chain dragging and hammer sounding	Green	Green	Red	Red	Green	Green	Green	Green
6	Air-coupled IE	Green	Green	Red	Green	Red	Green	Green	Green
7	IE	Green	Green	Red	Green	Green	Red	Green	Green
1	IE	Green	Green	Red	Red	Red	Green	Green	Green
2	Infrared	Green	Green	Red	Green	Green	Yellow	Green	Green
<b>Correct Detection</b>		<b>False Detection</b>		<b>Approximate Detection</b>			<b>No data available: NA</b>		

**Table 6.2. Detectability of Delamination by GPR**

Participant	C1	C2	C3	C4	C5	C6	C7	C8	
1	Green	Green	Red	Red	Yellow	Green	Green	Green	
8	Green	NA	NA	Green	Green	Red	Green	NA	
9	Green	Green	Red	Yellow	Yellow	Green	Yellow	Green	
4/5	Green	Green	Yellow	Green	Green	Green	Green	Green	
4	Green	Green	Red	Green	Red	Green	Green	Green	
<b>Correct Detection</b>		<b>False Detection</b>		<b>Approximate Detection</b>			<b>No data available: NA</b>		

**Repeatability Measurements**

The participants chose a number of ways to report their repeatability measurements. Some of the participants described and illustrated the repeatability of the technology in terms of the measured raw data, whereas others described the repeatability after some degree of analyzing the raw data. A third group reported the repeatability after the interpretation of the results. Figure 6.6 is a sample of the results extracted from the participants’ reports. The top figure illustrates the repeatability of a series of impact echo measurements described in terms of the frequency spectra (analyzed data). The next figure illustrates the repeatability of the impact echo measurements in terms of the delamination characterization (interpreted data). Finally, the two sets of repeatability results for half-cell potential and electrical resistivity are based on the raw field measurements.

**Laboratory Validation Testing: Fabricated Bridge Deck**

**Impact Echo**

Six participants conducted either the ground-coupled IE or air-coupled IE tests on the fabricated deck to primarily detect the delaminated areas simulated in the deck. The condition maps reported by the participants are shown in Figures 6.7 and 6.8. For comparison, the horizontal distribution of defects as-built in the deck is also shown in each figure. For example, the main features in Figure 6.7c correspond to the

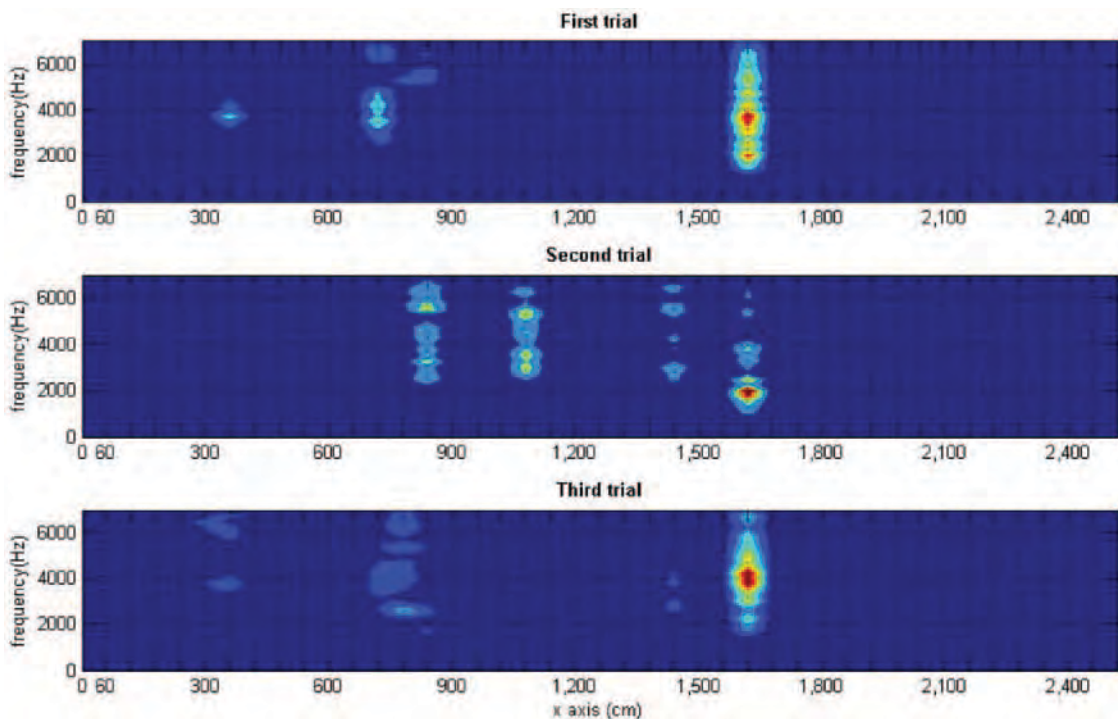
frequency of the peak amplitude across the tested surface. Cold colors in this figure correspond to a lowest-frequency response, which is an indication of delamination. Another way of presenting the data is the cloud plot as shown in Figure 6.7d. Inspecting the two plots simultaneously may help improve the interpretation of the results. The participant’s protocol is to mark regions that exhibit both dense data cloud formation up to 4 kHz (Figure 6.7d) and a dominant low frequency (Figure 6.7c), which indicate the likelihood of a near-surface delamination. Regions that exhibit only sparse cloud formation up to 4 kHz, yet do exhibit a dominant low frequency, indicate the likely presence of other types of degradation.

There is a good agreement between the maps provided by the participants, especially in identifying the shallow delaminated areas. Both the air-coupled IE and ground-coupled IE methods show an acceptable capacity for detecting shallow delaminations. Significant experience seems to be needed in deep delamination detection and characterization.

**Ground-Penetrating Radar**

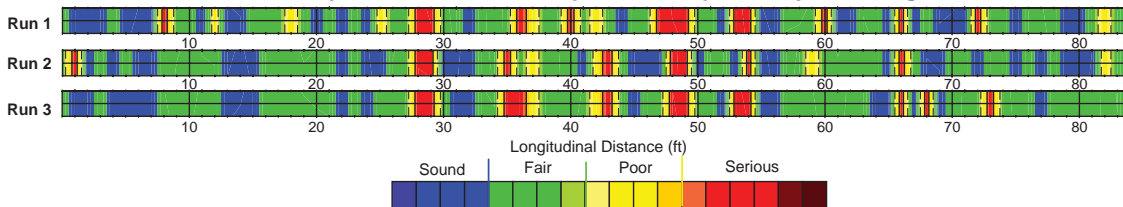
Five participants used GPR with only one system mounted on a vehicle. GPR condition maps are depicted in Figures 6.9 and 6.10. Some of the GPR condition maps identify the main areas of delamination, but in general the detection is not good. The likely reason for that can be explained in the following way. The artificial delamination in the fabricated deck

*(text continues on page 60)*



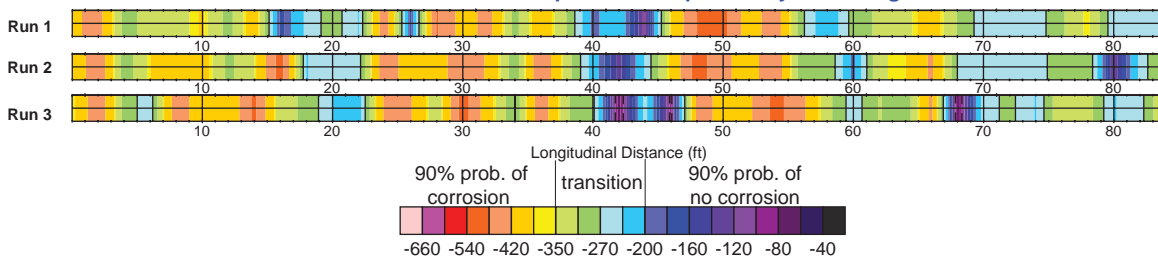
(a)

**Impact Echo Condition Map - Line D Repeatability - VA Bridge**



(b)

**Half-cell Potential Condition Map - Line D Repeatability - VA Bridge**



(c)

**Figure 6.6. Repeatability measurement results. Spectral amplitude, air-coupled IE (a); ratings based on spectral frequency, IE (b); voltage, HCP (c).**

(continued on next page)

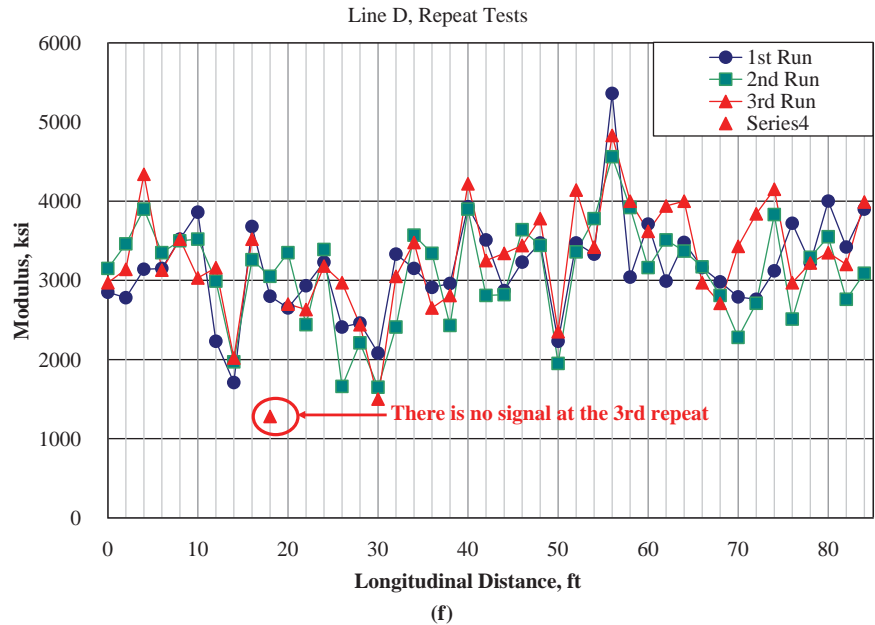
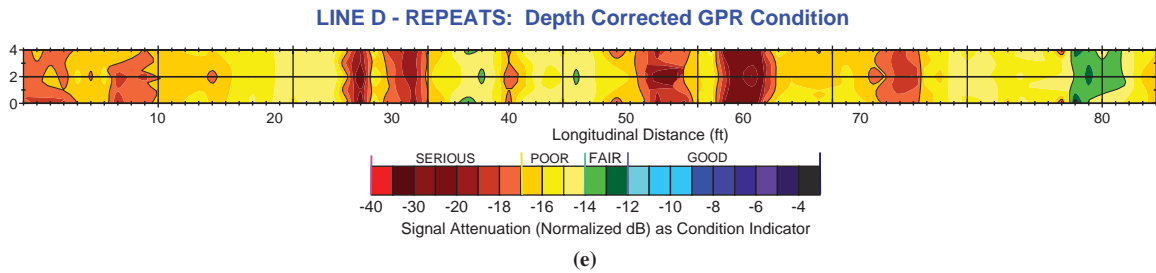
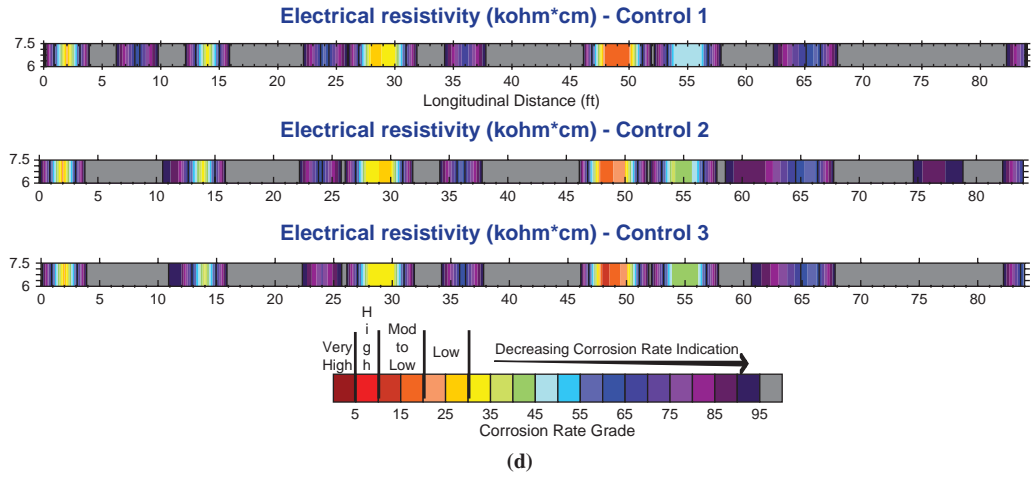
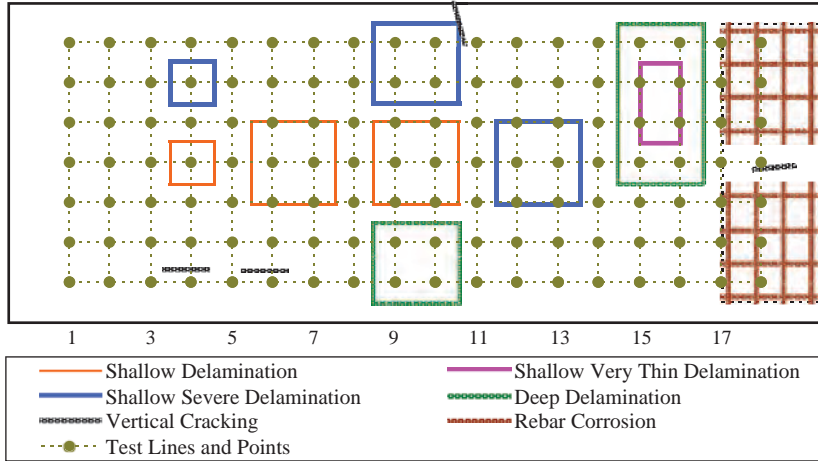
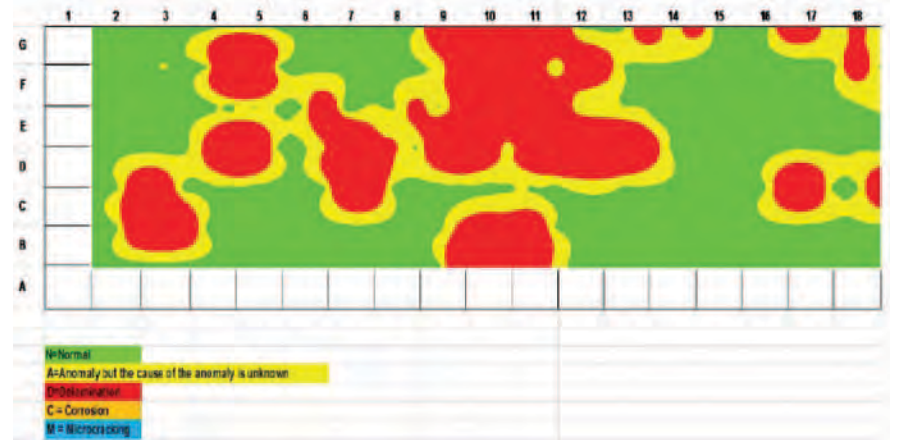


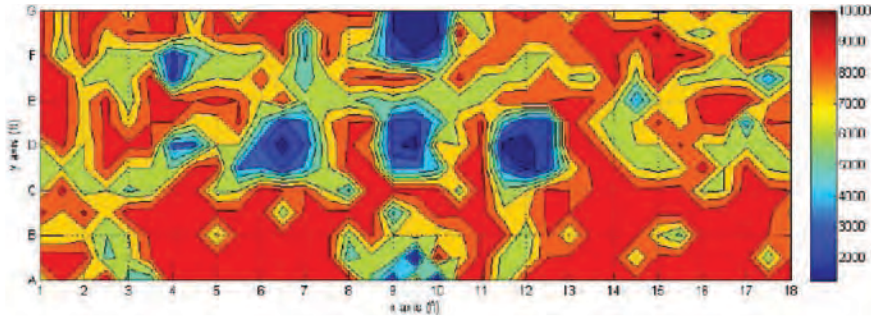
**Figure 6.6. (continued) Repeatability measurement results. Resistivity, ER (d); signal attenuation, GPR (e); and modulus, USW (f).**



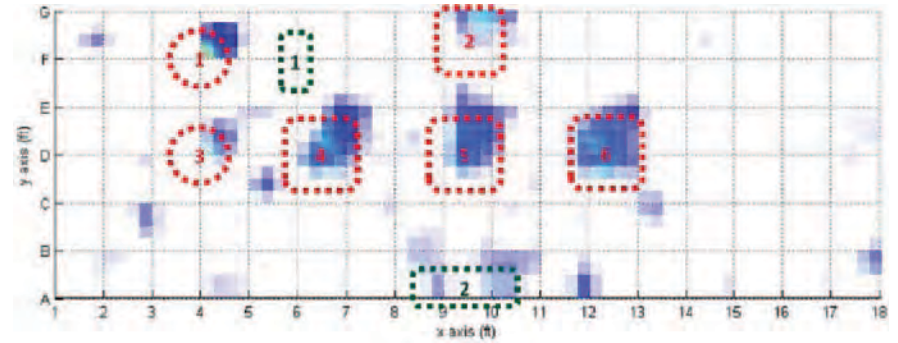
(a)



(b)



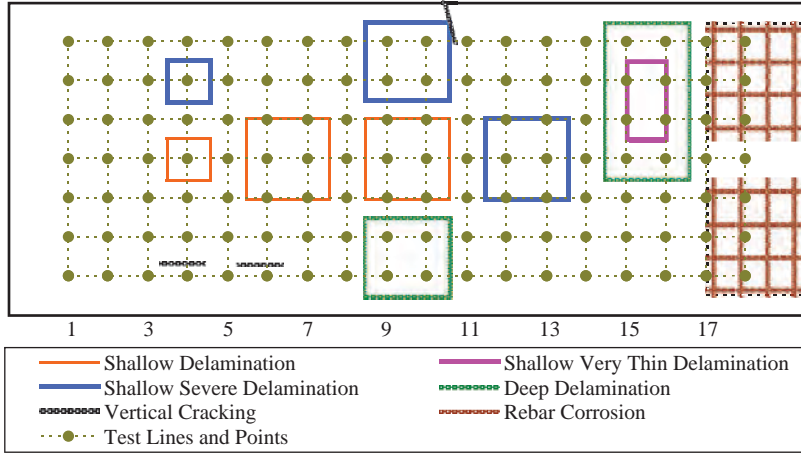
(c)



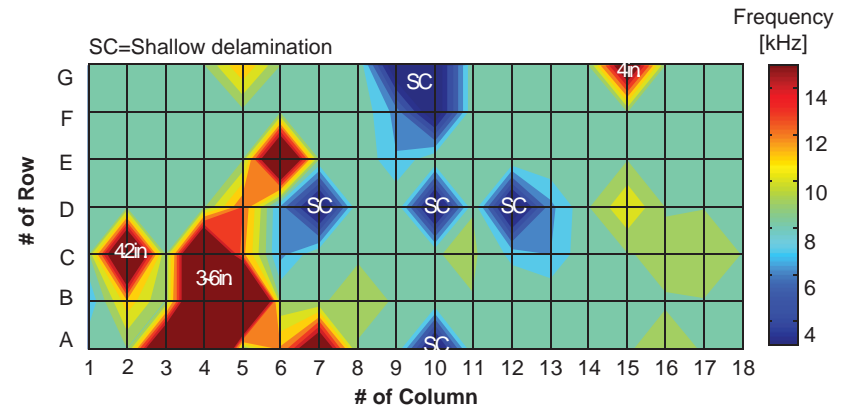
(d)

Figure 6.7. Impact echo condition maps: plan of fabricated deck (a), Participant 4 (b), and Participant 6 (c, d).

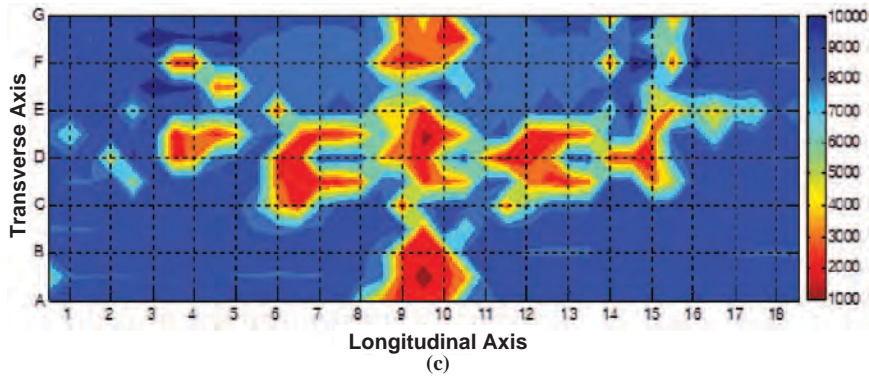




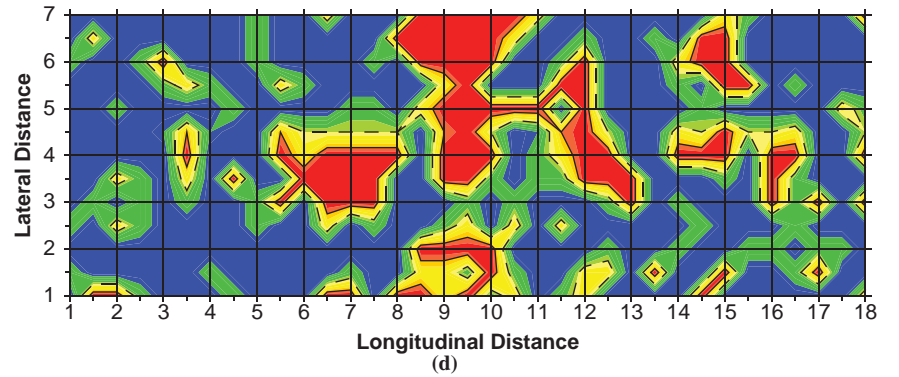
(a)



(b)

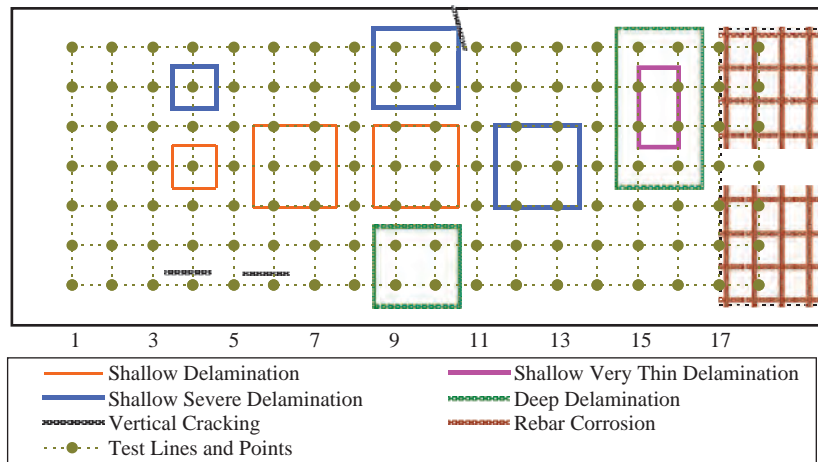


(c)

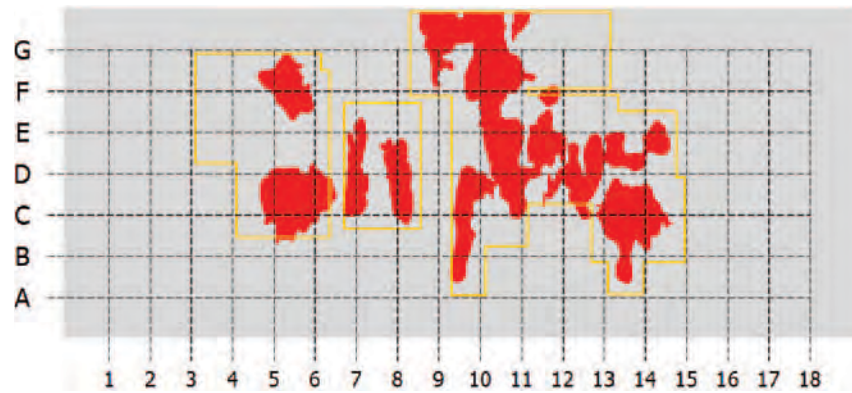


(d)

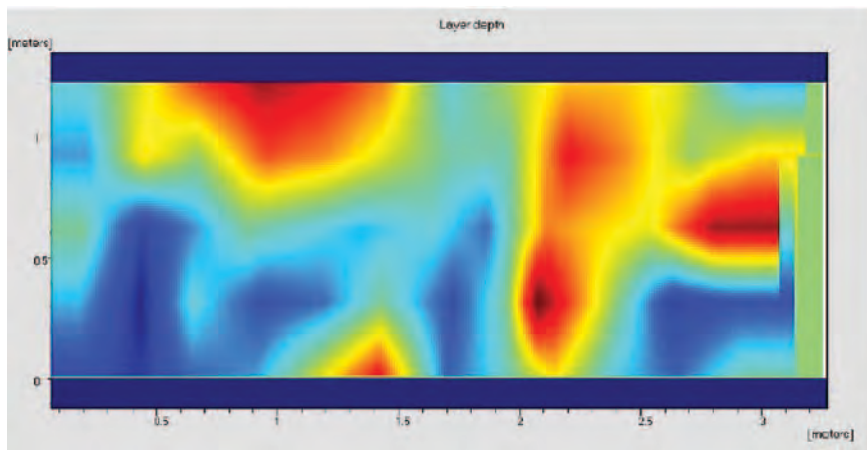
Figure 6.8. Impact echo condition maps: plan of fabricated deck (a), Participant 7 (b), Participant 10 (c), and Participant 9 (d).



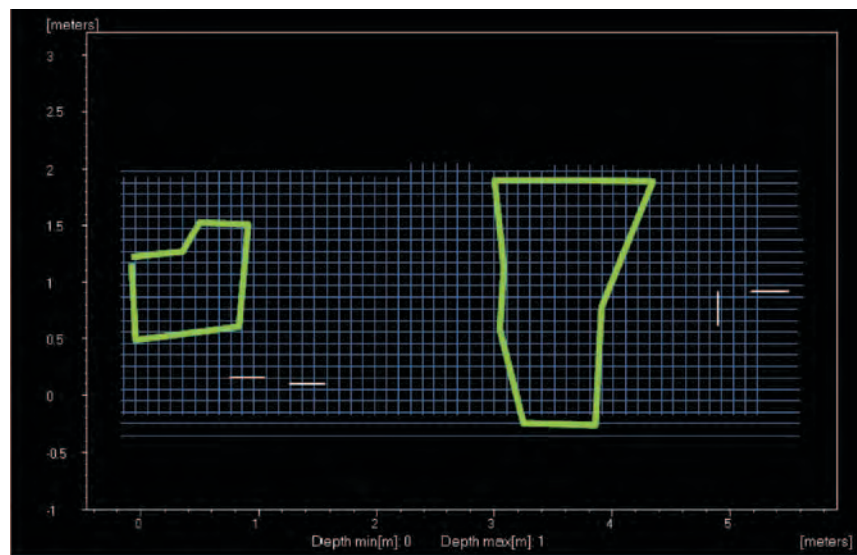
(a)



(b)

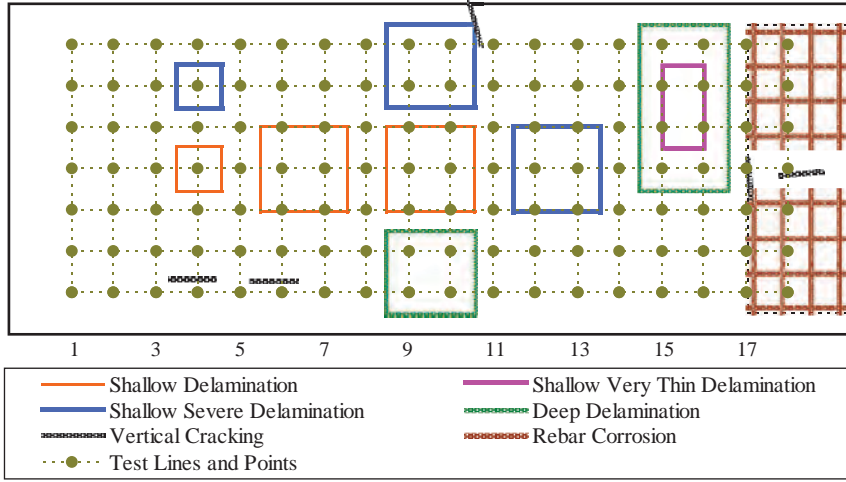


(c)

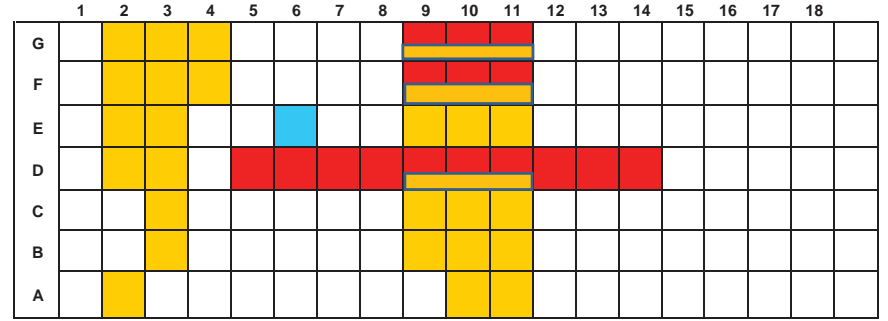


(d)

Figure 6.9. GPR condition maps: plan of fabricated deck (a), Participant 8 (b), Participant 4 (c), and Participant 5 (d).

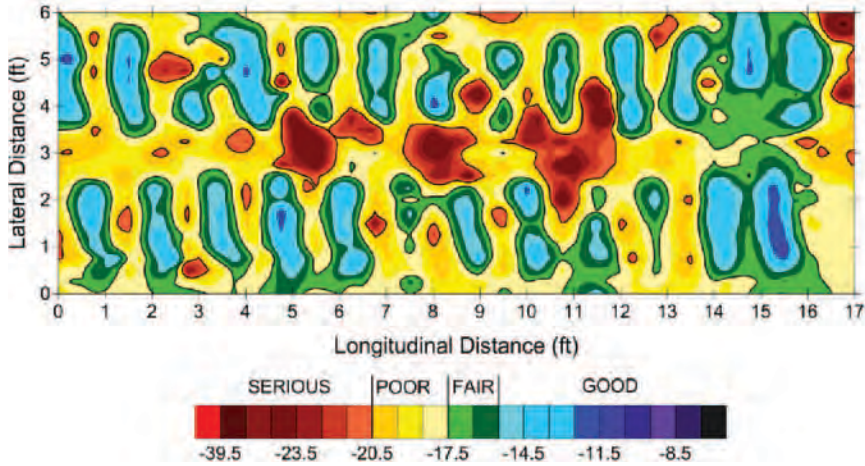


(a)

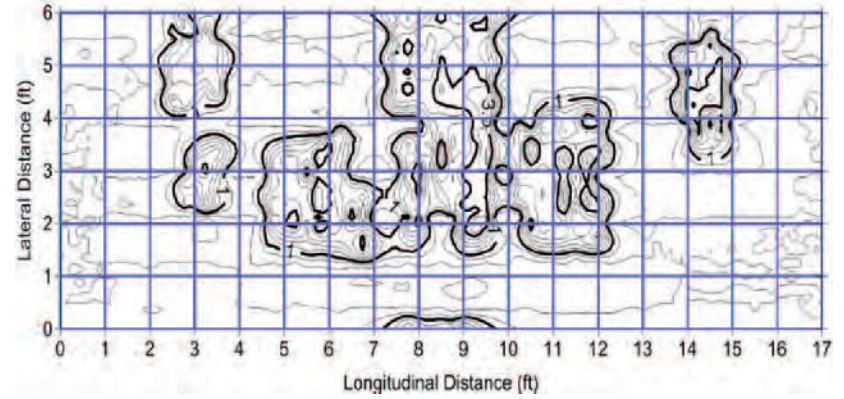


- N = Normal
- A = Anomaly but the cause of the anomaly is unknown
- D = Delamination
- C = Corrosion
- M = Microcracking

(b)



(c)



(d)

Figure 6.10. GPR condition maps: plan of fabricated deck (a), Participant 1 (b), and Participant 9 (c, d).

(continued from page 53)

was created through the placement of synthetic inserts and not through the penetration of moisture and chlorides that would create a corrosive environment leading to rebar corrosion. A corrosive environment that would foster concrete deterioration (and, in advanced stages, initiate delamination at the rebar level) manifests itself as a very high attenuation of the GPR signal. Therefore, employing GPR in this fashion, where attenuation-based deterioration is the key to identifying potentially delaminated zones, means nothing in this fabricated specimen. One of the participants was able to recognize plastic inserts as anomalies in the GPR B-scans but did not identify the same thing in the attenuation plot (Figure 6.10c and 6.10d). This is because the inserts happened to be thick enough and produced enough dielectric contrast to be directly imaged.

Results of this testing also confirm that corrosion-induced delaminations in real bridge decks are not easily reproducible in the laboratory using inserts. As shown previously, corrosion and corrosion-induced delamination were detected during the field validation using other NDT methods. These areas of delamination and highly active corrosion primarily existed in the areas where there was a highly attenuated GPR signal measured at the top rebar level. This confirms the indirect detection of delamination by GPR in real decks through EM wave attenuation caused by a conductive concrete, instead of through imaging.

### Infrared Thermography

The participant conducting passive infrared thermography tests used a FLIR T400 camera. Two sets of images from these tests at two different times and ambient temperatures are shown in Figure 6.11. Figure 6.11b (40 min after sunrise) shows much clearer images than those shown in Figure 6.11c (at about noontime) and provides information on the severity of the delamination by the significant difference in color. The difference in color indicates that the time and temperature are critically important to successfully detect the delamination with infrared methods. In addition, the fact that the delamination in this deck is simulated with plastic foam materials has to be considered. In heat capacity and heat conductivity, such materials are significantly different from air.

### Chain Dragging and Hammer Sounding, Half-Cell Potential, and Electrical Resistivity

The condition maps based on chain dragging and hammer sounding, HCP, and ER are shown in Figure 6.12. Chain dragging was able to detect shallow delaminations except for the thin or small ones, but was not able to detect the deep delaminations.

Half-cell potential could recognize some corrosion activity on the right side (upper right corner in Figure 6.12) of the

embedded reinforcement but not on the left side (lower right corner in Figure 6.12). The reason for this is that before HCP testing, the embedded electrical connection to the left section of steel was broken. This did not allow an electrical connection to be established with that portion of the reinforcement. Because the right and left sections of steel were not electrically continuous, an individual connection was required for each section in order to perform HCP. Finally, the resistivity map does not actually yield any information regarding the deck condition because the corrosion of the steel was not the result of a natural process, such as chloride and moisture ingress into the deck or concrete carbonation. Instead, the previously corroded rebars were placed in the deck.

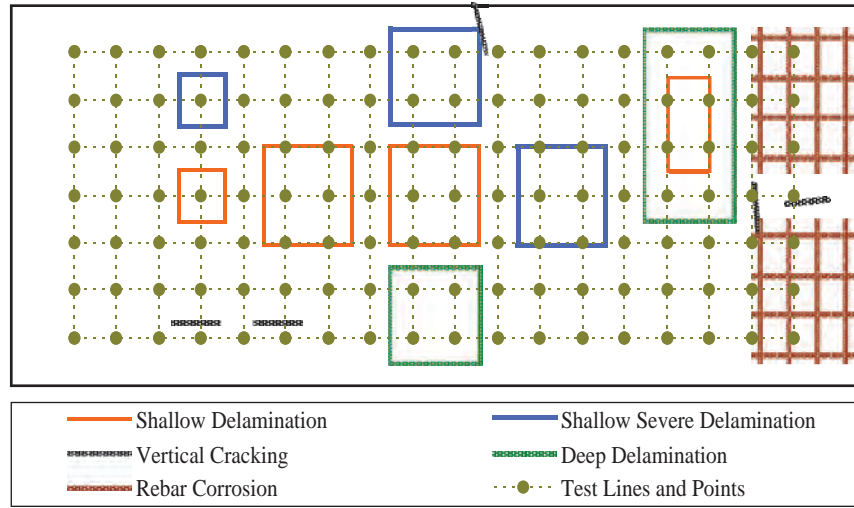
### Surface Wave Methods

Four participants reported their results from the surface wave methods. One participant mapped the variation in modulus along the depth (Figure 6.13). As anticipated, the variation in modulus is reasonably uniform except for the delaminated areas that show as degraded concrete. Three participants used the method to estimate the depth of the simulated cracks. One participant used the ultrasonic waves' time of flight and another participant used the SASW method. One participant used two alternative methods: surface wave transmission (SWT) and time-of-flight diffraction (TOFD). The results are presented in Table 6.3. The SWT method seems to be the most reasonable one.

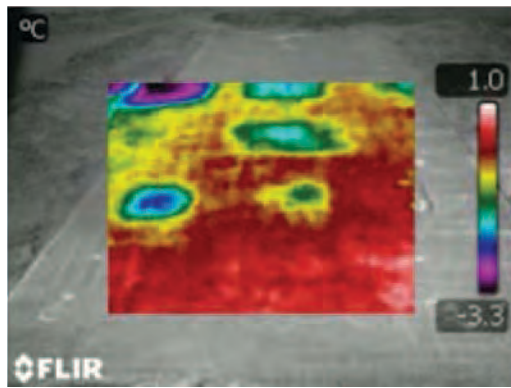
### Laboratory Validation Testing: Retrieved Bridge Deck

This deck, as shown in Figure 5.19 in Chapter 5, was seriously distressed. The deck almost universally contained stress-induced cracks of different orientations and was extensively delaminated. Information from coring further confirmed the seriously distressed situation of the deck (see Figure 5.20). The main goal of the deck validation tests was to evaluate the detectability of various NDT methods when a deck is severely distressed. The condition maps for the retrieved bridge section, as reported by different participants, are shown in Figures 6.14 through 6.18. Some of the participants chose not to report their results on this deck while others used the results from multiple tests they performed to interpret the results.

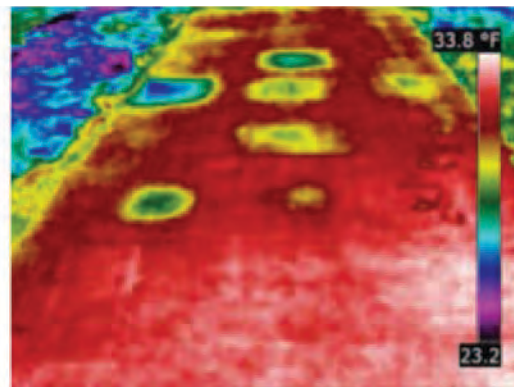
Table 6.4 and Table 6.5 show the comparisons (in the same format as for the Virginia bridge) between results reported by participants and the cores' conditions in terms of delamination detection. None of the participants could report with certainty that the deck was uniformly damaged. This may be because most methods rely on anomalies in the signal to decipher the condition of the deck.



(a)

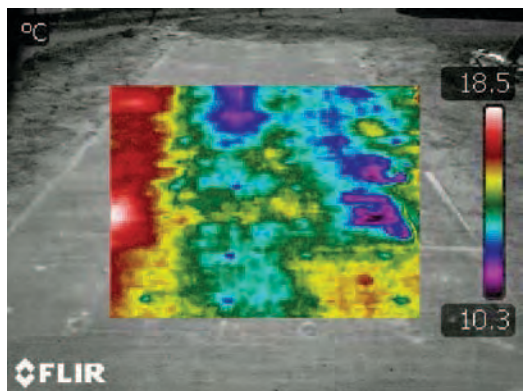


Fusion Image

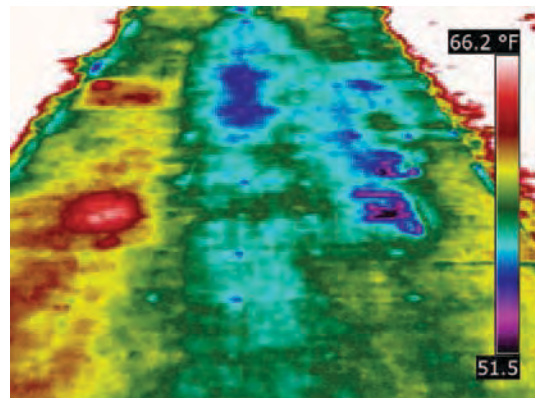


Infrared Image

(b)



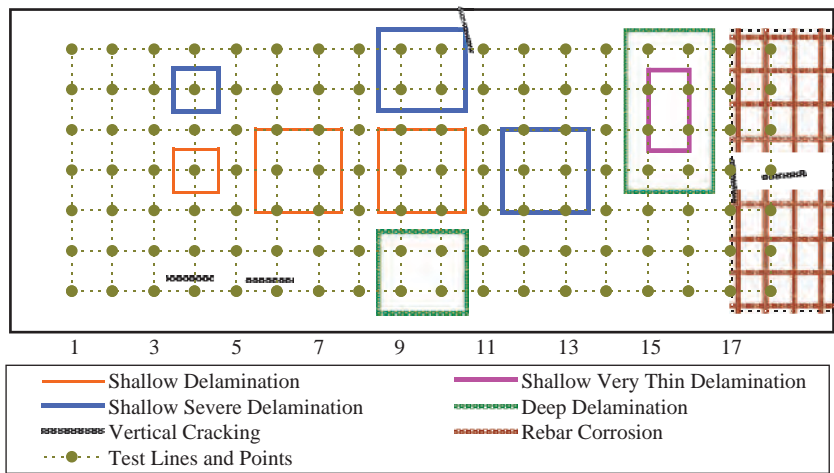
Fusion Image



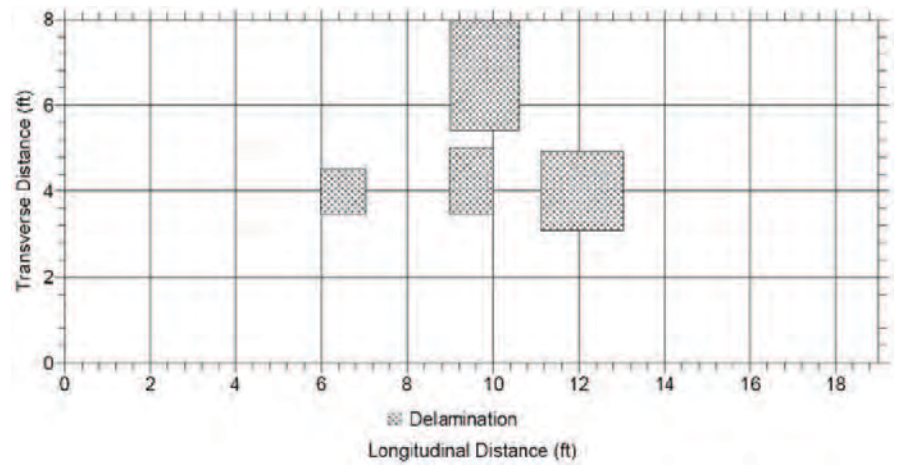
Infrared Image

(c)

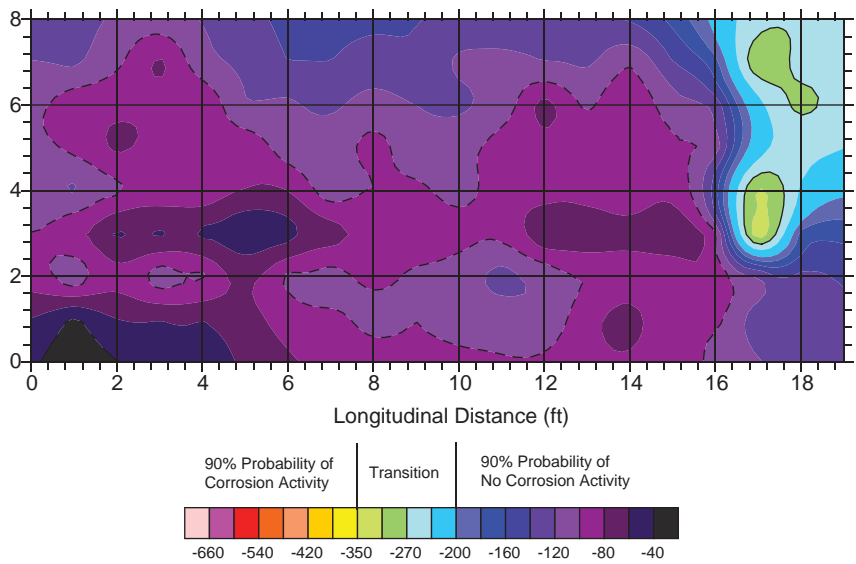
**Figure 6.11. Infrared images: plan of fabricated deck (a) and Participant 2 (b, c). Infrared image (c) is taken from the opposite side.**



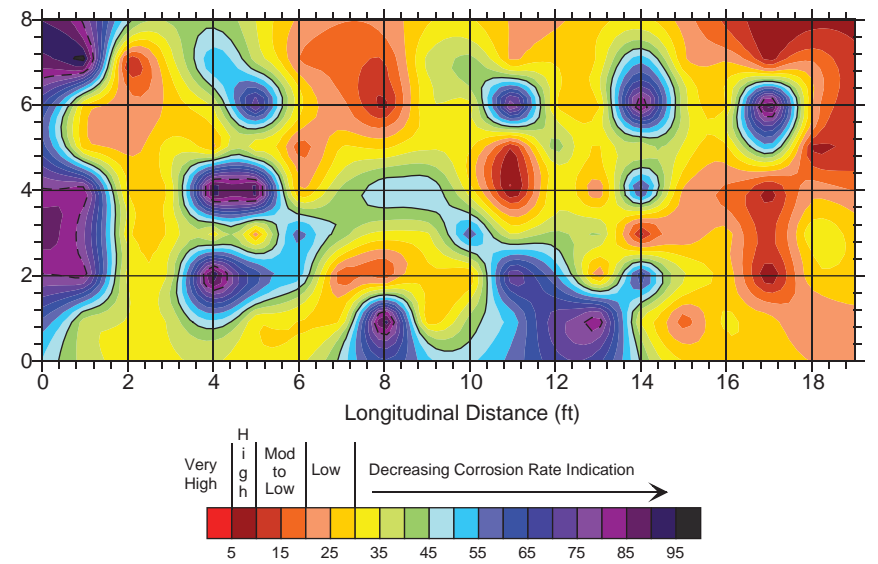
(a)



(b)



(c)



(d)

**Figure 6.12. Plan of fabricated deck (a), chain dragging and hammer sounding (b), HCP (c), and ER (d). Participant 9.**

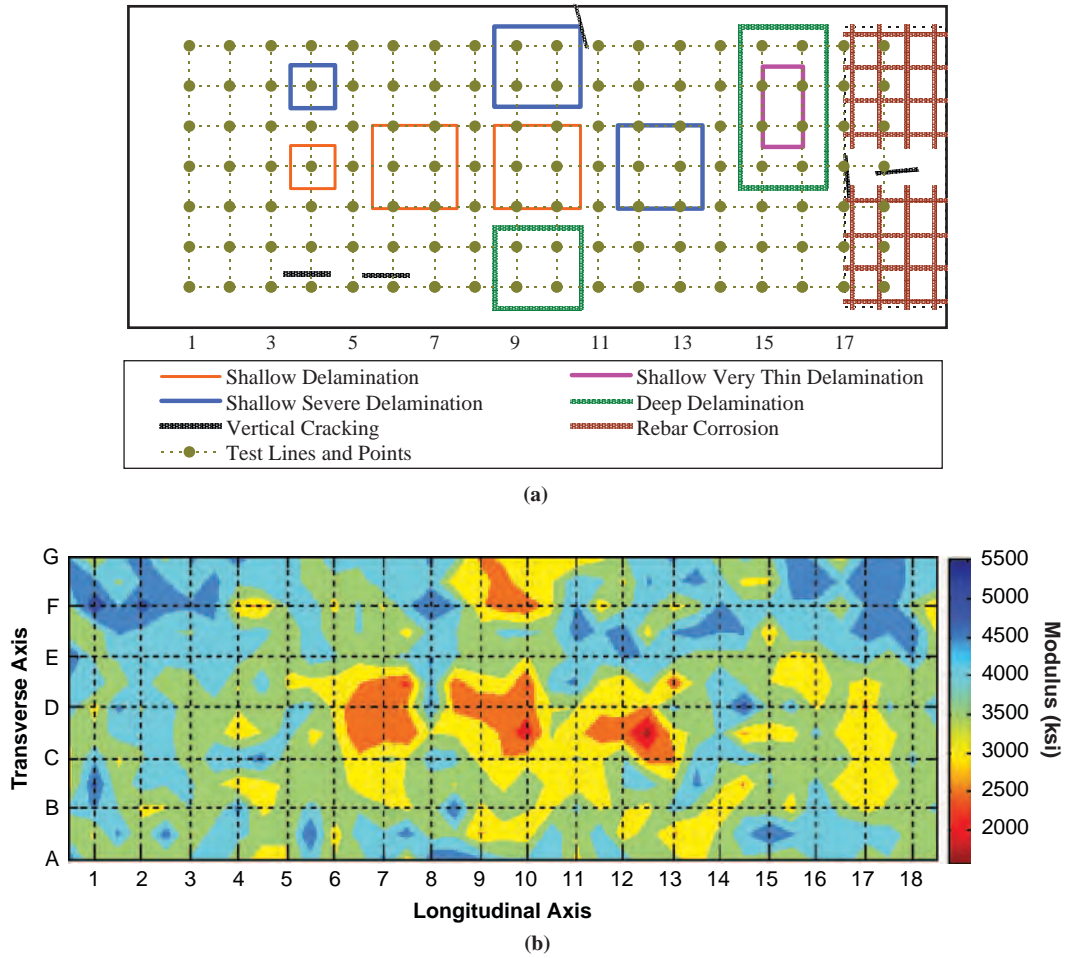


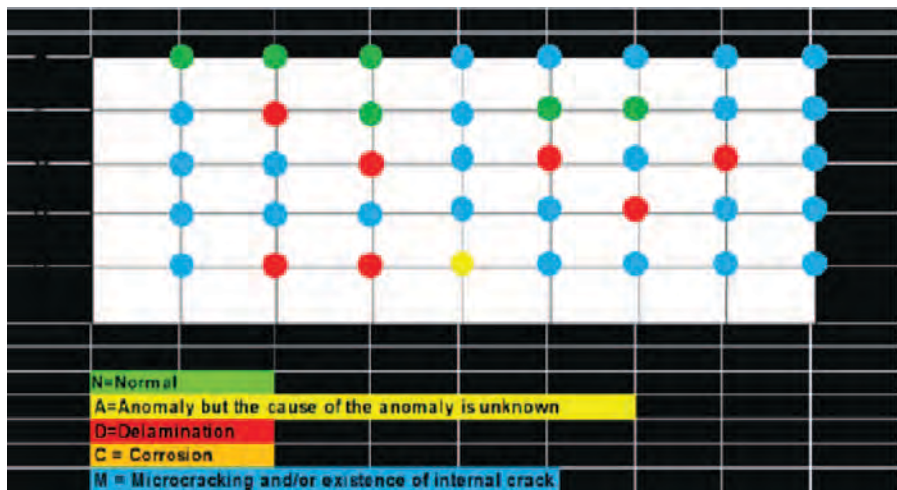
Figure 6.13. Plan of fabricated deck (a) and apparent modulus mapping for delamination (b). Participant 10.

Table 6.3. Comparison of Crack Depths (in.) Estimated by Participants and As Built

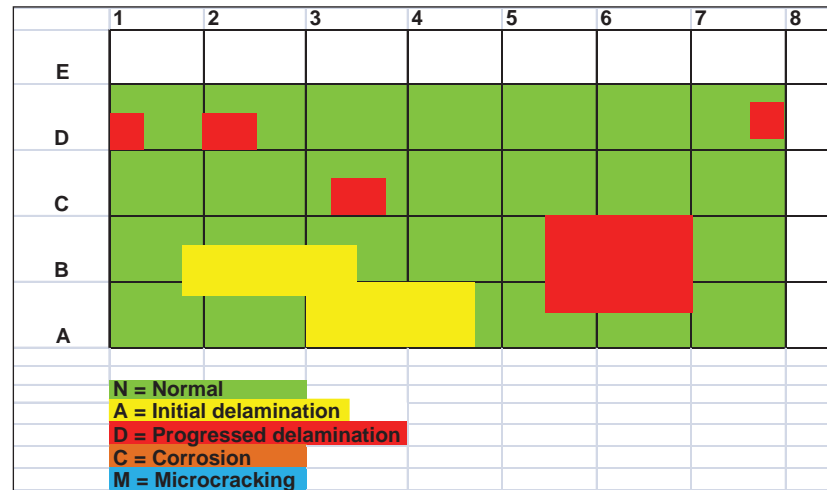
Crack	Ultrasonic	SASW	SWT	TOFD	As Built
CK1	Down to top rebar	6.0	2.0 ~ 2.5	NA	2.5
CK2	Surface	4.8	1.1 ~ 1.5	NA	2.5
CK3	Between two rebar mats	4.8	2.5 ~ 3.7	3.8	3.0
CK4	Down to top rebar	5.4	4.0 ~ 5.7	5.8	6.0
CK5 <sup>a</sup>	Down to top rebar	Shallow	NA	NA	2.5

Note: NA = not available.

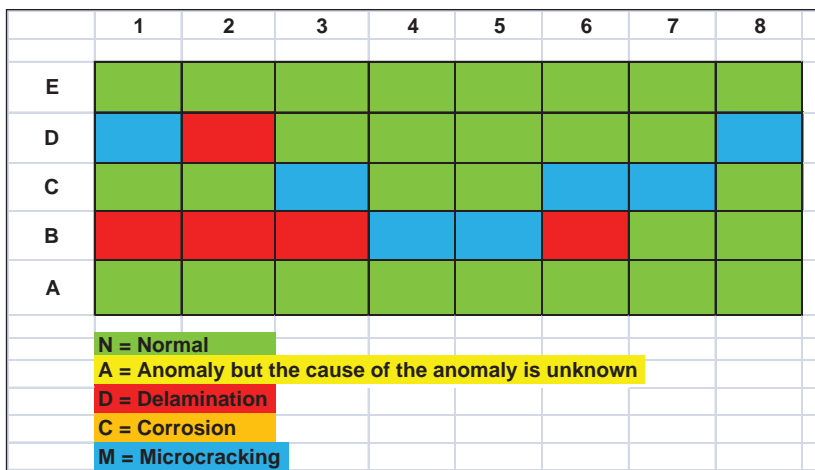
<sup>a</sup>Natural crack from the edge of the deck (depth was measured at the edge).



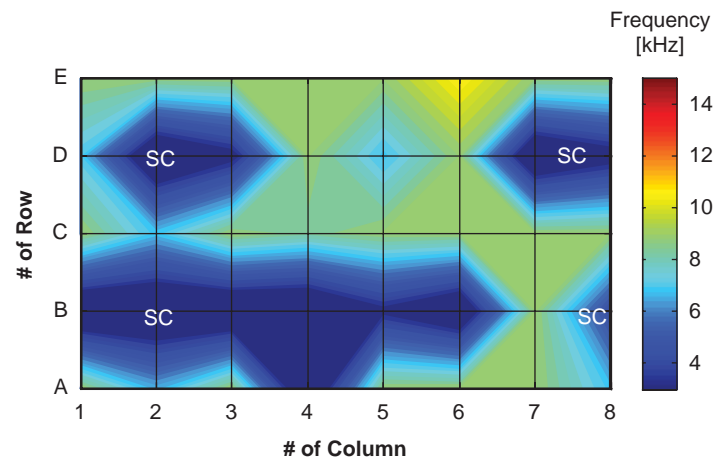
(a)



(b)



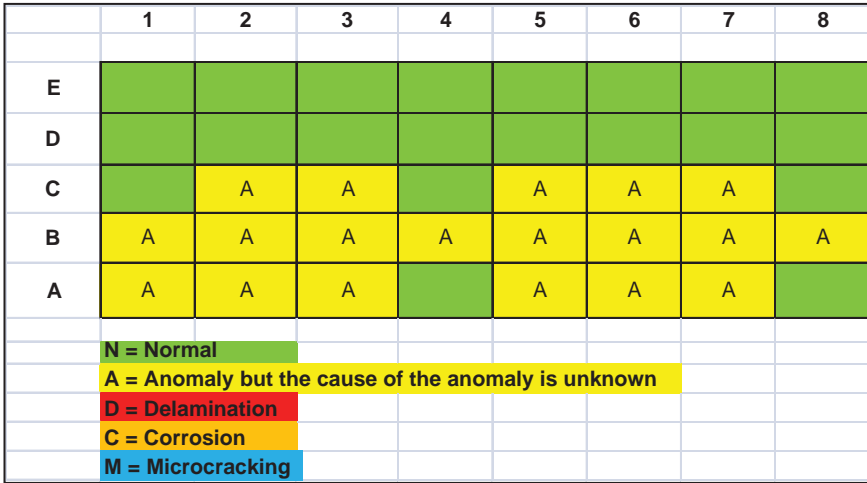
(c)



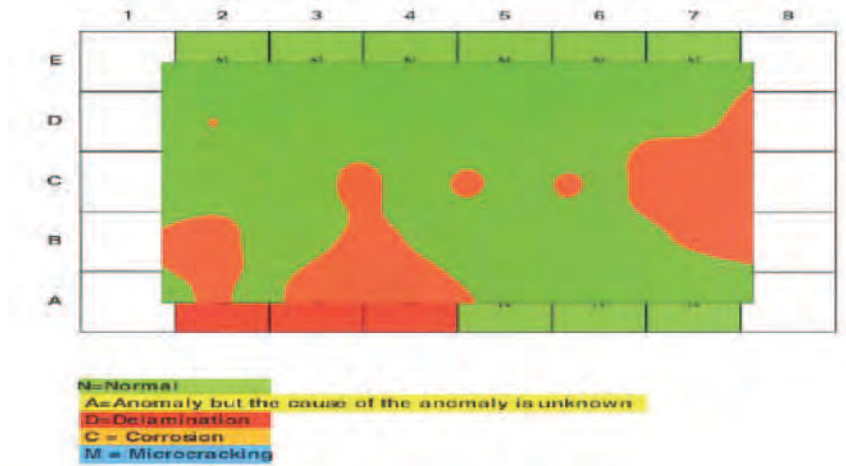
(d)

Figure 6.14. Impact echo condition maps: Participant 4 (a), Participant 6 (b), Participant 1 (c), and Participant 7 (d).

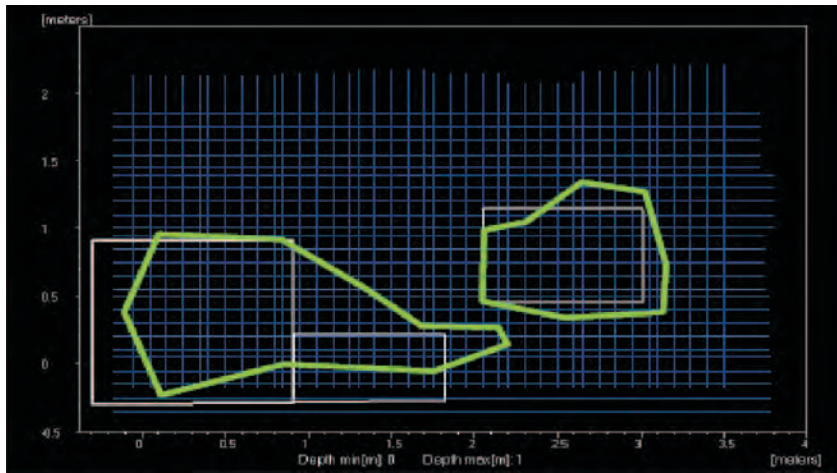




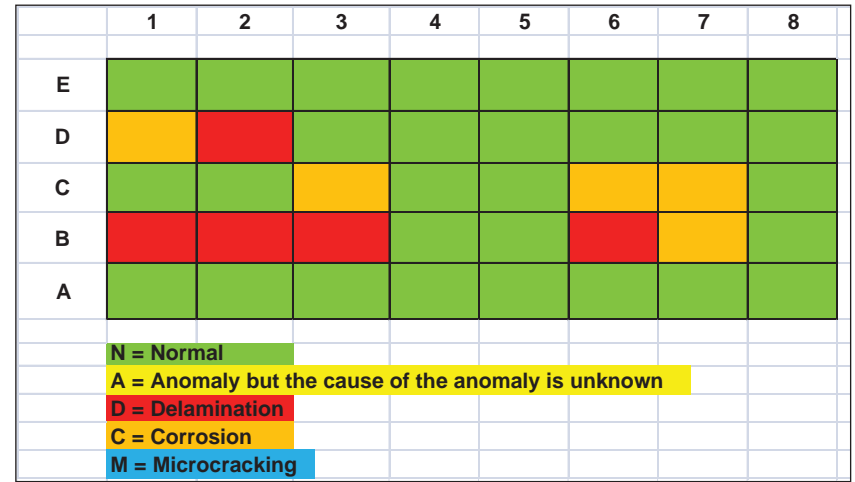
(a)



(b)



(c)



(d)

Figure 6.15. GPR condition maps: Participant 8 (a), Participant 4 (b), Participant 5 (c), and Participant 1 (d).

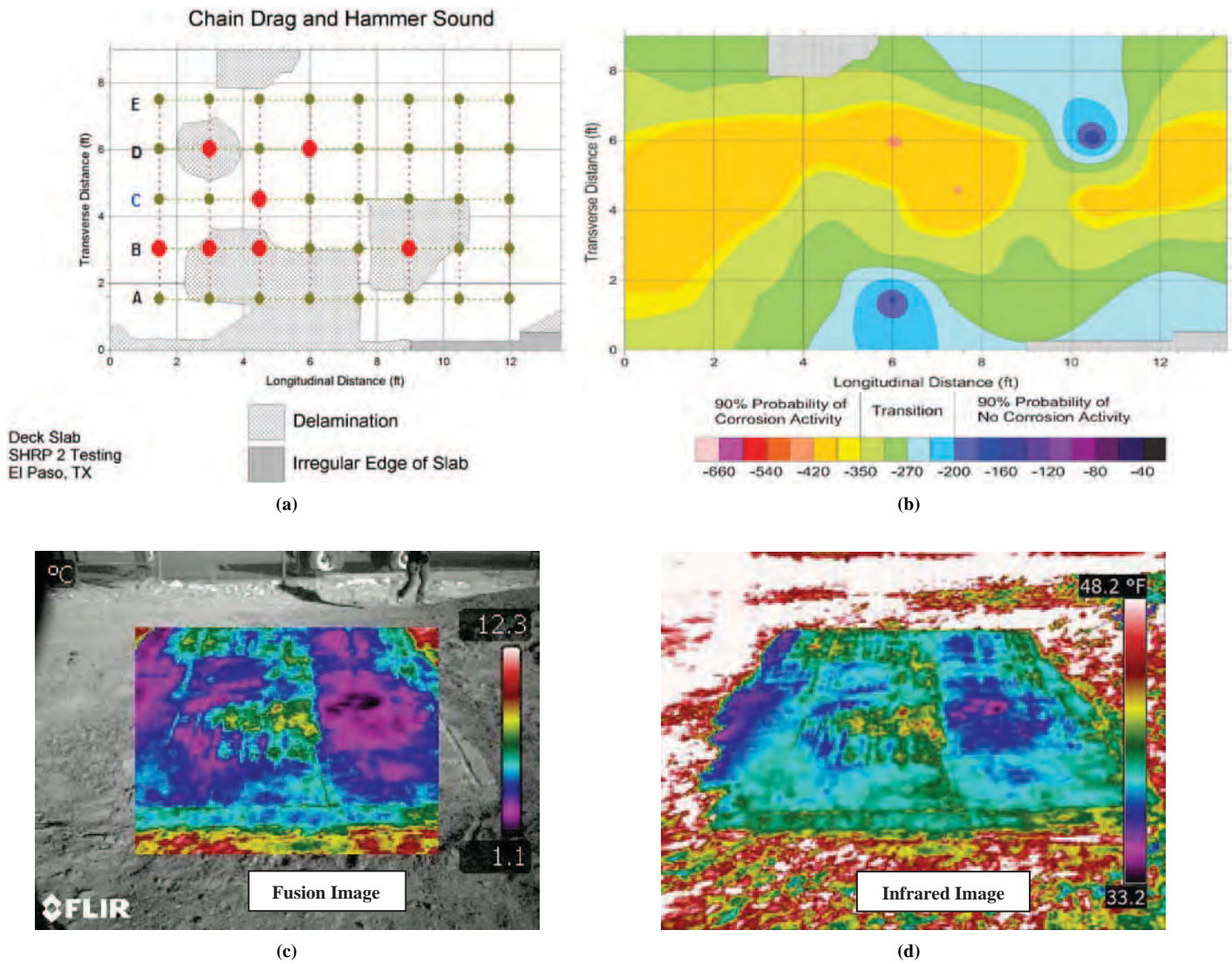


Figure 6.16. Condition maps of chain dragging and hammer sounding (a); HCP, Participant 9 (b); and infrared thermography, Participant 2 (c, d).

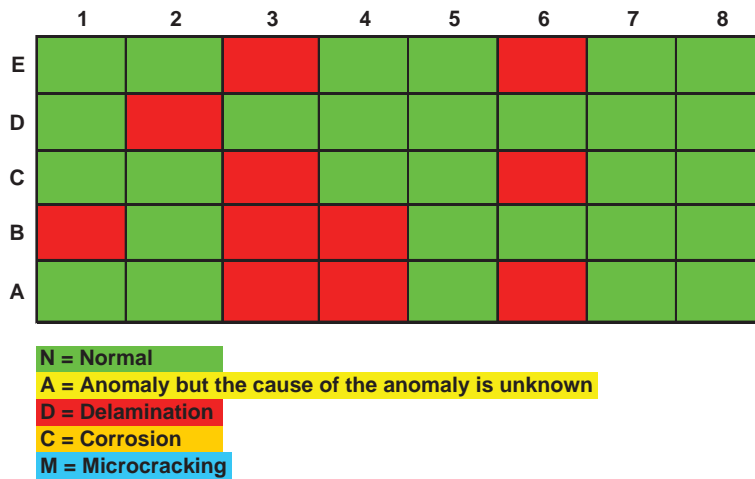


Figure 6.17. Impact echo condition maps: Participant 9.

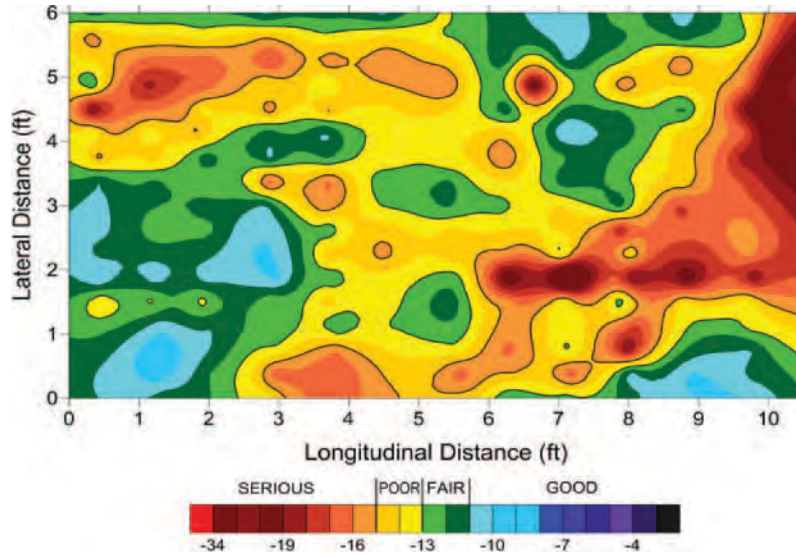


Figure 6.18. GPR condition maps: Participant 9.

Table 6.4. Delamination Detectability by Impact Echo, Infrared, and Chain Dragging and Hammer Sounding

Participant	Technology/Device	Coring Location							
		B1	B2	B3	B6	C3	D2	D4	
1	IE/Ultrasonic	Yellow	Yellow	Yellow	Yellow	Red	Yellow	Red	
4	IE Scanning	Red	Red	Red	Yellow	Yellow	Yellow	Red	
6	Air-coupled IE	Red	Yellow	Yellow	Yellow	Yellow	Yellow	Red	
7	Air-coupled IE	Yellow	Yellow	Yellow	Yellow	Red	Yellow	Red	
9	Air-coupled IE	Yellow	Red	Yellow	Red	Yellow	Yellow	Red	
2	Infrared (fusion image)	Yellow	Yellow	Yellow	Yellow	Red	Yellow	Yellow	
9	Chain dragging and hammer sounding	Red	Yellow	Yellow	Yellow	Red	Yellow	Red	
<i>False Detection</i>				<i>Approximate Detection</i>					

Table 6.5. Detectability of Delamination by GPR

Participant	Technology/Device	Coring Location							
		B1	B2	B3	B6	C3	D2	D4	
1	GPR	Yellow	Yellow	Yellow	Yellow	Red	Yellow	Red	
4	Aladdin 2 GHz	Yellow	Yellow	Yellow	Red	Yellow	Yellow	Red	
8	Geoscope 3 GHz	Yellow	Yellow	Yellow	Yellow	Yellow	Red	Red	
5	RIS Hi BrighT	Yellow	Yellow	Yellow	Yellow	Red	Red	Red	
9	2.6 GHz	Red	Red	Red	Yellow	Red	Yellow	Yellow	
<i>False Detection</i>				<i>Approximate Detection</i>					

## CHAPTER 7

# Evaluation and Ranking of NDT for Condition Assessment of Bridge Decks

The performance of NDT technologies was generally evaluated from the perspective of five performance measures: accuracy, precision (repeatability), ease of use, speed, and cost. The field validation testing focused mainly on the evaluation of speed, precision, ease of use, and cost, because the evaluation of accuracy was limited by the extent of ground truth information. Evaluation of the technologies' accuracy in detecting deterioration, however, was the primary objective of the laboratory testing.

### Assessment of NDT Technologies

The criteria for the evaluation and ranking of the NDT methods and devices were discussed in Chapter 4. Those criteria were applied, with some minor adjustments, using the quantitative results obtained from the field and laboratory studies.

#### Accuracy

The accuracy was judged on the basis of the following three criteria defined in Table 4.3: (1) detectability extent, (2) detectability threshold, and (3) severity of deterioration. Detectability is the most fundamental parameter for the evaluation of any NDT technology. If a certain defect cannot be detected by a given technology, the other four performance measures are meaningless. In principle, the detectability can be translated into the ability of a given technology to locate a given defect as accurately as possible. At the same time, the same technology should not report an intact location as defective. In other words, the number of false-positive and false-negative results should be minimal.

#### Delamination

Five groups of technologies were evaluated for the detection of delamination (see Table 6.4). For delamination detection,

the detectability extent was judged by how accurately each technology detected the area and existence of the delaminated areas. The detectability threshold was assessed by the smallest delaminated area that a technology could detect. The severity of the deterioration was judged by how well a technology could be delineated among advanced stages of delamination versus the onset of delamination and whether it can distinguish between a deep or shallow delamination. Based on the criteria defined in Table 4.3 and the preceding explanation, the accuracy of the five technologies is presented in Table 7.1. When multiple vendors used the same technology, the average and maximum points earned are reported. The average point can be considered as the status of the state of the practice at this time and the maximum point corresponds to the state of the art.

In general, the IE method is the most accurate technology with an average point of 2.8/5. The infrared thermography technology and the GPR were reasonably accurate as well. The main concern with the infrared thermography technology was that it was very sensitive to the environmental conditions and that there is a small window during the day during which the technology works well. The ranking of the GPR would have improved if the delaminated areas were moisture filled and chloride filled. The materials used in the laboratory experiments to simulate the delamination were more representative of the air-filled delamination. As reflected in Chapter 6, chain dragging was not very successful for detecting the delaminated areas that were small or deep. None of the vendors conducted the impulse response tests on the laboratory specimens; as such, the subsequent ranking of the method was primarily based on the work done on the Virginia bridge.

#### Rebar Corrosion

Three technologies were evaluated for rebar corrosion. The evaluation criterion was based on the ability of the participants to distinguish the difference between the area constructed with

**Table 7.1. Grading of NDT Technologies Based on Accuracy**

Defect	Technology	Participant	Device	Performance Parameters for Accuracy			Grade	Average Grade	Maximum Grade
				Detectability Extent (WF = 0.3)	Detectability Threshold (WF = 0.3)	Severity of Deterioration (WF = 0.4)			
Delamination	GPR	8	Air coupled	3	3	1	2.2	1.7	2.2
		4	Ground coupled	3	3	1	2.2		
		5	Ground coupled	1	3	1	1.0		
		9	Ground coupled	3	3	1	2.2		
	IE	4	Scanning system	3	3	3	3.0	2.8	3.4
		6	Air coupled	5	5	1	3.4		
		7	Air coupled	3	3	1	2.2		
		1	Scanning system	3	3	1	2.2		
	IE-USW	9	Stationary	3	5	1	2.8	2.8	2.8
		Infrared	2	Handheld camera	3	3	1	2.2	2.2
	Chain dragging	9	NA	3	1	1	1.6	1.6	1.6
Rebar corrosion	GPM-HCP	4	Stationary	3	1	3	2.4	2.4	2.4
	GPR	1	Ground coupled	1	3	1	1.6	1.6	1.6
		5	Ground coupled	1	3	1	1.6		
HCP	9	Stationary	3	3	1	2.2	2.2	2.2	
Crack depth	SASW	1	Stationary	3	1	1	1.6	2.3	3.0
		4	Stationary	3	3	3	3.0		
	SWT	7	Stationary	3	3	3	3.0	3.0	3.0
	TOFD	7	Stationary	3	1	1	1.6	1.6	1.6
Concrete degradation	USW	9	Stationary	3	3	5	3.8	3.8	3.8

corroded rebar and the rest of the deck that was built with new rebar. The GPM, HCP, and ER technologies were marginally successful in reporting changes in parts of the deck that were constructed with the corroded rebar. However, it should be also mentioned that the three technologies were not developed to detect or measure the degree of rebar corrosion. Instead, they are used to measure corrosion activity, corrosion rate, or to describe the corrosive environment of concrete.

One of the limitations of the reviewed and evaluated technologies is the assessment of the activity and rate of corrosion when epoxy-coated rebars are used in the deck. Although the measurements have been conducted and reported using GPM and HCP, no clear guidelines regarding the interpretation of the measurement results can be provided. The characterization of a corrosive environment using ER, however, is not affected by the rebar type in the deck.

### ***Depth of Vertical Crack***

The evaluation of the three sonic methods that were used to detect the depth of cracks was rather straightforward because the depth of the embedded cracks was known, as discussed in Chapter 6. The most promising methods were SWT and SASW used by one of the participants. Because the cracks were evident from the surface, a detectability extent of 3 was given to all methods.

### ***Concrete Degradation***

Only one participant reported information about concrete degradation. As reflected in Table 7.1 and based on tests of the Virginia bridge, the USW method was successful in quantifying the degradation of concrete. Strictly speaking, the limitation of that method is that the delaminated and cracked concrete show as degraded concrete as well.

### ***Repeatability***

One of the challenges in making an objective comparison between technologies and participants is that the repeatability of the presented results needed to be made for different data or results “levels.” A level indicates whether the repeated data are just collected, are collected and analyzed, or are analyzed and interpreted. For example, HCP and ER do not require any data reduction, and the condition maps are generated from the raw collected data. However, GPR and IE results must be analyzed before generating the contour maps.

One approach to measure the technology repeatability was by using the coefficient of variation (CV). For each individual test, CV at every test point was obtained by calculating the standard deviation  $\sigma$  of the three runs, divided by their corresponding mean value  $\mu$  ( $CV = \sigma/\mu$ ). The upper and lower

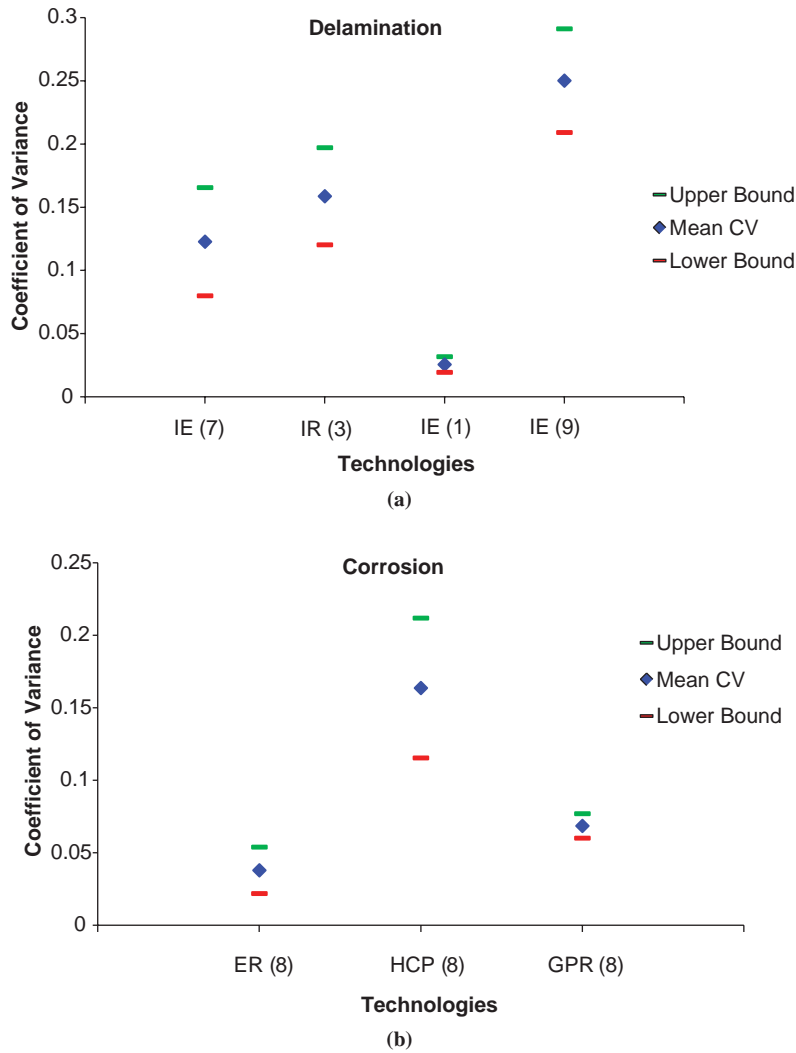
bounds of CVs with a 95% confidence interval (CI) were calculated for each test by adding and subtracting the CI to and from the mean CV.

Figure 7.1 depicts the CV, and the upper and lower bounds for each test. Figure 7.1a shows the repeatability results for the technologies detecting delamination, and Figure 7.1b demonstrates the results for technologies detecting and describing corrosion activity or environment. As can be seen from Figure 7.1a, the IE system of Participant 1 has the lowest CV (better repeatability), followed by Participants 7, 3, and 4. It should be mentioned that the data used in the repeatability study varied between the participants who presented the simple analyzed data and those who presented the interpreted data. Given that the CVs are all rather small ( $<0.25$ ), one can argue that all of them have an acceptable repeatability. The same argument is valid for the technologies detecting corrosion; electrical resistivity has the lowest CV followed by GPR and HCP (Figure 7.1b). Electrical resistivity and GPR have a smaller half-width compared with HCP, which shows that these two tests are more repeatable than HCP. However, the final repeatability grading of technologies could not be based on CV because some of the participants submitted their raw data for which it was not possible to calculate CV. This is the reason some of the participant results are missing in Figure 7.1. Therefore, grading based on the provided graphical presentations of the data and results, although somewhat subjective, was selected as a better approach to repeatability evaluation.

Unlike the other performance measures, repeatability is hard to quantify for infrared thermography. However, paying attention to the infrared thermography concept helps to clarify the issue. To detect damage in the deck, infrared thermography uses relative values (i.e., the temperature difference between the deteriorated sections and those that can be described to be in sound condition). The stronger the contrast is, the more pronounced the deterioration (delamination) will be. Thus, as long as the heat conduction conditions are the same, it will be repeatable. The effect of debris on the deck, vehicles and people casting shadows, markings on the deck, time of the day, and so forth, however, also need to be taken into account. The grades for repeatability are provided in the summary table (Table 7.7).

### ***Speed***

Speed as a performance measure has two main components: speed of data collection and speed of data analysis and interpretation. For most agencies, speed of data collection is more important because of the cost of traffic control and losses and inconveniences associated with traffic interruptions. The data collection speed of the participating technologies was evaluated on the basis of the records taken during the con-



**Figure 7.1. Repeatability for detection of delamination (a) and characterization of corrosion activity or corrosive environment (b).**

duct of the field validation testing. The data analysis and interpretation speed were graded on the basis of the information provided by the participants.

**Speed of Data Collection and Coverage**

Some technologies collect data in a continuous manner, whereas other technologies are spot measurements. Therefore, the speed of data collection is expressed in terms of the production rate, which is the area coverage per hour needed for high-density data coverage. The high density of data coverage in this case is the data collected on a 2-ft × 2-ft grid. Therefore, the speed was calculated by using the area coverage per hour for both continuous and point measurements. The time taken to perform the repeatability measurements was excluded in the speed calculation. A grade of 1 to 5 was

assigned to each technology, with 1 being the least favorable and 5 being the most favorable (the fastest technology in terms of speed of data collection). The grading was assigned as follows:

- 5: Area coverage greater than 2,000 ft<sup>2</sup>/h;
- 4: Area coverage between 1,500 and 2,000 ft<sup>2</sup>/h;
- 3: Area coverage between 1,000 and 1,500 ft<sup>2</sup>/h;
- 2: Area coverage between 500 and 1,000 ft<sup>2</sup>/h; and
- 1: Area coverage less than 500 ft<sup>2</sup>/h.

**Speed of Data Analysis and Interpretation**

Data analysis is defined as the processing of raw data collected by the device and includes preprocessing (e.g., background removal); data analysis and presentation, whether this is done

by a single parameter or a graphical output; and data interpretation. The grades are defined on the basis of the production rate. Again, the equivalency is expressed in terms of the number of spot measurements analyzed and interpreted. The speed evaluation results for each participant are presented in Table 7.2. The grades were assigned as follows:

- 5: Data analysis for more than 1,000 ft<sup>2</sup>/h;
- 3: Data analysis between 500 and 1,000 ft<sup>2</sup>/h;
- 1: Data analysis less than 500 ft<sup>2</sup>/h.

The overall grade was obtained by assigning a weight factor of 0.6 to the speed of data collection and a weight factor of 0.4 to the speed of data analysis and interpretation.

The overall grades for each particular technology are calculated for the ultimate ranking of the technology. The results for both the data collection and data analysis are summarized in Table 7.3. The average grade is the mean of all grades calculated for all the participants. A grade of 1, 3, or 5 was assigned to each technology, with 1 being the least favorable and 5 being the most favorable (the slowest technology in terms of speed of data analysis and interpretation).

Infrared thermography, ground-penetrating radar, electrical resistivity, half-cell potential, and impulse response can be conducted at a higher speed rate than the other technologies. Chain dragging and hammer sounding has a medium speed, and galvanostatic pulse measurement, ultrasonic surface waves, and impact echo are of the lowest speed.

**Table 7.2. Grading of the NDT Technologies Based on Speed**

Technology	Participant	Speed (ft <sup>2</sup> /h) (Raw Data)		Speed (Grade)		Overall Grade
		Data Collection	Data Analysis	Data Collection (WF = 0.6)	Data Analysis (WF = 0.4)	
Infrared	2	1,750	1,008	4	5	4.4
GPR (Aladdin)	4/5	2,931	Information not provided	5	3	4.2
GPR	8	2,871	600	5	3	4.2
GPR	9	2,313	800	5	3	4.2
GPR	4	2,032	Information not provided	5	3	4.2
Electrical resistivity	9	1,415	1,008	3	5	3.8
Infrared	10	1,227	Information not provided	3	5	3.8
Half-cell potential	9	1,156	1,008	3	5	3.8
Impulse response	3	1,217	1,008	3	5	3.8
GPR (hand cart)	1	2,188	252	5	1	3.4
GPR	5	2,060	120	5	1	3.4
Chain dragging and hammer sounding	9	802	1,008	2	5	3.2
IE-SASW (surface wave)	4	1,654	Information not provided	4	1	2.8
IE	4	1,569	Information not provided	4	1	2.8
IE	1	1,551	168	4	1	2.8
Galvanostatic pulse	4	517	Information not provided	2	3	2.4
PSPA	9	516	630	2	3	2.4
IE	9	1,018	336	3	1	2.2
IE	6	797	336	2	1	1.6
Air-coupled IE	7	575	336	2	1	1.6
USW (for vertical cracks)	4	na	na	na	na	na
Vertical cracks (surface wave: USW)	7	na	na	na	na	na

Note: WF = weight factor; PSPA = portable seismic property analyzer; na = not applicable.



**Table 7.3. Speed**

Technology	Number of Participants	Maximum Grade	Average Grade
Infrared	2	4.4	4.1
GPR	5	4.2	3.9
ER	1	3.8	3.8
HCP	1	3.8	3.8
Impulse response	1	3.8	3.8
Chain dragging	1	3.2	3.2
GPM	1	2.4	2.4
USW	1	2.4	2.4
IE	6	2.8	2.3

**Ease of Use**

The following parameters were considered in evaluating the ease of use of each technology: expertise in data collection, number of operators, ease of maneuvering, physical effort for the setup, expertise in data analysis, and potential for automation. The grades for some of the parameters are based on observations at sites where the tests were being performed, including expertise in data collection, number of operators, ease of maneuvering, and physical effort for setup and movement. Grading for “expertise in data analysis” and “potential for automation” is based on both the information provided by the participants and the judgment of the research team, which is based on the submitted reports from participants (Table 7.4). The results are summarized in Table 7.5.

**Table 7.4. Grading of NDT Technologies Based on Ease of Use**

Technology	Participant	Data Collection	Data Analysis	Potential for Automation	Overall Index for Ease of Use
		WF = 0.45	WF = 0.4	WF = 0.15	
Infrared	10	3.7	5	3	4.1
Chain dragging/hammer sounding	9	3.4	5	3	4.0
Infrared	2	3.2	5	3	3.9
Resistivity	9	3.7	3	5	3.6
HCP	9	3.2	3	5	3.4
Impulse response	3	2.3	3	3	2.7
GPM	4	2.1	3	3	2.6
IE	9	3.0	1	5	2.5
GPR	9	3.2	1	3	2.3
GPR	1	3.2	1	3	2.3
GPR	5	3.2	1	3	2.3
GPR	4	3.2	1	3	2.3
IE-SASW (surface waves)	4	3.2	1	3	2.3
Acoustic sounding	4	3.2	1	3	2.3
USW	9	3.2	1	3	2.3
GPR	4/5	2.8	1	3	2.1
IE	1	2.8	1	3	2.1
GPR	8	2.3	1	3	1.9
Air-coupled IE	7	2.3	1	3	1.9
USW (for vertical cracks)	4	1.9	1	1	1.4
Vertical cracks (USW)	7	1.9	1	1	1.4
IE	6	1.0	1	3	1.3

Note: WF = weight factor.

**Table 7.5. Ease of Use**

Technology	Number of Participants	Maximum Grade	Average Grade
Infrared	2	4.1	4.0
Chain dragging	1	4.0	4.0
ER	1	3.6	3.6
HCP	1	3.4	3.4
Impulse response	1	2.7	2.7
GPM	1	2.6	2.6
GPR	5	2.3	2.2
IE	6	2.5	2.1
USW	1	1.4	1.4

**Cost**

The cost of an NDT method includes the following:

- Cost of data collection. The cost of data collection is defined as the overall cost based on the workforce size, expertise level, and time needed to collect data.
- Cost of data analysis and interpretation. The cost of data analysis and interpretation is defined as the overall cost, based on the workforce expertise level and time needed to analyze and interpret.
- Cost of equipment, supplies, and equipment maintenance.
- Cost of traffic control. The cost needed to provide a safe work area on the bridge during data collection.

To evaluate the cost-effectiveness of each technology, each participant was asked to provide a cost estimate for two hypothetical bridges that have a deck area of 5,000 ft<sup>2</sup> and 10,000 ft<sup>2</sup>. The two bridges would be located within 100 miles of the participant’s office. Because this was assumed to be a production-type job, the cost of the equipment, supplies, maintenance, and so forth were included in the quoted cost. Consequently, the cost of the equipment is not considered as an independent parameter in the cost evaluation. The pricing provided by the participants includes the cost associated with data collection, data reduction, and data interpretation. Figure 7.2 represents the cost per square foot as reported by the participants.

As can be seen from Figure 7.2, a few of the participants provided quotes that were unrealistically low or high. The reason is that some of the participants are either researchers, equipment vendors, or manufacturers who rarely work on production-level jobs. The other, and well-expected, observation is that as the bridge size increased, the cost of the survey per unit area decreased.

The participants and technologies were divided into five categories: (1) radar (ground penetrating and air coupled); (2) acoustic (impact echo, impulse response, ultrasonic surface waves); (3) infrared thermography; (4) chain dragging and hammer sounding; and (5) electrochemical techniques (half-cell potential, electrical resistivity). The average survey cost per square foot was then calculated for each category. Figure 7.3 depicts the cost per square foot of the deck for each category.

The data presented in Figure 7.3 do not include costs associated with traffic control, which can often be substantial. The speed of surveying has a direct effect on the amount of time

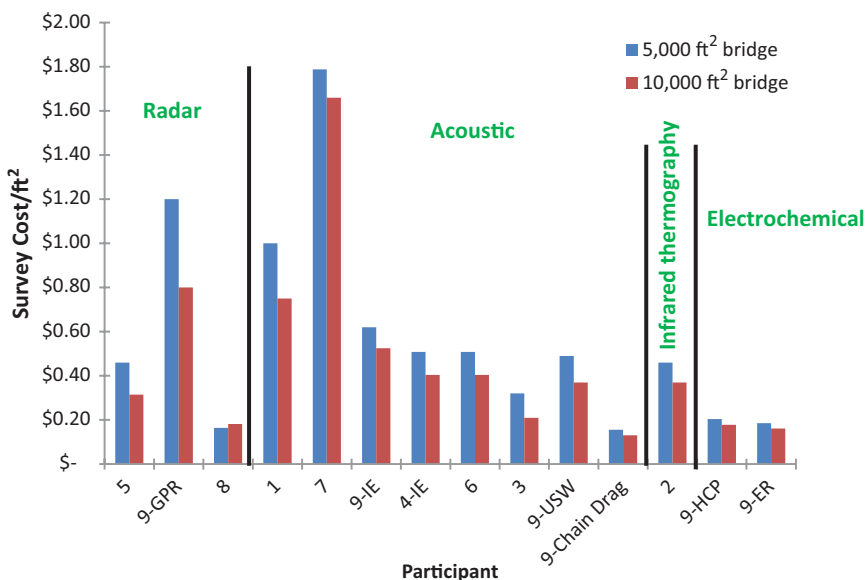


**Figure 7.2. Cost per square foot for the assumed surveys on 5,000-ft<sup>2</sup> and 10,000-ft<sup>2</sup> bridge decks (excluding traffic control).**

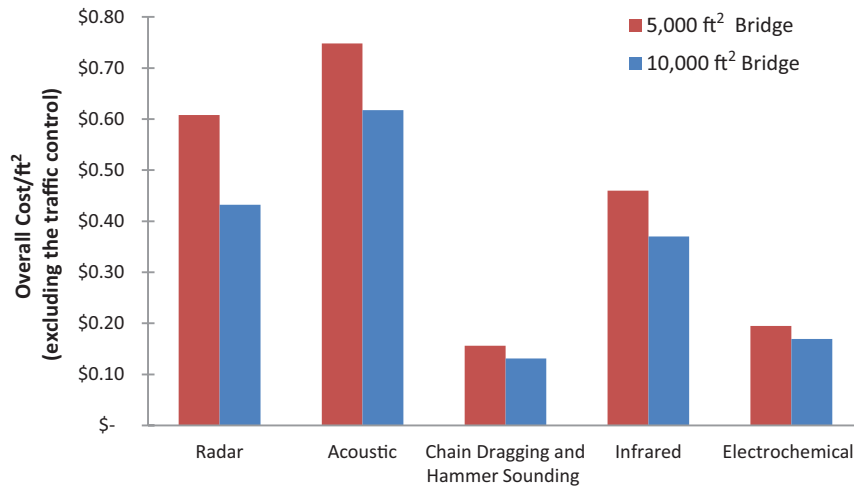


**Figure 7.3. Cost per square foot for each technology category (excluding traffic control).**

traffic control is needed. On the basis of the speed calculated for each technique during the field validation testing in Haymarket, Virginia (Table 7.2), the total time that each participant would need to survey the two hypothetical bridges was calculated. A full day of traffic control was considered to be 6 h: from 9 a.m. to 3 p.m. Because the typical minimum time frame for traffic control is half a day, the survey times were rounded to half-day increments: less than 3 h (0.5 day), between 3 and 6 h (1 day), between 6 and 9 h (1.5 days), and so forth. Figure 7.4 depicts the number of days needed for each participant to survey the bridge.

A typical full day of traffic control is assumed to cost \$2,000. For the air-coupled GPR, the assumed cost is \$1,000,

because an air-coupled GPR does not require an entire lane to be closed to perform the testing. Instead, an attenuator truck following the vehicle on which the air-coupled GPR is mounted would suffice in many situations. Figure 7.5 compares the overall cost of testing per square foot in the two situations: with and without traffic control.

Ground-penetrating radar is the fastest technology on the deck, and traffic control only adds about 27% to the overall cost. Conversely, in the case of the least expensive technologies such as chain dragging and hammer sounding and electrochemical methods, the traffic control significantly adds to the final cost: 384% and 205%, respectively. However, chain dragging and hammer sounding are the only techniques whose

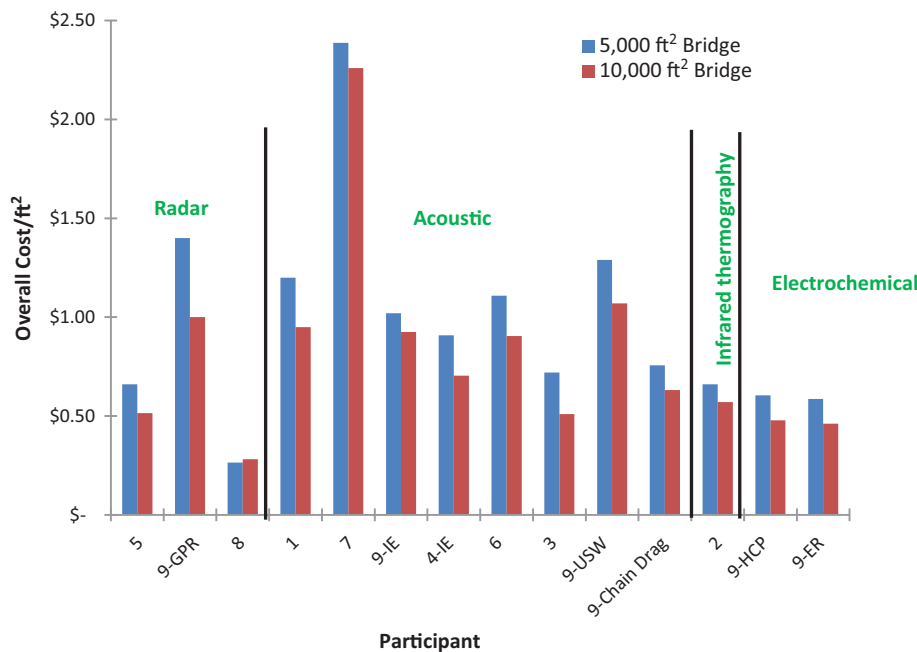


**Figure 7.4. Number of days to survey the bridge.**

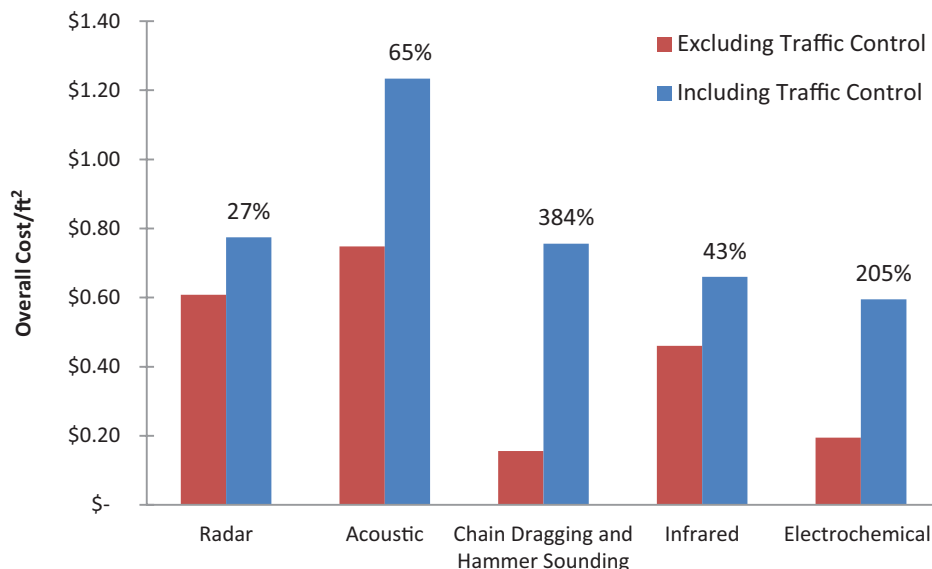


**Figure 7.5. The overall cost of survey (with and without traffic control).**

speed changes with the level of deterioration because there is no postprocessing involved and testing and data analysis are performed simultaneously on the bridge. The deck of the Haymarket Bridge in Virginia, which was used in the field validation phase of the project, has significant signs of deterioration. Therefore, the testing took a longer time than usual, which brought the cost of the chain dragging and hammer sounding to the same level as the infrared thermography.

The grading of the technologies is based on the unit cost for the hypothetical evaluation of a bridge deck of 5,000 ft<sup>2</sup> (Table 7.6). The technologies costing less than \$0.5/ft<sup>2</sup> were assigned Grade 5, and the grade was decreased one point for every additional \$0.25/ft<sup>2</sup>.

### Summary Grades

The grades for all the performance measures for all the NDT technologies are summarized in Table 7.7. Unlike the initial grading based on the literature search, the grading herein is made only for the deterioration types for which the technology was validated. For technologies that were represented by multiple participants, the performance measure grades are represented by mean values for the same group. Certainly, an argument can be made that a technology should

be represented by its best performers. In this case, the performance and corresponding grades would represent the true potential of the technology at this time. Also, the grading of the cost in the table is based on the cost, including the anticipated traffic control costs.

The overall grades span from 2.3 to 3.6, which puts all the technologies in the fair-to-good range with respect to the evaluation of a particular deterioration type. The overall good grades for a particular deterioration type by multiple technologies, however, come from different performance measures. The strengths of some technologies are higher accuracy and precision (repeatability), whereas some technologies are stronger in other performance measures, such as speed or cost. For example, impact echo, GPR, infrared thermography, and chain dragging and hammer sounding receive close grades for delamination detection. However, impact echo's higher grade derives primarily from the accuracy, GPR's and infrared thermography's grades from the speed, and chain dragging's grade from the ease of use. Therefore, a decision regarding the selection of the technology should also be based on the most important performance measure. In the case of corrosion, the selection should be guided by the objective of the assessment. Four technologies received good grades for corrosion characterization: electrical resistivity,

**Table 7.6. Grading of NDT Technologies Based on Cost**

	Radar	Acoustic	Chain Dragging and Hammer Sounding	Infrared Thermography	Electrochemical
<b>Grades (excluding traffic control)</b>	4	3	5	5	5
<b>Grades (including traffic control)</b>	3	2	3	4	4

**Table 7.7. Deterioration Type Grades for Validated NDT Technologies**

NDT Technology	Deterioration Type	Accuracy	Precision (Repeatability)	Speed	Ease of Use	Cost	Overall Deterioration
		WF = 0.3	WF = 0.3	WF = 0.2	WF = 0.1	WF = 0.1	Type Grade
Impact echo	Delamination	2.8	4.0	2.3	2.1	3.0	3.0
Ultrasonic surface waves	Delamination	2.8	3.0	2.4	1.4	3.0	2.7
	Crack depth	2.5	3.0	1.0	1.4	3.0	2.3
	Concrete deterioration	3.8	4.0	2.4	1.4	3.0	3.3
Ground-penetrating radar	Delamination	2.1	4.0	3.9	2.2	3.0	3.1
	Corrosion	1.6	4.0	3.9	2.2	3.0	3.0
Half-cell potential	Corrosion	3.0	3.0	3.8	3.4	4.0	3.3
Galvanostatic pulse measurement	Corrosion	2.4	3.0	2.4	2.6	4.0	2.8
Electrical resistivity	Corrosion	3.0	4.0	3.8	3.6	4.0	3.6
Infrared thermography	Delamination	2.2	2.0	4.1	4.0	4.0	2.9
Chain dragging	Delamination	2.2	3.0	3.2	4.0	3.0	2.9

Note: WF = weight factor.

half-cell potential, galvanostatic pulse measurement, and ground-penetrating radar. However, ER and GPR will describe the corrosive environment of concrete to a greater extent, while GPM and HCP will describe corrosion rate and activity, respectively.

The overall value of the NDT technology in concrete bridge deck deterioration detection is summarized in Table 7.8. The deterioration type grades were taken from Table 7.7, where the technology was applicable. Applications of IE in vertical crack depth and concrete quality estimation, and GPR in concrete degradation assessment, were described in Chapter 2.

Because those applications were not validated during the study, the technologies received a grade of 1 for the same. The technology that provides the highest value is GPR. The second most valuable technologies are impact echo and ultrasonic surface waves. However, the ultimate decision on which equipment to acquire and which technology to use will depend on a number of elements. Among others, it will depend on the type of deterioration that is of the highest concern to the agency and whether the evaluation is being done for network-level condition monitoring, or the project level for maintenance or rehabilitation.

**Table 7.8. Overall Value of NDT Technology in Bridge Deck Deterioration Detection**

Deterioration Type	Delamination	Corrosion	Vertical Cracks	Concrete Degradation	Overall Value	Ranking
	WF = 0.42	WF = 0.35	WF = 0.10	WF = 0.13		
Impact echo	3.0	0.0	1.0	1.0	1.5	2
Ultrasonic surface waves	2.7	0.0	2.4	3.3	1.8	2
Ground-penetrating radar	3.1	3.1	0.0	1.0	2.5	1
Half-cell potential	0.0	3.3	0.0	0.0	1.2	3
Galvanostatic pulse measurement	0.0	2.8	0.0	0.0	1.0	3
Electrical resistivity	0.0	3.6	0.0	0.0	1.3	3
Infrared thermography	2.9	0.0	0.0	0.0	1.2	3
Chain dragging/hammer sounding	2.9	0.0	0.0	0.0	1.2	3

Note: WF = weight factor.

## CHAPTER 8

## Implementation of the Results from the Study

The ultimate goal of SHRP 2 Renewal Project R06A was to develop an electronic repository of promising NDT technologies that target practitioners who evaluate bridge decks. The electronic repository or NDToolbox is a web-based open-source database system, which uses a very advanced caching system that makes the toolbox fast, lightweight, and efficient. The

administrator can give permission to users in various access levels from viewer-only to text viewer to a text/image editor. The NDToolbox arrangement makes it user friendly. Regular users can easily navigate through the content and find the information they seek. Searching within the toolbox is also possible. Figure 8.1 illustrates the home page of the repository.

The screenshot shows the NDToolbox home page. On the left, there is a sidebar with two main sections: 'Technologies' and 'Deterioration'. The 'Technologies' section lists: Electrical Resistivity, Galvanostatic Pulse Measurement, Ground Penetrating Radar, Half-Cell Potential, Hammer Sound / Chain Drag, Impact Echo, Impulse Response, Infrared Thermography, Ultrasonic Pulse Echo, and Ultrasonic Surface Waves. The 'Deterioration' section lists: Rebar Corrosion, Deck Delamination, Cracking, and Concrete Deterioration. The main content area is titled 'Technologies' and contains a table with the following data:

NDT Method	Application 1	Application 2	Application 3
Ground Penetrating Radar	Corrosion	Concrete Deterioration	Delamination
Impact Echo (IE)	Delamination	Concrete Deterioration	
Ultrasonic Surface Waves (USW)	Concrete Deterioration	Cracking	
Impulse Response (IR)	Delamination	Concrete Deterioration	
Half-Cell Potential	Corrosion		
Electrical Resistivity (ER)	Corrosion		
Galvanostatic Pulse Measurement (GPM)	Corrosion		
Ultrasonic Pulse Echo (UPE)	Delamination	Concrete Deterioration	Cracking
Chain Drag / Hammer Sounding	Delamination		
Infrared Thermography	Delamination		
Surface Waves For Crack Characterization	Cracking		

Figure 8.1. Home page of the NDToolbox.

The main menu gives the user two options for navigating the website: through the Technologies menu (Figure 8.1) or the Deterioration menu (Figure 8.2).

As shown in the preceding figures, the technologies are listed alphabetically on the left side of the page. Selecting a technology will direct the user to another page where each technology is described in eight sections:

1. Description of the method;
2. Physical principle;
3. Applications;
4. Performance;

5. Limitations;
6. Equipment;
7. Test procedures, protocols, guidelines, and so forth; and
8. Samples of data output, result presentation and interpretation, and so forth.

These sections can be found on the right side of the Technologies page (Figures 8.3 to 8.5).

It is also possible to see all these eight sections continuously in a single page. To do so, the user needs to click the name of the technology below the main menu.

The screenshot shows the NDToolbox website interface. The header includes the SHRP2 logo and navigation tabs for Home, Technologies, and Deterioration. A left sidebar lists various technologies and deterioration types. The main content area displays a table mapping defects to techniques.

Defect	Technique 1	Technique 2	Technique 3
Delamination	Impact Echo	GPR	Impulse Response
Corrosion	GPR	Electrical Resistivity	Half-Cell Potential
Concrete Deterioration	GPR	Ultrasonic Surface Waves	Ultrasonic Pulse Echo
Vertical Crack	Ultrasonic Pulse Echo		

**Figure 8.2. The NDToolbox: Deterioration.**

The screenshot shows the SHRP2 NDToolbox website interface. The main content area is titled 'PHYSICAL PRINCIPLE' and contains the following text:

**Infrared Thermography**

Infrared radiation is part of the electromagnetic spectrum with the wavelength ranging from 0.7 to 14  $\mu\text{m}$ . Infrared cameras measure the thermal radiation emitted by a body and based on thermal properties of various materials can capture the regions with temperature differences. The three main properties that influence the heat flow and distribution within a material include: the thermal conductivity ( $\lambda$ ), the specific heat capacity ( $C_p$ ) and the density ( $\rho$ ).

When the solar radiation or a heater, in the case of active thermography, heats up the deck, all the objects in the deck emit some energy back. Delaminations and voids are typically filled with water or air which have different thermal conductivity and thermal capacity than the surrounding concrete. These delaminated areas heat up faster and cool down more quickly comparing to concrete. They can develop surface temperatures from 1 to 3 degrees centigrade higher than the surrounding areas when ambient conditions are favorable.

Below the text are two diagrams illustrating the physical principle. The left diagram shows a cross-section of a concrete deck with a delamination. Red arrows point upwards from the warmer surface, and blue arrows point downwards to the colder surface. The right diagram shows the same cross-section but with red arrows pointing downwards from the warmer surface and blue arrows pointing upwards to the colder surface, indicating heat flow during cooling.

Figure 8.3. Physical principle of infrared thermography.

The screenshot shows the SHRP2 NDToolbox website interface. The main content area is titled 'DATA PRESENTATION' and contains the following text:


**Electrical Resistivity**

The contour map of electrical resistivity depicts the spatial distribution of the resistivity values. Areas with low resistivity have a high susceptibility to corrosion activity whereas areas with a high resistivity have a low susceptibility to corrosion activity. In the plot below, the electrical resistivity was correlated to the corrosion rate.

Below the text is a contour map titled 'Electrical resistivity (kohm\*cm)'. The x-axis is 'Longitudinal Distance (ft)' ranging from 0 to 80. The y-axis is 'Depth (ft)' ranging from 0 to 10. The map shows various colored regions representing different resistivity values. Below the map is a legend for 'Corrosion Rate Grade' with a color scale from 5 (Very High) to 95 (Low). The legend also includes a 'Decreasing Corrosion Rate Indication' arrow pointing from high to low resistivity values.

Figure 8.4. Data presentation: Electrical resistivity.





[Home](#)   [Technologies](#)   [Deterioration](#)

## NDToolbox

[My account](#)   [Log out](#)

---

**Technologies**

- Electrical Resistivity
- Galvanostatic Pulse Measurement
- Ground Penetrating Radar
- Half-Cell Potential
- Hammer Sound / Chain Drag
- Impact Echo
- Impulse Response
- Infrared Thermography
- Ultrasonic Pulse Echo
- Ultrasonic Surface Waves

**Deterioration**

- Rebar Corrosion
- Deck Delamination
- Cracking
- Concrete Deterioration

Home

### EQUIPMENT

[View](#)   [Edit](#)   [Revisions](#)

**Impulse Response**

The equipment used for IR testing includes an instrumented hammer, a geophone, and the processing units. The instrumented hammer or sledgehammer applies an impact that induces a low-strain deformation in the tested element. The maximum induced stress in concrete depends on the elastic properties of the hammer tip. Typical peak stress levels range from 5 MPa for hard rubber tips to more than 50 MPa for aluminum tips. The response of the medium to the input impulse is normally measured using a velocity transducer (geophone), whose stability at low frequencies and the robust performance of which in practice have made it preferable compared to others. Both the hammer and the geophone are linked to a portable field computer for data acquisition and storage (Figure 2), which enables recording of both the impact force and the response of the structure.




Figure 2. Illustration of the impulse-response testing with main equipment components: portable computer (left), and instrumented hammer and geophone (right).

**Sections**

- DESCRIPTION
- PHYSICAL PRINCIPLE
- APPLICATIONS
- PERFORMANCE
- LIMITATIONS
- EQUIPMENT
- TEST PROCEDURES
- DATA PRESENTATION

**Figure 8.5. Equipment: Impulse response.**

## CHAPTER 9

## Summary, Conclusions, and Recommendations

The primary objective of this research was to identify NDT technologies that can effectively detect and characterize deterioration in bridge decks. The research activity had the following five specific objectives:

- To identify and characterize NDT technologies for the rapid condition assessment of concrete bridge decks;
- To validate the strengths and limitations of applicable NDT technologies from the perspectives of accuracy, precision, ease of use, speed, and cost;
- To recommend test procedures and protocols for the most effective application of the promising technologies; and
- To synthesize the information regarding the recommended technologies needed in an electronic repository for practitioners.

The first phase of the project consisted of a thorough literature search to identify deterioration processes of concrete decks and existing and emerging NDT technologies for detecting deck defects. From a number of deterioration types, the following four types were given the highest priority for concrete bridge decks because of their importance to the transportation agencies: delamination, corrosion, vertical cracking, and concrete degradation. Of those four types, higher priority was given to the detection of delamination and corrosion. On the basis of their capability to detect a certain type of defect, the technologies were categorized as follows:

- Delamination: impact echo, chain dragging and hammer sounding, ultrasonic pulse echo, infrared thermography, and ground-penetrating radar.
- Corrosion: half-cell potential, electrical resistivity, and galvanostatic pulse measurement.
- Vertical crack: visual inspection, ultrasonic surface waves, ultrasonic pulse echo, and impact echo.
- Concrete degradation: ultrasonic surface waves and pulse echo, impact echo, and ground-penetrating radar.

Ten teams from research institutions and industry elite in the field of nondestructive evaluation of bridge decks participated in the validation phase of the project to assess the performance of each of the above-mentioned techniques. The following five performance measures were used in the evaluation of technologies: accuracy, precision, speed, ease of use, and cost. Accuracy and precision were given the highest importance, followed by speed, ease of use, and cost. The validation testing had two main components: field and laboratory validations. The field validation enabled testing under actual, production-level conditions. The main focus of the research team during field testing was on the evaluation of speed, ease of use, repeatability, and cost. The laboratory validation was conducted on samples with artificially introduced deterioration and defects at known locations providing broad ground truth information. Therefore, the laboratory validation concentrated on the evaluation of accuracy and repeatability of the NDT technologies.

The field and laboratory testing results confirmed the literature findings that there is no particular technology that is capable of detecting all four major deterioration types. Although a number of technologies can provide detailed and accurate information about a certain type of defect, complementary use of multiple technologies is required. Until new breakthrough technologies are available for production-level testing, a selection of technologies must be used for bridge deck condition evaluation. The selection of technologies must be primarily based on the accuracy of information they provide regarding the most important deterioration types. Those technologies should also meet or exceed certain criteria regarding the speed, ease of use, and cost. These performance measures were examined in this research study.

The following conclusions were drawn from this research study:

1. For each of the main deterioration types, there are technologies that have demonstrated fair-to-good abilities of

- detection. However, there is not a single technology that has shown capability in evaluating all deterioration types.
2. Four technologies were identified that can detect and characterize delamination with a fair-to-good level of confidence. Those are impact echo, chain dragging and hammer sounding, infrared thermography, and ground-penetrating radar.
  3. Four technologies were identified as having fair-to-good capabilities for corrosion detection or characterization of corrosive environment. Those include half-cell potential, electrical resistivity, galvanostatic pulse measurement, and ground-penetrating radar.
  4. Only one technology, surface wave testing, was validated as a fair technology in the vertical crack characterization.
  5. Three technologies were identified as having capabilities in concrete deterioration detection and characterization. Those are ultrasonic surface waves, impact echo, and ground-penetrating radar.
  6. The top technologies based on the overall value in detection and characterization of deterioration in concrete decks are impact echo, half-cell potential, ultrasonic surface waves, ground-penetrating radar, chain dragging and hammer sounding, electrical resistivity, infrared thermography, and galvanostatic pulse measurement.
  7. The overall value and ranking were to some extent influenced by the selected performance measures and the applied weights and significance factors in the grading process.

One of the encouraging outcomes from the validation testing is that a number of NDT technologies can generate data at a production rate that is comparable to the current practice of chain dragging and hammer sounding. The speed of operation is certainly going to improve as new technologies are being developed. In addition, the cost of evaluation using some of the

NDT technologies is gradually approaching that of chain dragging and hammer sounding. Considering the benefits of more accurate assessments and reduced traffic interruptions, transportation agencies should be moving toward implementing modern NDT technologies.

Both the documented benefits and limitations of the NDT technologies justify the strong need for investing in their continued development. Some of the promising technologies include seismic and ultrasonic tests, such as impact echo and surface waves, and ground-penetrating radar. Their potential especially increases as the technologies are being used in an air-coupled mode, thus increasing their speed and reducing the cost.

Transportation agencies that would like to build their own capability should select tools on the basis of the deterioration type of the highest concern and constraints related to lane closures, available funds, and so forth. If delamination is of greatest concern and is guiding agency decisions, impact echo with a higher degree of automation should be the NDE technology of choice. If corrosion is the deterioration type of greatest concern, either electrical resistivity or half-cell potential measurements are recommended because of their simplicity, low cost, and relative speed. The advantage of the electrical resistivity measurement is that it does not require an electrical connection to the rebar mesh. However, half-cell potential provides information on corrosion activity that might be of greater interest to the agencies. With respect to the assessment of the quality of concrete, the ultrasonic surface wave technology provides the best results. Finally, if the objective of the agency is to obtain the overall condition assessment on the network level, GPR is the recommended tool because of its speed and ability to identify delaminations and describe the corrosive environment. Ideally, the agencies should have access to four out of the five mentioned technologies.

# References

- American Concrete Institute. 2001. *Protection of Metals in Concrete Against Corrosion*. Report ACI 222R-01. American Concrete Institute, Farmington Hills, Mich.
- Afshari, A., D. Frazer, and R. Creese. 1996. Ultrasonic Techniques for the Bonding of Rebar in Concrete Structures. In *Structural Materials Technology—An NDT Conference* (P. Hartbower, ed.), San Diego, Calif., pp. 3–8.
- Baessler, R., A. Burkert, T. Frølund, and O. Klinghoffer. 2003. Usage of GPM-Portable Equipment for Determination of Corrosion Stage of Concrete Structures. *Proc., NACE Corrosion Conference*, San Diego, Calif.
- Barnes, C. L., and J. F. Trotter. 2000. Ground Penetrating Radar for Network Level Concrete Deck Repair Management. *ASCE Journal of Transportation Engineering*, Vol. 126, No. 3, pp. 257–262.
- Baumann, K. 2008. Practical Example of Interpretation of Half Cell Measurements on R.C. Structures. *Proc., 12th International Conference on Structural Faults and Repair*, Edinburgh, United Kingdom.
- Bien, J., L. Elfgren, and J. Olofsson (eds.). 2007. *Sustainable Bridges: Assessment for Future Traffic Demands and Longer Lives*, Wrocław, Poland. Contract TIP3-CT-2003-001653. European Union Within the Sixth Framework Programme.
- Bishko, A., V. Shevaldykin, and A. Samokrutov. 2008. Ultrasonic Echo-Pulse Tomography of Concrete Using Shear Waves Low-Frequency Phased Antenna Arrays. *Proc., 17th World Conference on Nondestructive Testing*, Shanghai, China.
- Böhni, H., and B. Elsener. 1991. Früherkennung von Bauwerkskonstruktionen: Potentialfeldmessung und galvanostatische Impulstechnik, Zerstörungsfreie Prüfung im Bauwesen. *Proc., International ZfPBau Symposium*, Berlin, pp. 101–122.
- Bürchler, D., B. Elsener, and H. Böhni. 1996. Electrical Resistivity and Dielectric Properties of Hardened Cement Paste and Mortar. In *Electrically Based Microstructural Characterization* (R. A. Gerhardt, S. R. Taylor, and E. J. Garboczi, eds.), Materials Research Society, Warrendale, Pa., pp. 407–412.
- Cheng, C., and M. Sansalone. 1995. Determining the Minimum Crack Width That Can Be Detected Using the Impact-Echo Method. *RILEM Journal of Materials and Structure*, Vol. 28, No. 6, pp. 74–82.
- Davis, A. G., C. A. Olson, and K. A. Michols. 2001. Evaluation of Historic Reinforced Concrete Bridges. *Proc., ASCE Structures Congress and Exposition*, Boston, Mass. (CD-ROM).
- El-Safty, A. 2008. Behaviour of RC Bridge Deck Slabs and Girders Strengthened with CFRP Laminates. *Proc., 12th International Conference on Structural Faults and Repair*, Edinburgh, United Kingdom.
- Elsener, B. 2003. Half-Cell Potential Measurements—Potential Mapping on Reinforced Concrete Structures. *Materials and Structures*, Vol. 36, pp. 461–471.
- Elsener, B., A. Hug, D. Bürchler, and H. Böhni. 1996. Evaluation of Localised Corrosion Rate on Steel in Concrete by Galvanostatic Pulse Technique. In *Corrosion of Reinforcement in Concrete Construction* (C. L. Page, P. Bamforth, J. W. Figg, eds.), Society of Chemical Industry, London, p. 264.
- Gebhardt, W., H. Rieder, M. Spies, K. Berns, and C. Hillenbrand, 2006. Kombination von ZfP- und Robotersystemen—Ein Konzept für Autonome Systeme zur Fahrbahnprüfung. *Proc., Fachtagung Bauwerksdiagnose*, Berlin, DGZfP BB 100-CD, Poster 1.
- Gowers, K. R., and S. G. Millard. 1999. Measurement of Concrete Resistivity for Assessment of Corrosion Severity of Steel Using Wenner Technique. *ACI Materials Journal*, Vol. 96, No. 5, pp. 536–542.
- Gowers, K. R., and S. G. Millard. 1991. The Effect of Steel Reinforcement Bars on the Measurement of Concrete Resistivity. *British Journal of Non-Destructive Testing*, Vol. 33, No. 11, pp. 551–554.
- Gu, P., and J. J. Beaudoin. 1998. Obtaining Effective Half-Cell Potential Measurements in Reinforced Concrete Structures. *Construction Technology Update No. 18*, National Research Council of Canada.
- Gucunski, N., G. R. Consolazio, and A. Maher. 2006. Concrete Bridge Deck Delamination Detection by Integrated Ultrasonic Methods. Special Issue on Non-Destructive Testing and Failure Preventive Technology. *International Journal of Material and Product Technology*, Vol. 26, No. 1/2, pp. 19–34.
- Gucunski, N., and H. Jackson. 2001. Void Detection Underneath Rigid Pavements: Numerical Simulation of the Impulse Response Method. *Proc., Symposium on the Application of Geophysics to Engineering and Environmental Problems* (CD-ROM), Denver, Colo.
- Hevin, G., O. Abraham, H. A. Pedersen, and A. Campillo. 1998. Characterization of Surface Cracks with Rayleigh Waves: A Numerical Model. *Non-Destructive Testing and Evaluation International*, Vol. 31, pp. 289–297.
- Hunkeler, F. 1996. The Resistivity of Pore Water Solution—A Decisive Parameter of Rebar Corrosion and Repair Methods. *Construction and Building Materials*, Vol. 10, No. 5, pp. 381–389.
- Jackson, H., and N. Gucunski. 2002. Improved Pavement Model for Reduction of Impulse Response Test Data. *Proc., Annual Meeting of the Environmental and Engineering Geophysical Society SAGEEP* (CD-ROM), Las Vegas, Nev.
- Klinghoffer, O., P. G. Shaw, T. K. Pedersen, T. Frølund. 2000. Non-Destructive Methods for Condition Assessment of Prestressed Cables

- and Reinforcement Corrosion. *Proc., Materials Week Conference*, Munich, Germany, pp. 1–17.
- Kozlov, V. N., A. A. Samokrutov, and V. G. Shevaldykin. 2006. Ultrasonic Equipment for Evaluation of Concrete Structures Based on Transducers with Dry Point Contact. *Proc., NDE Conference on Civil Engineering* (I. Al-Quadi and G. Washer, eds.), St. Louis, Mo., pp. 496–498.
- Krause, M., B. Milmann, F. Mielentz, D. Streicher, B. Redmer, K. Mayer, K. J. Langenberg, and M. Schickert. 2008. Ultrasonic Imaging Methods for Investigation of Posttensioned Concrete Structures: A Study of Interfaces at Artificial Grouting Faults and Its Verification. Special issue. *Journal of Non-Destructive Evaluation*, Vol. 27, pp. 67–82.
- Kruschwitz, S. 2007. *Assessment of the Complex Resistivity Behavior of Salt Affected Building Materials*. PhD thesis. Technical University, Berlin.
- Lemieux, M., R. Gagné, B. Bissonnette, and M. Lachemi. 2005. Behavior of Overlaid Reinforced Concrete Slab Panels Under Cyclic Loading—Effect of Interface Location and Overlay Thickness. *ACI Structural Journal*, Vol. 102, No. 3, pp. 454–461.
- Lin, J. M., and M. J. Sansalone. 1996. Impact-Echo Studies of Interfacial Bond Quality in Concrete. Part I: Effects of Unbonded Fraction Area. *ACI Materials Journal*, Vol. 93, No. 3, pp. 318–326.
- Maierhofer, C., A. Brink, M. Roellig, and H. Wiggenhauser. 2002. Transient Thermography for Structural Investigation of Concrete and Composites in the Surface Near Region. *Infrared Physics and Technology*, Vol. 43, pp. 271–278.
- Maierhofer, C., M. Krause, F. Mielentz, D. Streicher, B. Milmann, A. Gardei, C. Kohl, and H. Wiggenhauser. 2004. Complementary Application of Radar, Impact-Echo, and Ultrasonics for Testing Concrete Structures and Metallic Tendon Ducts. In *Transportation Research Record: Journal of the Transportation Research Board*, No. 1892, Transportation Research Board of the National Academies, Washington, D.C., pp. 170–177.
- Maierhofer, C., R. Arndt, M. Röllig, C. Rieck, A. Walther, H. Scheel, and B. Hillemeier. 2006. Application of Impulse-Thermography for Non-Destructive Assessment of Concrete Structures. *Cement and Concrete Composites*, Vol. 28, pp. 393–401.
- Maser, K., and M. Bernhardt. 2000. Statewide Bridge Deck Survey Using Ground Penetrating Radar. *Proc., Structural Materials Technology Conference IV*, Atlantic City, N.J.
- Maser, K. R., and A. Rawson. 1992. Network Bridge Deck Surveys Using High Speed Radar: Case Studies of 44 Decks (Abridgement). In *Transportation Research Record 1347*, TRB, National Research Council, Washington, D.C., pp. 25–28.
- Millard, S. G. 1991. Reinforced Concrete Resistivity Measurement Techniques. *Proc., Institution of Civil Engineers. Part 2: Research and Theory*, Vol. 91, pp. 71–88.
- Nazarian, S., M. R. Baker, and K. Crain. 1993. *Report SHRP-H-375: Development and Testing of a Seismic Pavement Analyzer*. TRB, National Research Council, Washington, D.C.
- Nazarian, S., K. H. Stokoe, and W. R. Hudson. 1983. Use of Spectral Analysis of Surface Waves Method for Determination of Moduli and Thicknesses of Pavement Systems. In *Transportation Research Record 930*, TRB, National Research Council, Washington, D.C., pp. 38–45.
- Nazarian, S., M. Baker, and S. Reddy. 1994. *Nondestructive Testing of Pavements and Backcalculation of Moduli: Second Volume*, STP 1198, ASTM Publication, Philadelphia, Pa., pp. 473–487.
- Newton, C. J., and J. M. Sykes. 1988. A Galvanostatic Pulse Technique for Investigation of Steel Corrosion in Concrete. *Corrosion Science*, Vol. 28, pp. 1051–1074.
- Page, C. L., P. B. Bamforth, and J. W. Figg (eds.). 1996. *Corrosion of Reinforcement in Concrete Construction*. Royal Society of Chemistry, Cambridge, United Kingdom.
- Romero, F. A., and R. L. Roberts. 2002. The Evolution in High-Resolution Ground Penetrating Radar Surveys from Ground-Coupled to High-Speed, Air-Coupled Evaluations. *Proc., Structural Materials Technology V: An NDT Conference*, Cincinnati, Ohio.
- Sansalone, M., and N. J. Carino. 1989. Detecting Delaminations in Concrete Slabs with and without Overlays Using the Impact-Echo Method. *ACI Materials Journal*, Vol. 86, No. 2, pp. 175–184.
- Smith, J. L., and Y. P. Virmani. 1996. *Performance of Epoxy Coated Rebars in Bridge Deck*. Report FHWA-RD-96-092. FHWA, U.S. Department of Transportation.
- Stokoe, K. H., S. G. Wright, J. A. Bay, and J. M. Roesset. 1994. *Characterization of Geotechnical Sites by SASW Method*. Technical Review: Geophysical Characterization of Sites, ISSMFE Technical Committee 10 (R. D. Woods, ed.), Oxford University Press, New Delhi.
- Taffe, A., and H. Wiggenhauser. 2006. Validation of Thickness Measurement in Civil Engineering with Ultrasonic Echo. *Proc., 9th European Conference on Non-Destructive Testing*, Berlin.
- Texas Department of Transportation (TxDOT). *Standard Specifications for Construction and Maintenance of Highways, Streets, and Bridges*. [www.txdot.gov/txdot\\_library/consultants\\_contractors/publications/specifications.htm](http://www.txdot.gov/txdot_library/consultants_contractors/publications/specifications.htm). Accessed October 9, 2012.
- Yuan, D., S. Nazarian, D. Chen, and F. Hugo. 1999. Use of Seismic Pavement Analyzer to Monitor Degradation of Flexible Pavements Under Texas Mobile Load Simulator. In *Transportation Research Record 1615*, TRB, National Research Council, Washington, D.C., pp. 3–10.

## **TRB OVERSIGHT COMMITTEE FOR THE STRATEGIC HIGHWAY RESEARCH PROGRAM 2\***

CHAIR: **Kirk T. Steudle**, *Director, Michigan Department of Transportation*

### **MEMBERS**

**H. Norman Abramson**, *Executive Vice President (retired), Southwest Research Institute*  
**Alan C. Clark**, *MPO Director, Houston–Galveston Area Council*  
**Frank L. Danchetz**, *Vice President, ARCADIS-US, Inc.*  
**Stanley Gee**, *Executive Deputy Commissioner, New York State Department of Transportation*  
**Michael P. Lewis**, *Director, Rhode Island Department of Transportation*  
**Susan Martinovich**, *Director, Nevada Department of Transportation*  
**John R. Njord**, *Executive Director, Utah Department of Transportation*  
**Charles F. Potts**, *Chief Executive Officer, Heritage Construction and Materials*  
**Ananth K. Prasad**, *Secretary, Florida Department of Transportation*  
**Gerald M. Ross**, *Chief Engineer, Georgia Department of Transportation*  
**George E. Schoener**, *Executive Director, I-95 Corridor Coalition*  
**Kumares C. Sinha**, *Olson Distinguished Professor of Civil Engineering, Purdue University*  
**Paul Trombino III**, *Director, Iowa Department of Transportation*

### **EX OFFICIO MEMBERS**

**John C. Horsley**, *Executive Director, American Association of State Highway and Transportation Officials*  
**Victor M. Mendez**, *Administrator, Federal Highway Administration*  
**David L. Strickland**, *Administrator, National Highway Transportation Safety Administration*

### **LIAISONS**

**Ken Jacoby**, *Communications and Outreach Team Director, Office of Corporate Research, Technology, and Innovation Management, Federal Highway Administration*  
**Tony Kane**, *Director, Engineering and Technical Services, American Association of State Highway and Transportation Officials*  
**Jeffrey F. Paniati**, *Executive Director, Federal Highway Administration*  
**John Pearson**, *Program Director, Council of Deputy Ministers Responsible for Transportation and Highway Safety, Canada*  
**Michael F. Trentacoste**, *Associate Administrator, Research, Development, and Technology, Federal Highway Administration*

## **RENEWAL TECHNICAL COORDINATING COMMITTEE\***

CHAIR: **Cathy Nelson**, *Technical Services Manager/Chief Engineer, Oregon Department of Transportation*

### **MEMBERS**

**Rachel Arulraj**, *Director of Virtual Design & Construction, Parsons Brinckerhoff*  
**Michael E. Ayers**, *Consultant, Technology Services, American Concrete Pavement Association*  
**Thomas E. Baker**, *State Materials Engineer, Washington State Department of Transportation*  
**John E. Breen**, *Al-Rashid Chair in Civil Engineering Emeritus, University of Texas at Austin*  
**Daniel D'Angelo**, *Recovery Acting Manager, Director and Deputy Chief Engineer, Office of Design, New York State Department of Transportation*  
**Steven D. DeWitt**, *Chief Engineer, North Carolina Turnpike Authority*  
**Tom W. Donovan**, *Senior Right of Way Agent (retired), California Department of Transportation*  
**Alan D. Fisher**, *Manager, Construction Structures Group, Cianbro Corporation*  
**Michael Hemmingsen**, *Davison Transportation Service Center Manager (retired), Michigan Department of Transportation*  
**Bruce Johnson**, *State Bridge Engineer, Oregon Department of Transportation, Bridge Engineering Section*  
**Leonnie Kavanagh**, *PhD Candidate, Seasonal Lecturer, Civil Engineering Department, University of Manitoba*  
**John J. Robinson, Jr.**, *Assistant Chief Counsel, Pennsylvania Department of Transportation, Governor's Office of General Counsel*  
**Michael Ryan**, *Vice President, Michael Baker Jr., Inc.*  
**Ted M. Scott II**, *Director, Engineering, American Trucking Associations, Inc.*  
**Gary D. Taylor**, *Professional Engineer*  
**Gary C. Whited**, *Program Manager, Construction and Materials Support Center, University of Wisconsin–Madison*

### **AASHTO LIAISONS**

**James T. McDonnell**, *Program Director for Engineering, American Association of State Highway and Transportation Officials*

### **FHWA LIAISONS**

**Steve Gaj**, *Leader, System Management and Monitoring Team, Office of Asset Management, Federal Highway Administration*  
**Cheryl Allen Richter**, *Assistant Director, Pavement Research and Development, Office of Infrastructure Research and Development, Federal Highway Administration*  
**J. B. "Butch" Wlaschin**, *Director, Office of Asset Management, Federal Highway Administration*

### **CANADA LIAISON**

**Lance Vigfusson**, *Assistant Deputy Minister of Engineering & Operations, Manitoba Infrastructure and Transportation*

---

\*Membership as of August 2012.

## Related SHRP 2 Research

Evaluating Applications of Field Spectroscopy Devices to Fingerprint Commonly Used Construction Materials (R06B)

Using Infrared and High-Speed Ground-Penetrating Radar for Uniformity Measurements on New HMA Layers (R06C)

Nondestructive Testing to Identify Delaminations Between HMA Layers (R06D)

Real-Time Smoothness Measurements on Portland Cement Concrete Pavements During Construction (R06E)

Assessment of Continuous Pavement Deflection Measuring Technologies (R06F)

Mapping Voids, Debonding, Delaminations, Moisture, and Other Defects Behind or Within Tunnel Linings (R06G)

Bridges for Service Life Beyond 100 Years: Innovative Systems, Subsystems, and Components (R19A)